EFFECTS OF PREPARATION, Ni/Co RATIO, AND SULFURE POISONING OF Ni-Co BIMETALLIC CATALYST FOR DRY REFORMING REACTION

A Thesis Submitted to the College of

Graduate Studies and Research

in Partial Fulfillment of the Requirements

for the Degree of Master of Science

in the Department of Chemical and Biological Engineering

University of Saskatchewan

Saskatoon

By

Mohsen Shakouri

PERMISSION TO USE

In presenting this thesis in partial fulfillment of the requirements for a Postgraduate degree from the University of Saskatchewan, I agree that the Libraries of this University may make it freely available for inspection. I further agree that permission for copying of this thesis/dissertation in any manner, in whole or in part, for scholarly purposes may be granted by Professor Hui Wang who supervised my thesis work. It is understood that any copying or publication or use of this thesis or parts for financial gain shall not be allowed without my written permission. It is also understood that due recognition shall be given to me and to the University of Saskatchewan in any scholarly use which may be made of any material in my thesis.

DISCLAIMER

The University of Saskatchewan was exclusively created to meet the thesis and exhibition requirements for the degree of Master of Science at the University of Saskatchewan. Reference in this thesis to any specific commercial products, process, or service by trade name, trademark, manufacturer, or otherwise, does not constitute or imply its endorsement, recommendation, or favouring by the University of Saskatchewan. The views and opinions of the author expressed herein do not state or reflect those of the University of Saskatchewan, and shall not be used for advertising or product endorsement purposes.

Requests for permission to copy or to make other uses of materials in this thesis in whole or part should be addressed to.

Prof. D.-Y. Peng,

Department of Chemical and Biological Engineering

University of Saskatchewan

College of Engineering

1C119, 57 Campus Drive

Saskatoon, SK S7N 5A9

Canada

OR

Dean

College of Graduate Studies and Research

University of Saskatchewan

107 Administration Place

Saskatoon, Saskatchewan S7N 5A2

Canada

ABSTRACT

Ni-Co/$AlMgO_x$ bimetallic, Ni/$AlMgO_x$ and Co/$AlMgO_x$ monometallic catalysts were prepared with various Ni/Co ratios by using the precipitation and impregnation methods for dry reforming reaction. The effects of Ni/Co ratio and preparation methods on the catalyst were analyzed by using different characterization techniques such as BET, ICP, EXAFS, and XANES. It was observed that due to the lack of metal-metal interactions between impregnated catalysts the Ni/Co ratio was better controlled as compared to the precipitated catalysts. On the other hand, with the same Ni/Co ratio the impregnated catalyst was reduced more than the precipitated catalyst. The performance of each catalyst for CO_2 reforming of CH_4 reaction at 710 °C was studied in a quartz tube reactor. Among the prepared catalysts, the precipitated Ni-Co bimetallic catalyst with Ni/Co ratio of 1 showed the best performance. The Co monometallic catalysts did not show desired activity for CO_2 reforming of CH_4. Therefore, to observe the stability of the selected catalyst with Ni/Co ratio of 1 a life-time test was carried out for 65 days at two different temperatures of 710 °C and 760 °C. The precipitated catalyst with Ni/Co ratio of 1 showed higher activity and better stability at 760 °C as compared to 710 °C. Finally, the prepared catalysts were poisoned by adding 30 ppm of H_2S for CO_2 reforming of CH_4 reaction. The Ni monometallic catalysts, whether prepared by impregnation or precipitation method, showed better resistance to H_2S in all cases. Moreover, the Ni monometallic catalysts had higher ability for regeneration as compared to the other prepared catalysts. It was observed that the prepared catalysts with impregnation were more active and had a higher capability for regeneration after H_2S poisoning as compared to precipitated catalysts.

ACKNOWLEDGMENT

I would like to acknowledge the people who contributed to a successful completion of this work. My appreciations go to my parent and sisters for their moral and financial support. I am very grateful to my supervisor, Professor Hui Wang, for all his unflinching support, encouragement and guidance. His deep understanding of situation is greatly valued and highly appreciated. My gratitude also goes to Dr. Ajay K. Dalai, Richard W. Evitts, and Dr. D.-Y. Peng for their valuable course of materials. To Dr. Mehdi Nemati, and Dr. Dae Kun Hwang, and Dr. Jafar Soltan my committee members, I say big thank you for your time. I also would like to thank Dr. Stephen R. Foley for his time as the external examiner. The financial support the Natural Sciences and Engineering Research Council of Canada (NSERC) for this research project in form of Discovery Grant to my supervisor is highly appreciated. I also wish to acknowledge Jianguo Zhang and Chunyu Xi for their assistance and support in my experimental work. I also would like to thank S. Sameen A. Ziadi and Armin Moniri for their helps in the writing of my thesis. Lastly, lots of thanks to all the department technicians, office support staff, other graduate students and especially my very supportive friends for their support.

DEDICATION

I would like to dedicate this thesis to my beloved mother (R.I.P.)

Also, the honor of this thesis is going to my lovely father who has been a great source of motivation and inspiration.

TABLE OF CONTENTS

PERMISSION TO USE ..... **I**

ABSTRACT ..... **III**

ACKNOWLEDGMENT ..... **IV**

DEDICATION ..... **V**

TABLE OF CONTENTS ..... **VI**

LIST OF TABLES ..... **X**

LIST OF FIGURES ..... **XII**

NOMENCLATURE ..... **XV**

ABBREVIATIONS ..... **XVII**

CHAPTER 1: INTRODUCTION **1**

1.1 OVERVIEW 1

1.2 MOTIVATION 2

1.3 THESIS ARRANGEMENT 4

CHAPTER 2: LITERATURE REVIEW **6**

2.1 GREENHOUSE GASES AND SYNTHESIS GAS 6

2.2 SYNTHESIS GAS PRODUCTION 12

2.2.1 STEAM REFORMING 12

2.2.2 PARTIAL OXIDATION OF METHANE 12

2.2.3 AUTO – THERMAL REFORMING 13

2.2.4 CO_2 REFORMING OF CH_4 13

2.3 CARBON DIOXIDE REFORMING OF METHANE (CDRM) 14

2.3.1 CALCOR PROCESS 15

2.3.2 SPARG PROCESS 16

2.3.3 CATALYSTS FOR DRY REFORMING REACTION 16

2.3.4 HYDROGEN AND SYNGAS PRODUCTION THROUGH CDRM REACTION 17

2.3.5 DEACTIVATION OF REFORMING CATALYST 19

2.4 CATALYST DESIGN 19

2.4.1 TARGET REACTION 20

2.4.2 STOICHIOMETRIC ANALYSIS 21

2.4.3 THERMODYNAMIC ANALYSIS 21

2.4.4 PROPOSED MECHANISM 21

2.4.5 DESIRED CATALYST PROPERTIES 23

2.4.6 CATALYST SELECTION 24

2.5 CATALYST PREPARATION METHODS AND PROCEDURES 28

2.5.1 PRECIPITATION METHOD 28

2.5.2 IMPREGNATION METHOD 31

2.6 KNOWLEDGE GAP 32

2.7 RESEARCH OBJECTIVES AND THESIS SCOPE 33

CHAPTER 3: EXPERIMENTAL SET-UP AND PROCEDURE 34

3.1 Experimental procedure 34
3.1.1 Catalyst preparation procedure 34
3.1.2 Catalyst test procedure 37
3.2 Catalyst characterization analyses 37
3.2.1 BET surface area 37
3.2.2 ICP analysis 38
3.2.3 XAS analysis 38
3.3 Experimental set-up of catalyst testing 39
3.3.1 Catalyst activity test 39
3.3.2 Catalyst life-time test 40
3.3.3 H_2S poisoning test 40
3.4 Data analysis procedure 41
Chapter 4: Results and Discussion 43
4. 1 Reproducibility of the results 43
4.2 Catalyst characterization 47
4.2.1 BET surface area 47
4.2.2 ICP analysis 48
4.2.3 XAS analysis 51
4.3 Catalyst activity test 56
4.3.1 Effect of Ni/Co ratio on CDRM reaction (precipitated catalysts) 56

4.3.2 Effect of Ni/Co ratio on CDRM reaction (impregnated catalysts)60

4.3.3 Effects of preparation methods for the Ni-Co/AlMgO$_x$ catalysts for CDRM reaction 64

4.3.3.1 Effect of preparation method for monometallic catalysts 64

4.3.3.2 Effect of preparation method for Ni-Co bimetallic catalysts 66

4.3.3.3 Overall comparison 68

4.4 Life-time activity and stability test of Ni-Co bimetallic catalyst (CopCat-Ni2Co4 with Ni/Co ratio of 0.6) 72

4.5 Catalyst poisoning with 30 ppm of H_2S 76

Chapter 5: Conclusion and recommendation 83

5.1 Conclusion 83

5.2 Recommendation 85

References 87

Appendix A: Calibration of mass flow (MFC) controller 95

Appendix B: Calibration of gas chromatography 98

Appendix C: Temperature calibration in the middle of the reactor 104

Appendix D: Carbon balance 105

Appendix E: Catalyst characterization analysis 107

Appendix F: Oven temperature profile of GC 111

LIST OF TABLES

Table 2.1 Processes produce synthesis gas 9

Table 2.2 Synthesis gas applications 10

Table 2.3 Natural gas compositions in Canada 11

Table 2.4 Proposed mechanism for carbon dioxide reforming of methane 22

Table 2.5 Physical data of common metals used as catalyst 25

Table 2.6 Comparison chart of catalyst preparation method..... 32

Table 3.1 Chemicals and amounts used for preparation of catalysts by precipitated..... 36

Table 3.2 Chemicals and amounts used for preparation of catalysts by impregnation .. 36

Table 4.1 Results of repeated BET analysis 44

Table 4.2 Reproducibility results of ICP analysis 44

Table 4.3 Repeated catalyst activity test results 45

Table 4.4 BET surface area of the prepared Ni-Co/$AlMgO_x$ bimetallic catalyst 47

Table 4.5 Metal composition of Ni-Co/$AlMgO_x$ bimetallic and Ni or Co metallic catalysts by ICP analysis 48

Table 4.6 Solubility products of metal hydroxides at 25 °C 49

Table 4.7 Co K-edge XANS and EXAFS results for Ni/Co ratio 0.6 52

Table 4.8 XANES results of the prepared catalysts 53

Table 4.9 EXAFS results of the prepared catalysts 54

Table 4.10 Reduced metal content (wt %) of precipitated catalysts 55

Table 4.11 Reduced metal content (wt %) of impregnated catalysts 55

Table 4.12 Activity and stability of Ni-Co precipitated catalysts 58

Table 4.13 Activity and stability of Ni-Co impregnated catalysts 62

Table 4.14 Formation rate of products and reactant conversions of the life-time..... 75

Table 4.15 Reactant conversions for the poisoning test, precipitated catalysts 79

Table 4.16 Reactant conversions for the poisoning test, impregnated catalysts 80

Table A.1 Heat capacity values of H_2, N_2, CO_2, and CH_4 at 21 °C. 95

Table B.1 GC calibration data for H_2..... 99

Table B.2 GC calibration data for N_2..... 100

Table B.3 GC calibration data for CO 101

Table B.4 GC calibration data for CH_4..... 102

Table B.5 GC calibration data for CO_2..... 103

Table D. 1 Carbon balance for CopCat-Ni3Co2 within 14h..... 106

Table F.1 GC oven temperature values..... 111

LIST OF FIGURES

Fig.2.1 Canada's total gas emissions breakdown by gas 7

Fig.2.2 Steps in catalyst design 20

Fig.2.3 Proposed surface mechanism for CDRM reaction on metallic catalyst 23

Fig.2.4 Brief chart of precipitation procedure 29

Fig.2.5 Schematic of the experimental set-up for catalyst preparation 30

Fig.2.6 Summary chart of impregnation procedure 31

Fig. 4.1 Methane conversion for the repeated catalyst activity test 46

Fig. 4.2 H_2/CO ratio of the repeated catalyst activity test 46

Fig. 4.3 Effect of preparation method on the intent Ni/Co ratios 50

Fig. 4.4 Effect of preparation method on the obtained Mg/Al ratios 51

Fig. 4.5 Activity and stability of precipitated catalysts in term of CH_4 conversion 57

Fig. 4.6 Activity and stability of precipitated catalysts in term of CO_2 conversion 58

Fig. 4.7 H_2/CO ratios of precipitated catalysts 59

Fig. 4.8 Activity and stability of impregnated catalysts in term of CH_4 conversion 61

Fig. 4.9 Activity and stability of impregnated catalysts in term of CO_2 conversion 62

Fig. 4.10 H_2/CO ratios of Impregnated catalysts 63

Fig. 4.11 Activity and stability of monometallic catalysts 65

Fig. 4.12 H_2/CO ratios of the monometallic catalysts 66

Fig. 4.13 Activity and stability of bimetallic catalysts 67

Fig. 4.14 H_2/CO ratios of Ni/Co bimetallic catalysts 67

Fig. 4.15 Activity and stability of Ni-Co catalysts 69

Fig. 4.16 H_2/CO ratios of Ni-Co catalysts 70

Fig. 4.17 CH_4 rates of CDRM reaction based on the total reduced metal weight 71

Fig. 4.18 CO_2 rates of CDRM reaction based on the total reduced metal weight 72

Fig. 4.19 Activity and stability of CopCat-Ni2Co4 (Life-Time). 74

Fig. 4.20 Production rates of the life-time CDRM test 74

Fig. 4.21 H_2/CO ratio during the life-time test period at 710 °C and 760 °C 76

Fig. 4.22 Activity of Ni-Co precipitated catalysts in term of CO_2 conversions during H_2S poisoning test 78

Fig. 4.23 Activity of Ni-Co precipitated catalysts in term of CH_4 conversions during H_2S poisoning test 79

Fig. 4.24 Activity of Ni-Co impregnated catalysts in term of CO_2 conversions during H_2S poisoning test 81

Fig. 4.25 Activity of Ni-Co impregnated catalysts in term of CH_4 conversions during H_2S poisoning test 81

Fig.A.1 Calibration curve for N_2 mass flow controller 96

Fig.A.2 Calibration curve for CH_4 mass flow controller 96

Fig.A.3 Calibration curve for CO_2 mass flow controller 97

Fig.A.4 Calibration curve for H_2 mass flow controller 97

Fig.B.1 GC calibration curve for H_2 99

Fig.B.2 GC calibration curve for N_2 100

Fig.B.3 GC calibration curve for CO 101

Fig.B.4 GC calibration curve for CH_4 102

Fig.B.5 GC calibration curve for CO_2 103

Fig.D. 1 Carbon flow in inlet and outlet streams of the reactor..... 105

Fig.C.1 Heater temperature calibration in the middle of the reactor 104

Fig.E.1 Three main regions in an XAS spectrum 109

Fig.F.1 Oven temperature profile of GC 111

NOMENCLATURE

A	molar mass of adsorbed species
b.b.c.	body centered cubic
c	BET constant
F_{in}, i	flow rate of component "i" before a reaction (mL/min)
F_{out}, i	flow rate of component "i" after a reaction (mL/min)
f.c.c.	faced centered cubic
HFCs	hydro-fluorocarbons
h.c.p.	hexagonal close packing
Me	metal
N	Avogadro's number = 6.022×1023
P	equilibrium pressure of the adsorbed gas,
P_0	saturation pressure of the adsorbed gas
PFCs	per-fluorocarbons
pH	a measure of the acidity or basicity

Q	the adsorbed gas quantity
Q_m	quantity of the monolayer adsorbed gas
s	molecular cross-sectional area
V	molar volume of adsorbed gas
wt %	weight percent

ABBREVIATIONS

ANL	Argonne National Laboratory
APS	Advanced Photon Source
ASTM	American Society for Testing Material
BET	Brunauer, Emmett, and Teller
CDRM	carbon dioxide reforming of methane
EXAFS	Extended X-ray Absorption Fine Structure
GC	gas chromatography
GHG	greenhouse gas
GHSV	gas hourly space velocity
ICP	Inductively Coupled Plasma
IPCC	Intergovernmental Panel on Climate Change
LUM	Lagrange Undetermined Multiplier
MTE	multi-reaction thermodynamic equilibrium
MFC	mass flow controller

NEXAFS	Near-edge X-ray Absorption Fine Structure
RDS	Rate Determining Step
RLS	Rate Limiting Step
RWGSR	reverse water gas shift reaction
SNG	synthetic natural gas
TCD	thermal conductivity detector
TOS	Time On Stream
XANES	X-ray Absorption Near-Edge Structure
XAS	X-ray Absorption Spectroscopy

CHAPTER 1: INTRODUCTION

1.1 OVERVIEW

CO_2 reforming of CH_4, or dry reforming, has attracted attentions among the other CH_4 reforming reactions, because it uses CO_2 and CH_4 which are greenhouse gases, and produces synthesis gas which is desired for industry.

Natural gas mainly contains CH_4 is in direct competition with oil and coal as a fuel in many applications. Besides, some low grades of natural gas contain significant amount of CO_2 as compared to its CH_4 content. In addition, land fill gas and coal gas contain significant amount of CH_4 and CO_2. Also, CO_2 is generated as a waste by-product in processes like fossil fuel combustion, synthesis fuels manufacturing, and chemical production. Therefore significant amount of CO_2 and CH_4 are easily available. Also, CO_2 and CH_4 are known as the main parts of greenhouse gas which is environmentally undesirable due to its direct effect on global temperature.

The conversion of gases to transportable fuels such as gasoline, diesel, and methanol has attracted much attention from both industrial and environmental aspects. Therefore, different methane reforming applications, like dry reforming, are studied to produce synthesis gas (mixture of H_2 + CO). As an example, syngas is used in Fischer–Tropsch synthesis that produces liquid hydrocarbons from synthesis gas.

Due to the importance of synthesis gas as feedstock for industry and an increase in H_2 demand, dry reforming is applied in landfill gas utilization and coal gas polygeneration. On the other hand, dry reforming reaction reduces the amount of CH_4 and CO_2[1] noticeably, therefore; many catalysts are being developed for dry reforming reaction. The major problem associated to this reaction is the lack of a stable catalyst to eliminate a significant amount of carbon formation during a long period of time on the stream.

1.2 MOTIVATION

Our research group in University of Saskatchewan has developed a Ni-Co/$AlMgO_x$ bimetallic catalyst with Ni/Co ratio of one prepared by precipitation method which is highly active and stable for dry reforming reaction (Zhang *et al.*, 2007). To find a good catalyst which has the lowest carbon formation for CDRM reaction Zhang made four different bimetallic catalysts. The catalysts were Ni-Me/$AlMgO_x$ (Me = Co, Fe, Cu, or Mn) which prepared by precipitation method. Among them Ni-Co/$AlMgO_x$ catalyst was tested for CDRM reaction for 2000h (GHSV of 110,000 mL/g.h; 750 °C; 1 atm; catalyst load of 0.05 g). The Ni-Co bimetallic catalyst showed 2000 h stability with relatively high conversion (CH_4 conversion: 90%, CO_2 conversion: 91%) and the carbon formation was as low as 0.44 g_{carbon}/g_c (Zhang *et al.*, 2007). Zhang also studied the mechanism and kinetic study of the reaction with Ni-Co catalyst. It is remarkable that the Ni-Co/AlMgOx bimetallic catalyst for dry reforming reaction was awarded a patent in July 2011 as a catalyst for production of synthesis gas (US Patent 7,985,710). Also, Carbon Science Inc. (Santa Barbara, USA) announced a worldwide

[1] The main part of greenhouse gases

exclusive licence agreement with University of Saskatchewan for the Ni-Co bimetallic catalyst, in December 2010.

Further observations on the Ni-Co/$AlMgO_x$ were done by Xi in our group. Xi studied effects of preparation conditions (especially pH value of precipitation) on the Ni-Co catalyst properties and performances (Xi and Wang, 2009).

Further investigations are going to be described for the Ni-Co catalyst for CDRM reaction during the thesis. The main observations are based on the following considerations:

1- A catalyst can be prepared by using different preparation methods such as precipitation method or impregnation method and each preparation method can affect the catalyst performance for a reaction.
2- Running CDRM reaction over related catalyst, metallic part is known as the active site. Ni-Co bimetallic catalyst contains both Ni and Co as the metals therefore various Ni/Co ratios may affect the catalyst performance for CDRM reaction.
3- H_2S is known as a poison for catalysts and may affect the catalyst performance. Since natural gas may contain few amounts of H_2S, therefore effect of H_2S on the Ni-Co/$AlMgO_x$ catalyst performance for CDRM reaction should be ivestigated.

To commercialize Ni-Co bimetallic catalyst, the effects of preparation methods, various Ni/Co ratios and effect of H_2S as a poison on the Ni-Co/$AlMgO_x$ catalyst performance for CDRM reaction need to be evaluated. To investigate the effects of

Ni/Co ratio on the Ni-Co bimetallic catalysts, the catalysts were prepared with Ni/Co ratio of 0.5, 1, and 2. Also, Ni and Co monometallic catalysts supported on AlMgOx were prepared. Furthermore, to observe the effects of preparation method on the catalyst performance all the catalysts were prepared with both impregnation and precipitation. The catalyst activity and stability for carbon dioxide reforming of methane were tested in a quartz fixed bed reactor. As Carbon Science Inc. requirement, the optimum catalyst was selected and used for CDRM reaction for almost 1600 h. Lastly, all the prepared catalysts were poisoned using H_2S in order to investigate the effects of H_2S on the catalysts.

1.3 THESIS ARRANGEMENT

The arrangement of the thesis is as follows:

Chapter 1: Introduction focuses on the general background and development of methane dry reforming technology.

Chapter 2: Literature review consists of relevant information for various methane reforming reactions. It also introduces the previous studies done for CDRM reaction using different catalysts. Then, the catalyst design and selection procedure is explained. The catalyst preparation methods are described as well.

Chapter 3: Experimental set-up and procedure focuses on the procedure of the catalysts preparation, catalyst characterization techniques and the activity tests. The data analysis method and equations are explained.

Chapter 4: Results and discussion contains the results of the research and related discussion. Briefly, the results of BET, ICP and XAS as catalyst characterization analyses are shown and discussed. Also, the effects of various Ni/Co ratios and preparation methods on catalyst performance for CDRM reaction are discussed. Furthermore, the stability of Ni-Co/AlMgO_x with Ni/Co ratio of 1 for CDRM reaction is described. The effects of H_2S poisoning on the catalyst performance for CDRM are explained as well.

Chapter 5: Conclusion and recommendation are made for future work.

CHAPTER 2: LITERATURE REVIEW

2.1 GREENHOUSE GASES AND SYNTHESIS GAS

The greenhouse gases (abbreviated as GHG) adsorb and emit infrared radiation in the earth's atmosphere. The major greenhouse gases in the atmosphere are water vapor, carbon dioxide, nitrous oxide, and methane. Since the industrial revolution, the concentration of carbon dioxide, methane, and nitrous oxide have being increased because of fossil fuel combustion, human activities, and land-use changes.

The assessment report compiled by the Intergovernmental Panel on Climate Change (IPCC, 2007) has observed that the changes in atmospheric concentrations of greenhouse gases, aerosols, land cover, and solar radiation are altering the energy balance of the climate system. The report has concluded that the increase in anthropogenic greenhouse gas (GHG) concentration is very likely to have caused most of the increase in global average temperature since the mid-20th century. The Canada's total emissions breakdown by gas, reported by the Environment Canada, is shown in Figure 2.1.

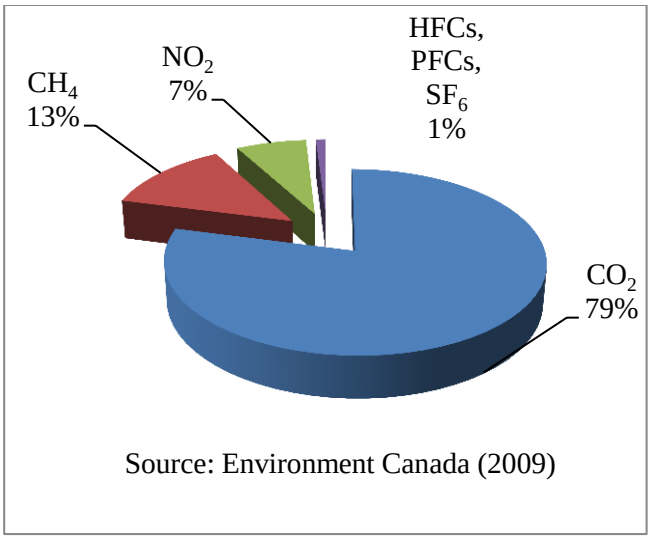

Fig. 2.1 Canada's total gas emissions breakdown by gas

Figure 2.1 shows that the CO_2 was the major greenhouse gas mainly caused by combustion of fossil fuels. Methane was laid on the second place with 13%, which mainly came from the activities in the Agriculture and Waste sectors, and emissions from oil and natural gas. The third place was given to nitrous oxide with 7%. Also, Per-fluorocarbons (PFCs), sulphur hexafluoride (SF_6) and hydro-fluorocarbons (HFCs) were close to 1% of total emissions.

Syngas[1] is a gas mixture containing various amounts of carbon monoxide and hydrogen. Because highly usage of H_2 and CO mixture as an intermediate feed in production of synthetic natural gas (SNG), the name of synthesis gas is given to the mixture of H_2 and CO. The examples of syngas production methods are steam reforming of natural gas or liquid hydrocarbons to produce hydrogen, the gasification of

[1] Short from of synthesis gas

coal. Syngas is also used as a feed in Fischer Tropsch synthesis process to produce methanol and is used for ammonia production as well.

The production of hydrogen is of great importance due to its use in the chemical and fuel industries (Barreto *et al.*, 2003; Goff *et al.*, 1987). Currently, the dominant method of hydrogen production is the catalytic reforming of CH_4 with steam[1]. Industrially, the reaction is carried out at high temperatures (1073 – 1103 K) and high pressures (20 – 40 bar) to obtain high yields of the products (Goff *et al.*, 1987). The hydrogen is used in many applications. As a pure product, it can be used in refinery processes, ammonia synthesis, hydrogenation, and fuel cells.

As a mixture with CO, hydrogen also has extensive usages, such as methanol synthesis, hydroformylation, and long-chain hydrocarbon synthesis via Fisher-Tropsch reaction. Hydrogen can be used more efficiently in fuel cells than the other fuels which need combustion to convert their potential to mechanical energy. In addition, the breakdown of hydrogen does not generate pollutants, unlike the fossil fuels. It is noteworthy that hydrogen is the only fuel whose production and use can contribute directly in eliminating many of environmental, economic, and health problems.

The synthesis gas produced from various reactions with different H_2/CO ratio. Based on H_2/CO ratio, the produced syngas can be consumed by various processes. Some of the reactions that can produce synthesis gas from methane are partial oxidation of methane, steam reforming, dry reforming, and auto-thermal reforming. Based on the

[1] $CH_4 + H_2O \rightleftharpoons CO + 3H_2$

H_2/CO ratio of the synthesis gas which is produced by different processes, it can be used in different reactions. Table 2.1 shows reaction which can produce synthesis gas.

Table 2.1 Processes produce synthesis gas

Process	Reaction Equation	H_2/CO ratio	$\Delta H°$
Partial oxidation	$CH_4 + 0.5O_2 \rightleftharpoons CO + 2H_2$	2	-36
Steam reforming	$CH_4 + H_2O \rightleftharpoons CO + 3H_2$	>3	+206
	$CO + H_2O \rightleftharpoons CO_2 + H_2$		-41
Dry reforming	$CH_4 + CO_2 \rightleftharpoons 2CO + 2H_2$	1	+247
Auto-thermal reforming	$CH_4 + 2O_2 \rightleftharpoons CO_2 + 2H_2O$		-802
	(Methane in excess)		
	$CH_4 + CO_2 \rightleftharpoons 2CO + 2H_2$		+247
	or		
	$CH_4 + H_2O \rightleftharpoons CO + 3H_2$		+206

Table 2.2 shows some applications of synthesis gas in various processes. Table 2.3 shows the composition of natural gas as reported by Uniongas Company in Canada, Ontario.

Table 2.2 Synthesis gas applications

Reaction	H_2/CO ratio	Application
Dry reforming	1	e.g. Oxo alcohols, formaldehyde production
Partial oxidation	2	e.g. Methanol synthesis, Fischer-Tropsch synthesis
Steam reforming	>3	e.g. H_2 Production, ammonia synthesis

Table 2.3 shows that the main part of the natural gas is composed of methane. Therefore the feed needed for syngas reaction can be found easily. On the other hand, due to high cost of natural gas transporting on site natural gas conversion to other more valuable and easily transportable products is desirable.

Table 2.3 Natural gas compositions in Canada (by Uniongas Company)

Component	Typical Analysis (mole %)	Range (mole %)
Methane	95.2	87.0 - 96.0
Ethane	2.5	1.5 - 5.1
Propane	0.2	0.1 - 1.5
iso - Butane	0.03	0.01 - 0.3
normal - Butane	0.03	0.01 - 0.3
iso - Pentane	0.01	trace - 0.14
normal - Pentane	0.01	trace - 0.04
Hexanes plus	0.01	trace - 0.06
Nitrogen	1.3	0.7 - 5.6
Carbon Dioxide	0.7	0.1 - 1.0
Oxygen	0.02	0.01 - 0.1
Hydrogen	trace	trace - 0.02

***** Typical sulphur content is 5.5 mg/m^3 which, based on 25 °C and 1 atm, means 4 ppm, Water vapour content is typically between 16-32 mg/m^3.

2.2 SYNTHESIS GAS PRODUCTION

2.2.1 STEAM REFORMING

Steam reforming is known as the main and well-developed process for producing synthesis gas and/or hydrogen. The steam reforming reaction is as follows:

$$CH_4 + H_2O \rightleftharpoons CO + 3H_2; \qquad \Delta H°_{298\ K} = +206\ kJ/mole$$

This endothermic reaction can be mixed with methane dry reforming to adjust the H_2/CO ratio as a feedstock for other processes. All group VIII metals show good activity for steam reforming. Among them, Ni for its cheap availability is the most commonly used catalyst while Ru and Rh show the highest activity for the process. Also, MgO and α-Al_2O_3 were used as the common support for these metals because of their good stability under high reaction temperature. (Bitter *et al.*, 1997)

2.2.2 PARTIAL OXIDATION OF METHANE

The syngas is also obtained by the partial oxidation of CH_4 as follows:

$$CH_4 + 0.5O_2 \rightleftharpoons CO + 2H_2; \qquad \Delta H°_{298\ K} = +247\ kJ/mole$$

While steam reforming needs a huge amount of energy, partial oxidation seems to be a good alternative process to produce synthesis gas. From economical point of view, the main problem related to this process is the cost of pure oxygen supply. The partial oxidation process can be operated both catalytically and non-catalytically. According to non-catalytic process methane and oxygen typically react at high temperature (1350-1800 K); therefore, most of the researchers were attracted to use catalyst for the process.

Typical reaction condition for catalytic partial oxidation is atmospheric pressure and temperature in range of 673 K to 1273 K (Bjørn Christian Enger *et al.*, 2008).

2.2.3 AUTO – THERMAL REFORMING

The combination of non-catalytic partial oxidation and reforming of methane developed by Haldor Topsøe in the late 1950s was named auto-thermal reforming. The process was developed by having both partial oxidation and reforming of methane in a single reactor. Due to the occurrence of undesired in combustion zone, the reaction may lead to carbon deposition on downstream tubes. The carbon deposition may cause various operational problems like catalyst deactivation, pressure drop, damaging the equipment, and poor heat transfer (Pena *et al.*, 1996).

2.2.4 CO_2 REFORMING OF CH_4

In recent years, the reforming of CH_4 with CO_2 has attracted great attention as an alternative method for hydrogen production since this reaction utilizes an environmentally problematic greenhouse gases. The CDRM reaction is as follows:

$$CH_4 + CO_2 \rightleftharpoons 2\,CO + 2\,H_2; \qquad \Delta H^{\circ}_{298\,K} = +247.4\ \text{kJ/mole}$$

However, the CH_4 reforming reactions are energy extensive, because they are endothermic in nature and must be carried out at high temperatures to obtain high conversions (high yield of H_2). Therefore different applications are studied to reduce the amount of greenhouse gases and produce syngas. One of the best processes which attract

great attention in the last decade is catalytic CO_2 reforming of methane (Ramachandran *et al.*, 1998).

As before mentioned, a beneficial procedure for producing syngas (CO and H_2) is dry reforming of methane which is an endothermic reaction producing a mixture of low molar ratio of CO and H_2.

$$CH_4 + CO_2 \rightleftharpoons 2CO + 2H_2 \quad ; \Delta H^0_{298\,K} = +247.4 \text{ kJ/mole} \quad (2.1)$$

$$CO_2 + H_2 \rightleftharpoons CO + H_2O \text{ (Reverse Water Gas Shift)} \quad ; \Delta H^0_{298\,K} = +41.4 \text{ kJ/mole} \quad (2.2)$$

2.3 CARBON DIOXIDE REFORMING OF METHANE (CDRM)

A number of studies have been performed on dry reforming of methane. Some of them have compared the conversion of the reactants and the yield of product in various ranges of conditions of temperature and pressure. For dry reforming of methane different types of reactors are used such as packed bed, fluidized bed, and membrane reactors. Also, Different catalyst materials and supports are used for this reaction and many efforts have been focused to develop the catalyst activity, selectivity, and resistance to deactivation (Cornaglia *et al.*, 2004). According to the reaction, the production of water through the reverse water gas shift reaction and some other side reactions in dry reforming of methane will limit the maximum yield of products, i.e. hydrogen and CO.

It is also reported that the major problems for catalyst deactivation in dry reforming reaction are carbon formation and sulphur poisoning. These problems are

preventing CDRM reaction technology from large-scale industrial application. The CALCOR and SPARG processes are currently known as the two commercial processes using CDRM reaction. The following sections briefly describe these processes (Teuner et al., 2001 and Udengaard et al., 1992).

2.3.1 CALCOR PROCESS

Since carbon monoxide is required as raw material for different applications, therefore various processes were developed for CO production. The limitation in transporting CO due to its toxicity and economical aspects, the on-site production of CO is desired. The standard CALCOR process is designed to produce CO under low pressure and high temperature using catalytic reforming of methane or liquefied petroleum gas (LPG). Figure 2.2 shows a schematic of the process as developed by Teuner *et al.* (2001).

In order to protect the catalyst, the feed has to be desulfurized before mixing with CO_2. Then mixture of CH_4 and CO_2 is passed through the reformer which is charged with reforming catalyst. The product consists of syngas, H_2O, CO_2, and traces of CH_4. The syngas is then cooled down to ambient temperature to recover CO_2. Finally, in the CO purification unit, H_2, CH_4 and traces of CO_2 are removed from carbon monoxide. The recovered CO_2 is recycled to the feed line for further use and the tail gas from the purification step is burned as fuel.

2.3.2 SPARG PROCESS

To produce synthesis gas with the H_2/CO ratio lower than steam reforming product, the sulfur passivated reforming process was designed (Udengaard *et al.*, 1992). The process was commercially developed in Sterling Chemical Inc. (Texas City, USA) in 1987. In order to achieve lower H_2/CO ratio, a part of steam in the reforming process is replaced by CO_2. Therefore, H_2/CO ratio lower as compared to steam reforming is obtained to be used in the synthesis of acetic acid, dimethyl ether, and oxo-alcohols. In SPARG process, due to adding CO_2 to the process, the possibility of increasing carbon formation and catalyst deactivation is minimized by introducing partially sulfur-poisoned reforming catalyst which is mainly nickel based.

2.3.3 CATALYSTS FOR DRY REFORMING REACTION

Different catalyst materials and supports are used for dry reforming of methane. Many efforts have been focused to develop the catalyst activity, selectivity, and resistance to catalyst deactivation (Cornaglia *et al.*, 2004). It is generally known that the transition metals are used for catalytic carbon dioxide reforming of methane. Researchers have used the catalysts such as Ni (Bradford *et al.*, 1996), Pt (Bradford *et al.*, 1998), Pd (ErdoÈhelyi *et al.*, 1994), Rh (Zhang *et al.*, 1996), and Ir (ErdoÈhelyi *et al.*, 1997).

A catalyst is usually composed of an active element, a promoter, and a support. In our research group, Zhang *et al.* (2007) found that the Ni-Co/$AlMgO_x$ bimetallic catalyst which was produced by precipitation method from Ni, Co, Al, and Mg exhibited an excellent performance on carbon dioxide reforming of methane. The developed

catalyst not only has a higher activity, but also because of its resistance to carbon deposition has a better stability as compared to the other Ni-Me bimetallic catalysts (Me = Fe, Cu, and Mn). Also, the Ni-Co catalyst has the higher surface area and the lower pore diameter in contrast the other Ni-Me bimetallic catalysts. Zhang was able to obtain higher conversion of the reactants by using this catalyst (Zhang *et al.*, 2007).

Section 2.4 will describe the method which will lead to the selection of this catalyst.

2.3.4 HYDROGEN AND SYNGAS PRODUCTION THROUGH CDRM REACTION

Yaw and Amin (2005) found that equilibrium compositions of the reaction improved from 600 K to 1000 K, but the effect of temperature above the 1000 K was insignificant. They also found that a lower CO_2/CH_4 ratio of unity was favourable in order to produce syngas besides reducing the water formation as a product of side reaction (RWGSR). Although they reported that the higher CO_2/CH_4 feed ratio above unity, the higher H_2 and CO yields, but higher occurrence of side reaction (RWGSR). For these approaches, they used multi-reaction thermodynamic equilibrium (MTE) method, and minimization of Gibbs free energy using Lagrange Undetermined Multiplier (LUM) method. Figure 2 and Figure 3 of Yaw and Amin (2005) paper showed the results for MTE and LUM, respectively.

Tsai and Wang (2008) worked on thermodynamic equilibrium prediction for natural gas dry reforming in a thermal plasma reformer. By using the HSC Chemistry 5.1® software, they tested temperature in the range of 500-1150 ˚C and CH_4/CO_2 flow ratios of 1/1, 1/1.25, 1/1.5, 1/1.75, and1/2. They found that the optimum operating

conditions for temperature and CO_2/CH_4 flow ratio were 850 ˚C and was 1.25, respectively.

Aparicio (*et al.,* 2002) calculated the theoretical conversion of the reaction by using equivalent volume proportion of CH_4 and CO_2 from Gibbs free energy values of the reactants and products at different temperatures as shown in Figure 5 of Aparicio's (*et al.,* 2002) report.

Múnera *et al.* (2003) and Cornaglia's (*et al.,* 2004) studied the CDRM reaction in a plug flow reactor and a dense Pd/Ag membrane reactor. The catalyst used was Pt/La_2O_3 and Rh/La_2O_3. They found that Rh/La_2O_3 was more stable than Pt/La_2O_3, and the highest conversion was achieved by the membrane reactor. As shown in Figure 3 of Cornaglia's (*et al.,* 2004) paper, they obtained the highest conversion of 34% by using Rh/La_2O_3 (containing 0.6% of Rh) in a membrane reactor.

Zhang *et al.* (2011) studied "in-situ synthesis of nickel modified molybdenum carbide catalyst" for CDRM reaction. They have observed up to 83% of CH_4 93% of CO_2 conversions for the Ni-Mo_2C catalysts that were in-situ synthesized in CH_4/CO_2 and CH_4/H_2 from $NiMoO_x$. Also, they have obtained the H2/Co ratio of 0.54 in a period of 35 h (at 800 °C).

Guo *et al.* (2004) examined Ni/Al_2O_3 and $Ni/MgAl_2O_4$ for CDRM reaction. Their conditions were GHSV of 500 $ml^{-1}g^{-1}h^{-1}$, CH_4/CO_2 ratio of 1 and T of 1023 °C. They observed methane conversion of 31.8 % and 85.3 % using Ni/Al_2O_3 and $Ni/MgAl_2O_4$ catalyst, respectively. Also, they reported that continuous catalyst deactivation was found for both Ni/Al_2O_3 and $Ni/MgAl_2O_4$ catalyst.

Bouarab *et al.* (2004) reported that supported Co catalysts (Co/SiO_2, $Co/5\%MgO\text{-}SiO_2$, $Co/35\%MgO\text{-}SiO_2$) gave better results in comparison with Ni in terms of carbon formation. However, they could not reach to a methane conversion over 42.7% using $Co/35\%MgO\text{-}SiO_2$ catalyst.

2.3.5 Deactivation of reforming catalyst

The deactivation of CDRM reaction catalysts is mainly due to losing the metal active sites from the available surface area of the catalysts. The problem may be caused by coke formation or sintering of the metal active sites. Because of the mechanism of CDRM reaction, the main reason for catalyst deactivation is carbon formation. Therefore various efforts have been done to develop a catalyst with noticeable stability while reducing carbon formation. Our research group has developed $Ni\text{-}Co/AlMgO_x$ bimetallic catalyst for CDRM reaction (Zhang *et al.*, 2007). Zhang reported that the Ni-Co bimetallic catalyst with Ni/Co ratio of 1 did not show any carbon formation after 250 h TOS. For industrial use, the natural gas is mainly used as the feedstock for CDRM reaction. The natural gas generally contains sulphur compounds, which may deactivate the catalyst through sintering. Therefore, it is desired to study the effects of sulphur compounds on the catalyst which may be used for CDRM reaction.

2.4 Catalyst Design

This section includes the methods of the $Ni\text{-}Co/AlMgO_x$ catalyst selection and preparation. The selection is briefly described through the procedure presented by

Dowden *et al.* (1968) According the procedures of Dowden *et al.* (1968) the following steps are used as shown in Figure 2.2.

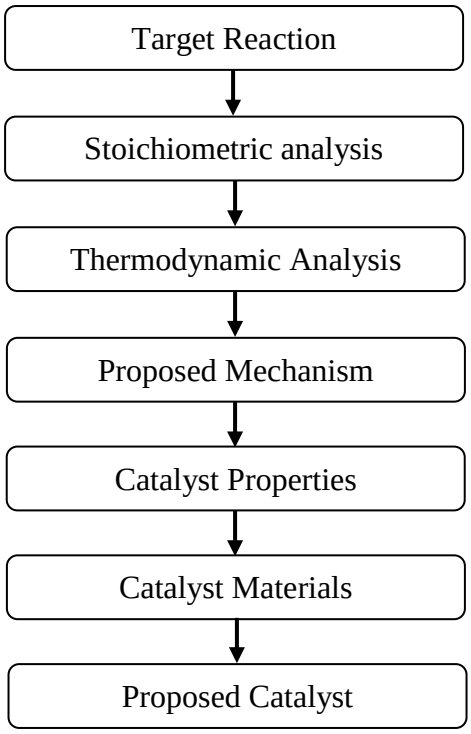

Fig.2.2 Steps in catalyst design (Dowden *et al.* 1968)

2.4.1 TARGET REACTION

CO_2 reforming of methane is used as the target reaction to produce synthesis gas:

$$CH_4 + CO_2 \rightleftharpoons 2CO + 2H_2; \qquad \Delta H°_{298\ K} = +247\ kJ/mole \quad (2.3)$$

The reaction is highly endothermic, and at temperature lower than 916 K the Gibbs free energy change is positive ($\Delta G^0_{T<916k}>0$). Therefore, temperature higher than 916 K should be selected for the reaction to take place. Also, it should be considered that at

higher temperature the possibility of reaction sites will be increased. According to literature (Bradford and Vannice, 1999), commonly used temperature for this reaction is 1023 K.

2.4.2 STOICHIOMETRIC ANALYSIS

Probable reactions are listed below (Richardson 1989):

1- primary reactant reactions

2- reactant self-interactions

3- reactant cross-interactions

4- reactant-product reactions

5- product-product reactions

2.4.3 THERMODYNAMIC ANALYSIS

Regarding thermodynamic analysis the equilibrium figures; such as composition vs. temperature, equilibrium constant vs. temperature, composition vs. pressure, conversion vs. temperature, H_2 selectivity vs. temperature, effects of inert gas, are considered which facilitating the prediction of reaction performance.

2.4.4 PROPOSED MECHANISM

For CDRM reaction, methane dissociation is believed to be one of the initial steps (Hickman and Schmidt, 1993). Also, it is reported that at equilibrium the methane adsorption on the surface of the catalyst leads to the methane cracking which is the rate determining step (Schuurman et al., 1998; Tsipouriari and Verykios, 1999; 2001). Bitter

et al. (1997, 1998) observed that CO_2 can dissociate into Oxygen and CO that are adsorbed on the support site. Solymosi (1991) reported the CO-S releases to gas phase CO immediately.

The reaction steps are briefly mentioned in Table 2.4 (Zhang, 2008).

Table 2.4 Proposed mechanism for carbon dioxide reforming of methane

Reaction	Description	
$CH_4 + M^* \rightleftharpoons CH_4\text{-}M$	CH_4 adsorption, equilibrium step	(2.4)
$CH_4\text{-}M \rightarrow C\text{-}M + 2H_2$	CH_4 cracking, Rate Determining Step (RDS)	(2.5)
$CO_2 + 2S^* \rightleftharpoons CO\text{-}S + O\text{-}S$	CO_2 dissociative chemisorption	(2.6)
$C\text{-}M + O\text{-}S \rightarrow CO + M + S$	Oxidation step, Rate Limiting Step (RLS)	(2.7)
$CO_2 + C\text{-}M \rightarrow 2CO + M$		(2.8)

***** M and S orderly stand for Metal active site species and Support active site species.

The rate limiting step (RLS) in each reaction is the step which controls the rate of the reaction. Kroll *et al.* (1996) suggested for CDRM reaction, that the reaction between M-C species and activated S-CO_2 can be assumed as the rate limiting step. It is believed that carbon deposition is the dominant catalyst deactivation reason for the catalysts which are used for CDRM reaction. Carbon deposition occurs when the rate of carbon species removal is lower than that of carbon species accumulation. Therefore, oxidation step (Eq. 2.7) is RLS and CH_4 dissociation is RDS. In addition, CO_2 may react directly with C-M species to form CO (Erdohelyi *et al.*, 1994; Schuurman *et al.*, 1998).

Based on the above-mentioned description, a surface reaction mechanism is proposed for catalytic CO_2 reforming of methane. Figure 2.3 shows the schematic of proposed mechanism (Zhang, 2008).

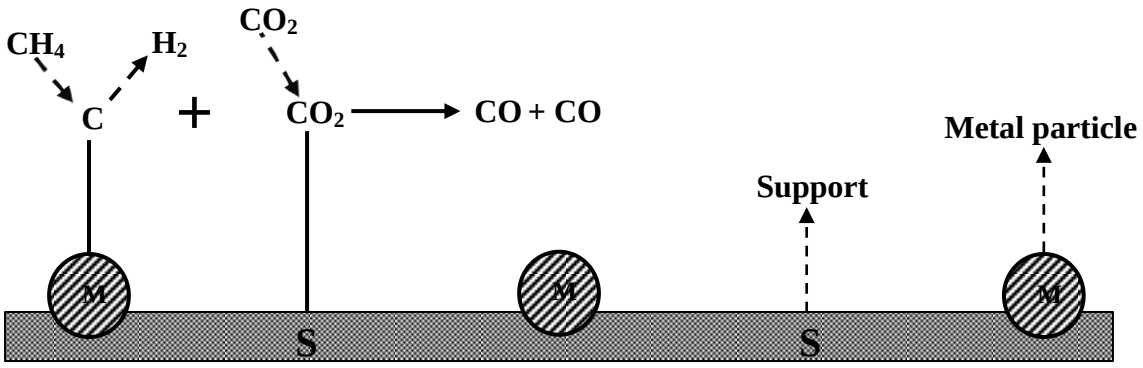

Fig. 2.3 Proposed surface mechanism for CDRM reaction on metallic catalyst (Zhang, 2008).

2.4.5 DESIRED CATALYST PROPERTIES

In general, if a catalyst has a higher activity, a better selectivity, and more stability then it will be closed to an ideal catalyst. A catalyst can enhance the rate of a reaction by accelerating the rate of RLS. On the other hand, a good selective catalyst produces the desired products more as compared to the potential products that can produce form the possible side reaction(s). Furthermore, if a catalyst has more life-time and lower rate of deactivation, then it will be a more stable catalyst.

In accordance to the proposed mechanism, it is desired that the catalyst enhance the ease of RLS occurrence. In our reaction system the side reaction is Reverse Water Shift Gas Reaction (RWSGR):

$CO_2 + H_2 \rightleftharpoons CO + H_2O$; $\Delta H°_{298\,K} = 247$ kJ/mole (2.9)

Therefore, a good catalyst should affect RWSGR and carbon formation reactions. The major problems of catalyst deactivation in CO_2 reforming of CH_4 are carbon deposition on surface, sintering, and metal oxidation. The desired properties of the catalyst, according to aforesaid mechanism and analysis, should have the following description:

D1- To increase dissociation of methane to CH_x species and to move out H atom from intermediate species to form hydrogen, the catalyst should have dehydrogenation sites on the surface.

D2- To remove C species obtained from the decomposition of methane on the surface, the catalyst should have surface sites which can adsorb CO_2 in order to enhance contribution of CO_2 on surface reaction.

D3- To have higher reaction rate, the catalyst should have the adjusted D1 and D2 sites for assisting the reaction between C and the activated CO_2.

D-4 Because of the high temperature of reaction (1023 K), the catalyst should have thermal stability in order to preserve its physical properties.

2.4.6 CATALYST SELECTION

The major objectives for designing the catalyst are in general:

1- Recognition of the required properties of catalyst for CO_2 reforming of CH_4,
2- Composition of desired catalyst,
3- Selecting the catalyst materials,
4- Low cost and availability.

A catalyst is usually composed of active element, promoter, and support. In Table 2.5, the most commonly used metals used in catalysts are shown (Anderson, 1975).

Table 2.5 Physical data of common metals used as catalyst

Metal	Atomic weight	Crystal structure	Lattice parameter (nm)	Neighbour atomic distance (nm)	Melting point (K)
Al	26.98	f.c.c.	0.404	0.286	1033
Ba	137.34	b.c.c.	0.501	0.434	998
Cr	52.00	b.c.c.	0.289	0.249	2163
Co	48.93	f.c.c.	0.355	0.251	1768
Cu	63.54	f.c.c.	0.361	0.255	1356
Ir	192.20	f.c.c	0.383	0.271	
Fe	55.85	b.c.c.	0.286	0.248	1808
La	138.91	h.c.p.	0.372; 0.606	0.371	1193
Mg	24.31	h.c.p.	0.321; 0.521	0.320	924
Mn	54.94	Complex	-	-	1517
Mo	95.94	b.c.c.	0.314	0.272	2883
Ni	58.71	f.c.c.	0.352	0.249	1726
Pd	106.40	f.c.c.	0.388	0.275	1825
Pt	195.09	f.c.c.	0.392	0.277	2042
K	39.10	b.c.c.	0.531	0.462	337
Re	186.20	h.c.p.	0.276; 0.445	0.274	3453
Rh	102.91	f.c.c.	0.380	0.268	2239

Table 2.5 Continued

Metal	Atomic weight	Crystal structure	Lattice parameter (nm)	Neighbour atomic distance (nm)	Melting point (K)
Ru	101.07	h.c.p.	0.270; 0.427	0.267	2523
Ag	197.87	f.c.c.	0.408	0.288	1234
Na	22.99	b.c.c.	0.428	0.371	371
Ti	47.96	h.c.p.	0.295; 0.468	0.293	1948
W	183.85	b.c.c.	0.316	0.274	3683
V	50.94	b.c.c.	0.302	0.263	2163
Zn	65.37	h.c.p.	0.266; 0.494	0.266	692
Zr	91.22	h.c.p.	0.322; 0.512	0.319	2125

It is well known that the transition metals are mainly used for dry reforming reaction. Trimm (1980) has reported the order of activity of metal catalysts that are used for hydrogenation or dehydrogenation as follows:

Ru, Pd, Ir, Pt, Rh > Ni, Co, Fe > W, Cr-Cu

From another point of view, the stability of number of metals increases in the following order (Satterfield, 1991):

Cu < Au < Pd < Ni < Co < Pt < Rh < Ir

The industry prefers non-precious metal-based catalyst for their lower cost and ease of availability. Ni is chosen because of its high activity and ease of use. The

deactivation of Ni is the main area of concern. An optimum selection of promoter and support may resolve the deactivation related issue of Ni. Takanabe *et al.* (2005) found that a homogeneous alloy of Ni and Co and a small Ni substitution of Co increase the activity, stability, and resistance to metal oxidation.

From thermodynamic point of view in order to achieve more conversion of reactants, the reaction should take place at high temperatures. Therefore, the support should be composed of high melting point materials to enhance the resistance to sintering by producing a stable surface (D4). The stability against sintering will decrease in the following order (Satterfield, 1991):

$$MgO > Al_2O_3 > SiO_2 > TiO_2$$

Therefore MgO is selected because of its high melting point (3346 K) and stability against sintering. Also, since MgO has more basic sites, it can enrich the activation and participation of acidic CO_2 in the reaction (D2). The major problem of MgO is its low surface area. To increase the total surface area, Al_2O_3 was selected because of having large surface area to be combined with MgO. Therefore, $AlMgO_x$ has a high thermal stability due to MgO, and high surface area due to Al_2O_3. Also, by choosing the optimum catalyst preparation method, we can achieve the purpose of D3 (Zhang, *et al.*, 2007). Therefore, it was decided to prepare Ni-Co/$AlMgO_x$ bimetallic catalyst for CO_2 reforming of CH_4.

2.5 CATALYST PREPARATION METHODS AND PROCEDURES

Usually, the industrial catalysts are produced by using either impregnation or precipitation method. Each method has its own advantages and disadvantages comparing with the other method. The following sections describe both precipitation and impregnation methods.

2.5.1 PRECIPITATION METHOD

This method is commonly comprised of a solution of aqueous metal salt which is combined with a reagent to cause precipitation (co-precipitation) of an insoluble metal species. After that the filtration and washing, drying, calcination, and forming of the catalyst are carried out to finally produce the catalyst. The following steps are used for the participation procedure:

1) **Solution Preparation:** Metal solution is prepared by dissolving the metal (Ni, Co, Al, and Mg) nitrates in di-ionized water. The solution made is based on the composition of the desired catalyst.
2) **Precipitation:** The precipitation of metal in solution is carried out by adjusting the pH of the solution. This is done by adding ammonium hydroxide (NH_4OH) as a reagent.
3) **Filtering and washing:** To remove undesired ions and water, the solution is washed and filtered at room temperature. The washing step is stopped when the pH value of the water after washing reaches to 7. The phenomena can be observed from the color of the after-wash water which needs to be clear. Through this step, a precipitated cake is produced.

4) **Drying:** To remove the water content in the precipitated cake, the cake is dried in an oven at 120 °C for overnight (i.e. 16 h minimum). The presence of water in the catalyst may lead to severe effects on the catalyst.

5) **Calcination:** This is one of the most important pre-treatment steps for making the catalyst. The dried catalyst is generally calcined in an oven at temperatures slightly higher than the reaction temperature. The catalyst is calcined at 850 °C in air for 6 h.

6) **Forming operation:** after calcination, the catalyst is grinded and sieved to particle sizes between No.45 and No.60 U.S.A standard testing sieves (A.S.T.M. E-11 specification) which correspond to catalyst size between 250 and 355 micrometer. The selection of the catalyst size is based on a smaller pressure drop in the packed bed reactor.

Figure 2.4 briefly shows the precipitation procedure. Also, Figure 2.5 Shows a schematic of the experimental set-up which used for catalyst production.

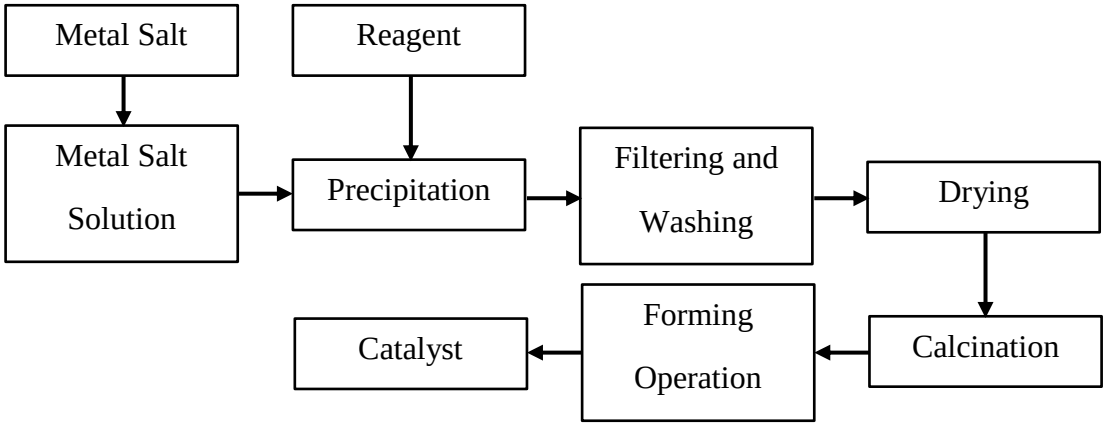

Fig. 2.4 Brief chart of precipitation procedure

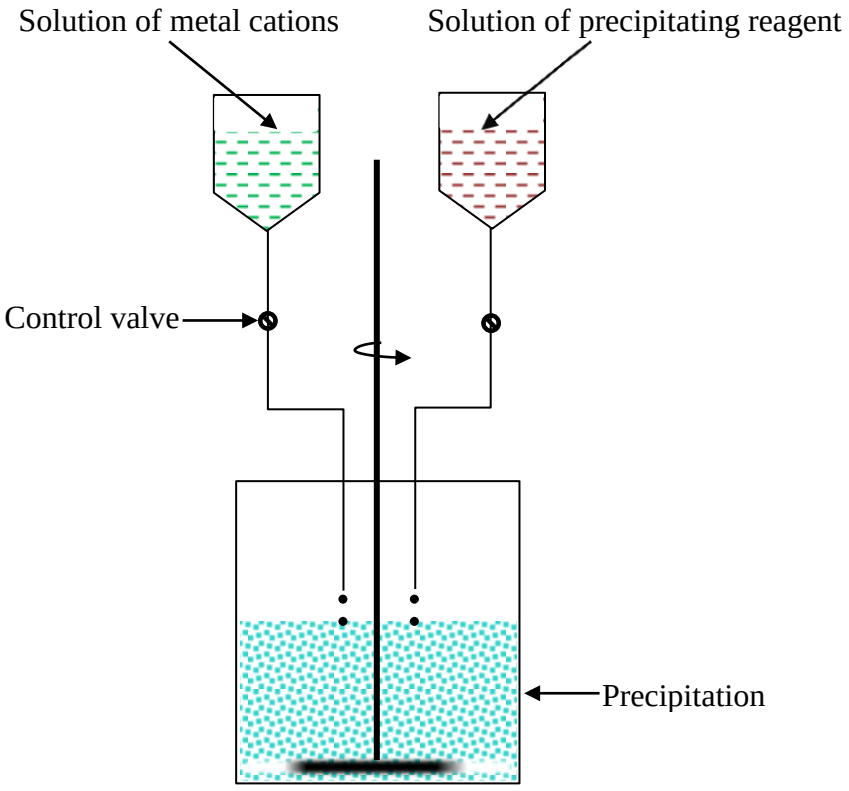

Fig. 2.5 Schematic of the experimental set-up for catalyst preparation.

Catalysts which are prepared with the precipitation method have some advantages as compared to the impregnated method. The major advantages can be generalized as:

1) On molecular level the catalyst components form a uniform mixture.
2) Catalyst has uniform distribution of active species.

However, precipitation method may be costly than the impregnation method because a significant amount of active components remain inside the catalyst bulk in comparison with the impregnated method. Also, it is hard to produce a catalyst with very small particle size and surface area greater than 200 m^2/g (Wijngaarden *et al.*, 1998).

2.5.2 IMPREGNATION METHOD

In this method, a support is made first which is based upon the participated procedure. Then the support is dipped into excess amount of solution of metal salts, or the metal solution is sprayed on the support. The metal uptake by the support is the sum of the solution occluded inside the pores of the support and the material adsorbed on the pore surface. The catalyst is finally produced after drying and calcination. Figure 2.6 shows the procedure of impregnation method.

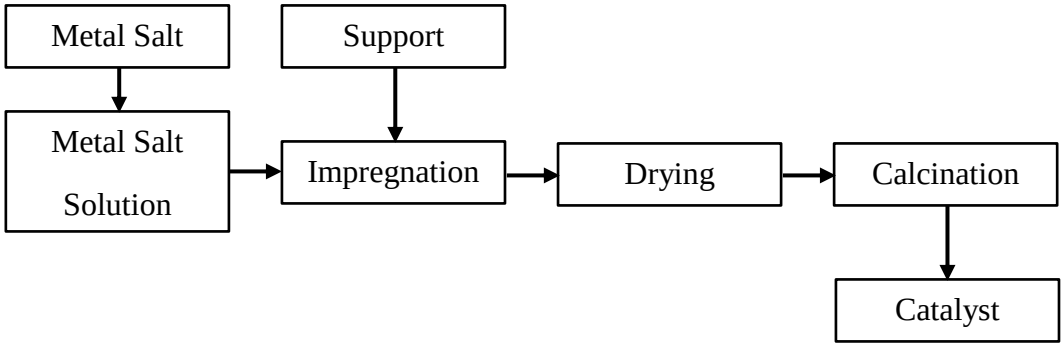

Fig. 2.6 Summary chart of impregnation procedure

The major advantages of impregnation method are:

1) Ability to use commercially available catalyst
2) Lower cost than precipitation method, especially in case of valuable metals,
3) Separation between the metal active phase and the support phase is clear

Based on the above description a comparison is made in Table 2.6 between the impregnation method and the precipitated method.

Table 2.6 Comparison chart of catalyst preparation method

	Description	Impregnation method	Precipitation method
1	Molecular scale mixing of catalyst components	Difficult	Easy
2	Uniform distribution of multi-active components	Difficult	Easy
3	Surface area up to 200 m^2/g	Easy	Easy
4	Surface area more than 200 m^2/g	Easy	Difficult
5	High metal loading	Difficult	Easy
6	High metal dispersion	Easy	Easy
7	Instrument availability	Easy	Easy
8	Relative cost	Easy	Difficult

2.6 KNOWLEDGE GAP

The Ni-Co bimetallic catalyst prepared by precipitation method in our research group is known as a novel and new-developed catalyst for CDRM reaction. Based on the previous work and literature review the following knowledge gaps are concluded toward commercialization:

1- Effect of preparation methods of Ni-Co/$AlMgO_x$ bimetallic, Ni/$AlMgO_x$ monometallic and Co/$AlMgO_x$ monometallic catalyst performance on CDRM reaction need to be evaluated.

2- Effect of various Ni/Co ratios on performance of Ni-Co/$AlMgO_x$ bimetallic catalyst running CDRM reaction has not been studied.

3- Performance of the Ni-Co/$AlMgO_x$ bimetallic, Ni/$AlMgO_x$ monometallic and Co/$AlMgO_x$ monometallic catalyst while poisoned by H_2S during CDRM reaction has not been investigated yet.

2.7 RESEARCH OBJECTIVES AND THESIS SCOPE

The following questions will be answered as the specific objectives:

- What are the effects of different Ni/Co ratios on the activity and stability of the Ni-Co bimetallic catalyst for CDRM reaction?
- What are the effects of the Ni monometallic and Co monometallic catalysts for CDRM reaction?
- What are the effects of preparation method on the Ni-Co/$AlMgO_x$ bimetallic, Ni monometallic and Co monometallic catalysts for CDRM reaction?
- How the Ni-Co/$AlMgO_x$ bimetallic, Ni monometallic and Co monometallic catalysts prepared by precipitation and impregnation with various Ni/Co ratios will act for CDRM reaction if the catalysts are poisoned by H_2S? Which catalyst(s) have the best performance after the H_2S poisoning?

CHAPTER 3: EXPERIMENTAL SET-UP AND PROCEDURE

This chapter describes the reactor set-up and the experimental procedure used for the catalyst activity for CDRM reaction.

3.1 EXPERIMENTAL PROCEDURE

3.1.1 CATALYST PREPARATION PROCEDURE

According to Zhang's observations Ni-Co bimetallic, Ni monometallic, and Co monometallic catalysts can be prepared by both precipitation and impregnation methods (Zhang, 2008). Different catalysts were prepared in order to observe the effects of preparation methods and various Ni/Co ratios. In the following sections, the term "catalyst" is used for Ni-Co/$AlMgO_x$ bimetallic catalyst. (Zhang *et al.*, 2007)

In preparing precipitated catalysts, all of the Ni-Co/$AlMgO_x$ catalysts (5-7 metal wt %) were prepared by using nickel nitrate (hexahydrate; Alfa Aesar), cobalt nitrate (hexahydrate; Alfa Aesar), aluminum nitrate (nanohydrate; Alfa Aesar), and magnesium nitrate (hxahydrate; Alfa Aesar). The ammonium hydroxide (EMD Chemicals) was used as a reagent. After preparation, the obtained product was washed and filtered with 2 L of de-ionized water, and then dried and calcined in air at 120 ˚C (overnight) and 850 ˚C (for 6h), respectively. Finally, the product was grinded and sieved to get the desired catalyst.

In order to prepare impregnated catalysts, the Al-Mg support was prepared first. The support was prepared by using the precipitation technique, and then the metal solution was added to it. The important part in this preparation was the volume of the metal solution that is added to the support. Several ways are available to find the amount of metal solution that is required to be added to the support. One of the methods adopted after support preparation and calcination was that, the required volume of the metal solution measured by adding water to the known amount of support. The procedure was the addition of water on the support until the first drop of water appeared on the surface of the support which indicated that the catalyst support was saturated and was not able to absorb water anymore. At this point the support and the water were mixed together like a paste. This condition was indicative of the amount of metal solution that was required by the support. As an example, for each gram of prepared support 1.2 mL of de-ionized water was added.

Based on the desired Ni/Co ratio, the metal solution was prepared and sprayed onto the surface of the prepared support. The catalysts were then dried and calcined to obtain the desired catalyst.

Ni-Co/$AlMgO_x$ bimetallic catalysts were prepared by both precipitation and impregnation methods using different Ni/Co ratios of 0.5, 1, and 2. Also, Ni/$AlMgO_x$ and Co/$AlMgO_x$ monometallic catalysts were prepared using both impregnation and precipitation methods. In Tables 3.1 and 3.2, the names and compositions of the prepared catalysts are summarized.

Table 3.1 Chemicals and amounts used for preparation of catalysts by precipitated

Name	Intent Ni/Co	$Ni(NO_3)_2$ (g)	$Co(NO_3)_2$ (g)	$Al(NO_3)_3$ (g)	$Mg(NO_3)_2$ (g)	Water (mL)
CopCat-Co6	Only Co	-	6.0000	50.0005	124.0004	500
CopCat-Ni1Co4	0.5	2.0001	4.0003	50.0004	124.0004	500
CopCat-Ni2Co4	1	3.0008	3.0008	25.0000	124.0006	600
CopCat-Ni3Co2	2	3.9198	1.9600	48.9923	121.5005	500
CopCat-Ni4	Only Ni	6.0000	-	50.0004	124.0005	500

Table 3.2 Chemicals and amounts used for preparation of catalysts by impregnation

Name	Intent Ni/Co	$Ni(NO_3)_2$ (g)	$Co(NO_3)_2$ (g)	$AlMgO_x$ (g)	Water (mL)
ImpCat-Co5	Only Co	-	0.7974	2.5300	3
ImpCat-Ni2Co3	0.5	0.2649	0.5267	2.5030	3
ImpCat-Ni3Co3	1	0.3960	0.3947	2.5030	3
ImpCat-Ni3Co2	2	0.5278	0.2633	2.5020	3
ImpCat-Ni5	Only Ni	0.7913	-	2.5020	3

3.1.2 CATALYST TEST PROCEDURE

After preparing all the Ni-Co/$AlMgO_x$ bimetallic and monometallic catalysts by using precipitation and impregnation methods the following analytical and experimental procedures were used for each catalyst:

1) BET surface area of all the samples was analyzed by using the prepared catalysts in powder form. The BET was re-analyzed for couple of catalysts to make sure the reproducibility of the results.
2) ICP analysis was done to observe the amount of Ni, Co, Al, and Mg in the catalyst. Also, the analysis was repeated for couple of catalysts for reproducibility.
3) XAS analysis of the catalysts was done by professor Hui Wang at ANL after catalyst reduction (H_2 (3.5%) + He at 750 °C in a cell reactor).
4) The activity test was done on each catalyst by carrying out the reaction of carbon dioxide reforming of methane. A quartz tube was used as the reactor.
5) After the activity test, the sulfur poisoning was carried by using 30 ppm of H_2S as a catalyst poison.
6) The results from above were analyzed and are reported in the subsequent sections.

3.2 CATALYST CHARACTERIZATION ANALYSES

3.2.1 BET SURFACE AREA

BET surface area is known as an important property for many kinds of materials and especially solid catalysts. B.E.T. (or BET) stands for Brunauer, Emmett, and Teller,

the scientists who proposed the theory for measuring the surface area (Brunauer *et al.*, 1938). The concept of the theory is based on the Langmuir theory. Different methods are used to calculate and measure the BET surface area, but most of them are based on isothermal adsorption of nitrogen. The BET is measured by the use of nitrogen adsorption/desorption isotherms at liquid nitrogen temperature and relative pressures. For the experiments, the BET surface area machine form Micromeritics (ASAP 2020, Surface Area and Porosity Analyzer) in Department of Chemical and Biological Engineering, University of Saskatchewan was used.

3.2.2 ICP ANALYSIS

Inductively Coupled Plasma or ICP is an analytical technique used for elemental determination. By using ICP, the compositions of prepared catalyst are analyzed. The ICP analysis was done with analysing the catalysts in the Department of Geology, University of Saskatchewan using ICP-MS machine from Perkin Elmer (Nexion 300D).

3.2.3 XAS ANALYSIS

To observe the electronic arrangement and/or local geometry of the catalyst, X-ray Absorption Spectroscopy (XAS) is a well-developed technique. The experiment usually is performed in a synchrotron by using X-ray beam-lines.

To further understand of particle size growth of the catalysts during the reduction condition, XAFS and EXANS analysis were analyzed by professor Hui Wang by using the Advanced Photon Source (APS) synchrotron at Argonne National Laboratory (ANL).

3.3 EXPERIMENTAL SET-UP OF CATALYST TESTING

Three sets of experiments were carried out for CDRM reaction. The catalyst activity test was used to determine the most active catalyst among the prepared catalysts. The life-time test was conducted to determine the stability of the optimum catalyst. Finally the catalyst poisoning test was carried out to determine the regeneration trend of the prepared catalysts.

3.3.1 CATALYST ACTIVITY TEST

The catalysts were evaluated in a fixed bed quartz reactor with 6 mm ID and 30 cm in length. The test was carried out until the catalyst activity became stable for methane conversion. In order to compare the effects of both Ni/Co ratio and preparation method, a 0.02 g of each catalyst was mixed with 0.48 g of quartz sand. The average particle size of the catalysts was 300 nm. The catalysts were loaded in the middle of the reactor. Before the testing, the catalysts were reduced in presence of H_2:N_2 with ratio of 1:4 at 800 °C for 4 h. For reduction H_2 (99.9% purity, Praxair Canada Inc.), and N_2 (99.9% purity, Praxair Canada Inc.) were used. The testing was carried out at 710 °C and GHSV (Gas Hour Space Velocity) of 558,000 ($mL/g_c.h$). The reactant gas consisting of an equimolar mixture of N_2 (99.9% purity, Praxair Canada Inc.), CH_4 (99.2% purity, Praxair Canada Inc.) and CO_2 (99.9% purity, Praxair Canada Inc.) was injected to the reactor. The product gas was analysed by an on-line Agilent 6890N GC, equipped with TCD and a GS-GASPRO capillary column (J&W Scientific) of 60 m in length and 0.32 mm of inner diameter using GC ChemStation software (Rev.b.04.02(96)). Helium (Ultra high purity 5.0, PRAXAIR Canada Inc.) was used as

the carrier gas. Finally, the obtained data was analyzed, based on the procedure and equations which are explained in section 3.4.

3.3.2 CATALYST LIFE-TIME TEST

The Ni-Co/$AlMgO_x$ bimetallic catalyst as prepared by precipitation method was evaluated for life-time test for 65 days in the same set-up as explained in section 3.3.1. The reaction conditions were different from the catalyst activity test. The catalyst load was 0.05 g which was mixed with 0.45 g of sand. The average particle size was 300 nm. The catalyst was loaded in the middle of the reactor and reduced at 800 °C for 4 h in presence of H_2:N_2 mixture with the ratio of 1:4. The testing was carried out at 710 °C and GHSV (Gas Hour Space Velocity) of 110,000 ($mL/g_c.h$) with equimolar flow rates of CH_4, CO_2 and N_2.

3.3.3 H_2S POISONING TEST

Running the tests three sections are distinguished called “before poisoning” (P-1), “during poisoning” (P-2), and “after poisoning” (P-3). The reaction conditions for the P-1 and P-3 sections were the same as explained in section 3.3.1. For the P-2, the flow rates of the gases were adjusted in order to keep the equimolar mixture of CH_4, CO_2, and N_2. Depending on instrument limitations, catalyst loadings, and poison availability a certain value of poisonous gas is chosen. The catalysts were poisoned by 30 ppm of H_2S and the temperature of the reaction was kept constant at 710 °C (the beginning of P-2). Then to make sure that all the catalysts are poisoned, the H_2S poisoning was stopped as soon as GC could not recognize the H_2 peak (the end of P-2).

Disappearance of hydrogen peak indicates that the catalyst is totally poisoned with H_2S. Then the flow rates of CH_4, CO_2, and N_2 gases were adjusted to the condition prior to the poisoning (beginning of P-3). It is notable that in this section time zero points to the time at which H_2S was injected to the reactor (beginning of P-2).

3.4 DATA ANALYSIS PROCEDURE

The conversion of reactants and yield of the products are calculated based on the following explained procedure. Consider X_i (volume/volume) obtained as the GC result:

$$X_i = \frac{F_{out},i}{\sum_i F_{out},i} \quad (3.1)$$

where, F_{out}, i is flow rate of component "i" after the reaction (mL/min) and "i" could be CO_2, CH_4, N_2, H_2,or CO.

The flow rate of each component exiting from the rector is calculated based on N_2 which is constant during the reaction. N_2 does not react with the other existing components in the CDRM reaction.

For example the flow rate of product containing methane can be calculated by the following procedure:

$$X_{N_2} = \frac{F_{out},N_2}{\sum_i F_{out},i}, \quad (3.2)$$

$$X_{CH_4} = \frac{F_{out},CH_4}{\sum_j F_{out},i}, \quad (3.3)$$

Dividing Eq. 3.3 by Eq. 3.2:

$$\frac{F_{out,CH_4}}{F_{out,N_2}} = \frac{X_{CH_4}}{X_{N_2}} \rightarrow F_{out}, CH_4 = F_{out}, N_2 \times \frac{X_{CH_4}}{X_{N_2}} \quad (3.4)$$

So, like the above procedure, Eq. 3.4 is generalized for the other component.

$$F_{out}, i = F_{out}, N_2 \times \frac{X_{N_2}}{X_i}, \text{ i: } CO_2, CH_4, N_2, H_2, CO \quad (3.5)$$

where, F_{out}, i means the flow rate of component "i" which is exiting from reactor.

Since N_2 does not react during CDRM reaction, therefore $F_{N_2}^{out}$ is equal to $F_{N_2}^{in}$. The values of X_i are obtained from GC, therefore F_{out}, i can be calculated from Eq. 3.5.

The reactant conversion can be obtained from Eq. 3.6 and 3.7.

$$\text{Methane } (CH_4)\text{conversion}, \% = \frac{(F_{in,CH_4} - F_{out,CH_4})}{F_{in,CH_4}} \times 100 \quad (3.6)$$

$$\text{Carbon Deoxide } (CO_2)\text{conversion}, \% = \frac{(F_{in,CO_2} - F_{out,CO_2})}{F_{in,CO_2}} \times 100 \quad (3.7)$$

where, F_{out}, i means flow rate of component "i" after the reaction (mL/min), and F_{in}, i is flow rate of component "i" before the reaction (mL/min).

To calculate consumption rate of reactants and formation rate of products, the following equations were used:

$$-r_{reactant} = \frac{(F_{in,reactant} - F_{out,reactant})}{m_{catalyst}}, \text{ (mol/g}_c\text{.h)} \quad (3.8)$$

$$r_{product} = \frac{F_{out,product}}{m_{catalyst}} \text{ (mol/g}_c\text{.h)} \quad (3.9)$$

where flow rates are used based on mol/h.

CHAPTER 4: RESULTS AND DISCUSSION

In this chapter the reproducibility of the results are firstly covered. Then a detailed discussion is carried out on the results obtained from ICP, XAS and BET surface area of the prepared catalysts. Also, the effects of Ni/Co ratios and the preparation methods on the activity and selectivity of Ni or Co monometallic and Ni-Co bimetallic catalysts running CDRM reaction are discussed. Following the catalyst tests, the stability of highly performed catalysts was evaluated for 60 days TOS. Finally, the performance of the poisoned catalysts was investigated with CDRM reaction.

4. 1 REPRODUCIBILITY OF THE RESULTS

In order to observe whether the results of the study are reproducible, some of the catalysts were characterized at the second time. The percent difference of two experimental values (x_1 and x_2) is calculated by dividing the absolute difference of them by their average value. Equation 4.1 shows the formula which was used.

$$\text{Diff.} = \left| \frac{x_1 - x_2}{\frac{(x_1 + x_2)}{2}} \right| \times 100, \% \qquad (4.1)$$

For BET surface area analysis, the precipitated CopCat-Ni1Co4 catalyst with (Ni/Co ratio of 0.37) and the impregnated ImpCat-Ni3Co3 catalyst (Ni/Co ratio of 0.97) were selected. The results are shown in Table 4.1.

Table 4.1 Results of repeated BET analysis

Analysis	Try	CopCat-Ni1Co4	Diff., %	ImpCat-Ni3Co3	Diff., %
BET (m^2/g)	x_1	94	5.5	103	1.0
	x_2	89		102	
Pore volume (ml/g)	x_1	0.189	4.9	0.297	1.0
	x_2	0.180		0.300	
Pore size (Å)	x_1	80.4	0.3	115.4	1.8
	x_2	76.9		117.5	

Table 4.1 indicates that the errors of the BET results, pore volume and pore size were significantly negligible.

The ICP analysis was repeated for the impregnated ImpCat-Ni2Co3 catalyst (Ni/Co ratio of 0.52) as presented in Table 4.2.

Table 4.2 Reproducibility results of ICP analysis

ICP analysis	Mg (ppm)	Al (ppm)	Co (ppm)	Ni (ppm)	Mg/Al	Ni/Co
x_1	298262	130774	36707	19050	2.28	0.52
x_2	333000	165000	37600	19400	2.02	0.51
Diff., %	11.0	23.1	2.4	1.8	12.0	1.9

The measured metal content values of the same ImpCat-Ni2Co3 catalyst by ICP analysis are fairly close indicating acceptable measurement error especially in terms of Ni and Co content.

The catalyst activity test for the CopCat-Ni3Co2 (Ni/Co ratio of 1.51) catalyst prepared by precipitation method was repeated on CDRM reaction. The reaction was carried out with the same conditions which described in section 3.3.1. The first 5 h results of both tests are summarized in Table 4.3. Also, Figure 4.1 and 4.2 show reactant conversion and H_2/CO ratio for the first and second runs.

Table 4.3 Repeated catalyst activity test results

Time (h)	CH_4 Conversion, %		Diff.%
	x_1	x_2	
1	52.2	54.8	4.8
2	48.7	51.0	4.6
3	46.5	48.0	3.2
4	43.8	45.2	3.1
5	41.4	42.5	2.6

The methane conversions are significantly close to each other for the selected catalyst (CopCat-Ni3Co2 with Ni/Co ratio of 1.51) in both runs as illustrated in Table 4.3 and Figure 4.1. Also, the calculated H_2/CO ratios are following the same trend in term of reproducibility for both runs. It can be concluded that the CopCat-Ni3Co2 (Ni/Co ratio of 1.51) catalyst showed almost the same performance (2-8% difference) during CDRM reaction implying acceptable results accuracy.

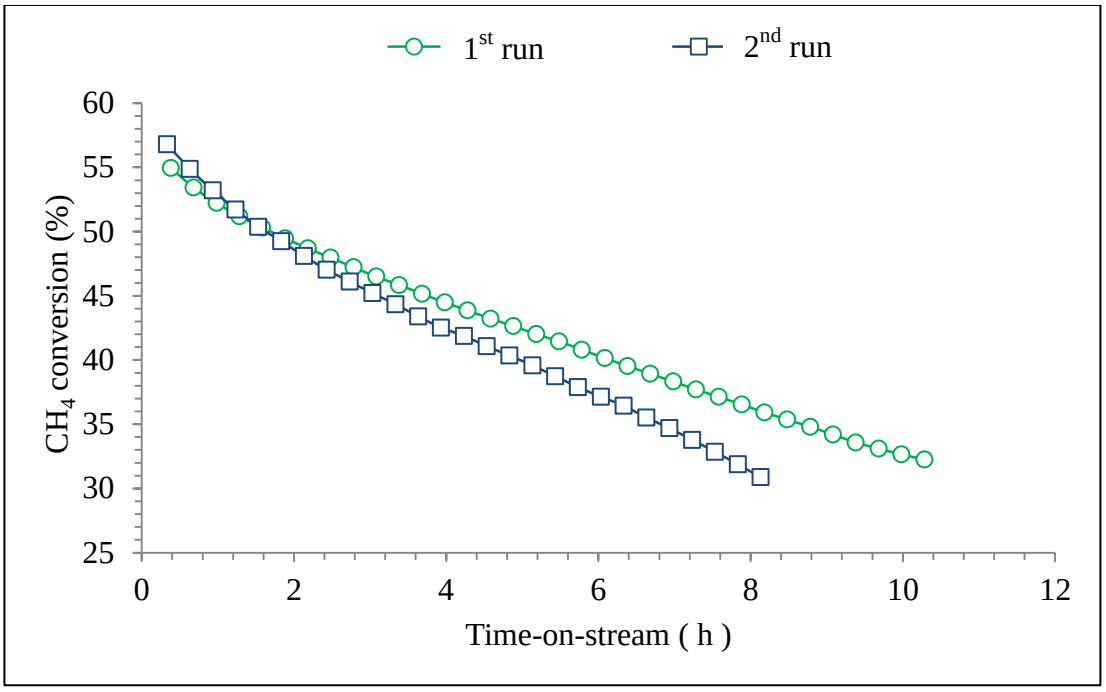

Fig. 4.1 Methane conversion for the repeated catalyst activity test; reaction conditions: 710 °C, 1atm, 558000 mL/g_c.h (GHSV), $CH_4/CO_2/N_2$=1/1/1, catalyst loading of 0.02 g

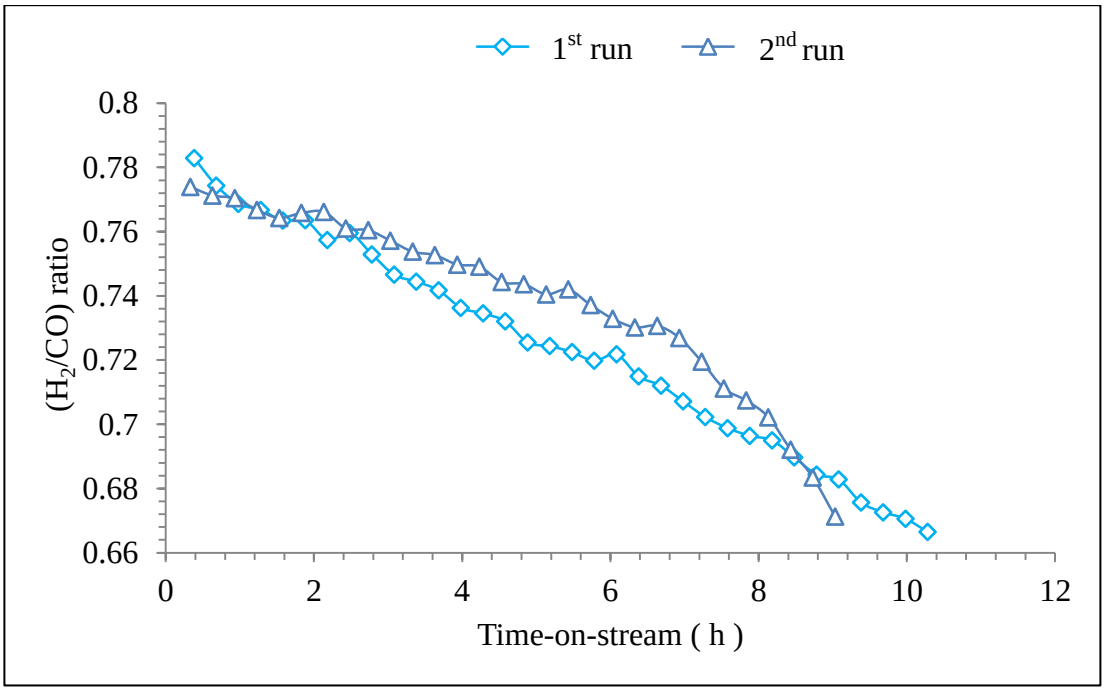

Fig. 4.2 H_2/CO ratio of the repeated catalyst activity test; reaction conditions: 710 °C, 1atm, 558000 mL/g_c.h (GHSV), $CH_4/CO_2/N_2$=1/1/1, catalyst loading of 0.02 g

4.2 CATALYST CHARACTERIZATION

4.2.1 BET SURFACE AREA

Table 4.4 shows BET analysis results of prepared catalyst.

Table 4.4 BET surface area of the prepared Ni-Co/$AlMgO_x$ bimetallic catalyst

Catalyst	BET (m^2/g)	Pore volume (mL/g)	Pore size (Å)
CopCat-Co6	106	0.277	105
CopCat-Ni1Co4	94	0.189	80
CopCat-Ni2Co4	111	0.287	104
CopCat-Ni3Co2	110	0.246	89
CopCat-Ni4	113	0.227	81
Support ($AlMgO_x$)	85	0.226	106
ImpCat-Co5	102	0.296	116
ImpCat-Ni2Co3	124	0.359	116
ImpCat-Ni3Co3	103	0.297	115
ImpCat-Ni3Co2	112	0.328	118
ImpCat-Ni5	114	0.340	119

Table 4.4 indicates that the difference between BET surface areas of all the prepared catalysts is negligible. BET surface area of almost all the prepared catalysts was greater than 100 (m^2/g) which is good enough for CDRM reaction. The other basic information from Table 4.4 is that the impregnated catalysts have larger pore volume and pore size as compared to precipitated catalysts. Moreover, the difference in pore

sizes of all the impregnated catalysts is negligible. Also, the precipitated catalyst with Ni/Co ratio of 1 (CopCat-Ni2Co4) had the largest pore volume and pore size among the other precipitated catalysts.

4.2.2 ICP ANALYSIS

According to Table 4.5 the Ni/Co ratios of the precipitated catalysts are lower than the intent Ni/Co ratio, while that of impregnated samples are fairly close the intent one.

Table 4.5 Metal composition of Ni-Co/$AlMgO_x$ bimetallic and Ni or Co metallic catalysts by ICP analysis (Intent Mg/Al ratio for all the catalysts is 2)

Catalyst	Intent Ni/Co	Ni	Co	Mg	Al	Ni/Co	Mg/Al
		atom %*					
CopCat-Co6		0	6	69	26		2.7
CopCat-Ni1Co4	0.5	1	4	67	28	0.4	2.4
CopCat-Ni2Co4	1.0	2	4	68	26	0.6	2.6
CopCat-Ni3Co2	2.0	3	2	60	35	1.5	1.7
CopCat-Ni4		4	0	69	27		2.6
Support ($AlMgO_x$)				69	31		2.2
ImpCat-Co5		0	5	65	30		2.1
ImpCat-Ni2Co3	0.5	2	3	68	27	0.5	2.5
ImpCat-Ni3Co3	1.0	3	3	67	27	1.0	2.5
ImpCat-Ni3Co2	2.0	3	2	66	29	1.9	2.3
ImpCat-Ni5		5	0	65	30		2.2

***** All the numbers are rounded based on the ICP results

The metal nitrates solutions affect the pH controlling step of precipitation method. Because of pH variation the obtained Ni/Co ratios might be different from the intent Ni/Co ratios. On the other hand, controlling the amount of metal contents is much easier in impregnation method than the precipitation method resulting in the similarity of intent and obtained Ni/Co ratio which is attributed to the nature of impregnation method.

Regarding the obtained Mg/Al ratio of $MgAlO_x$ support prepared by precipitation method, the same behaviour is observed as for the Ni/Co ratio.

Using precipitation procedure for catalyst preparation, the metal nitrates will dissolve in water in the form of metal ions which will precipitate as metal hydroxides. The amount of precipitated metal hydroxide is dependent of the related solubility product (K_{sp}). The higher obtained ratio of Mg/Al than the intent one may be due to the higher K_{sp} value of $Mg(OH)_2$ than $Al(OH)_3$. The same phenomenon clarifies the variant values for metal ratios (Ni/Co ratio). K_{sp} values are shown in Table 4.6.

Table 4.6 Solubility products of metal hydroxides at 25 °C

Metal hydroxide	$Mg(OH)_2$	$Al(OH)_3$	$Ni(OH)_2$	$Co(OH)_2$
K_{sp}	$5.61*10^{-12}$	$3*10^{-34}$	$5.48*10^{-16}$	$5.92*10^{-15}$

Unlike precipitation method, the Ni and Co nitrates do not contribute to the pH controlling step of preparation; therefore, by using impregnation method, the possibility of Ni and Co hydroxides precipitations is reduced resulting in a negligible difference

between Ni/Co intent ratio and the actually obtained. The results are shown in Table 4.5 and Figure 4.5.

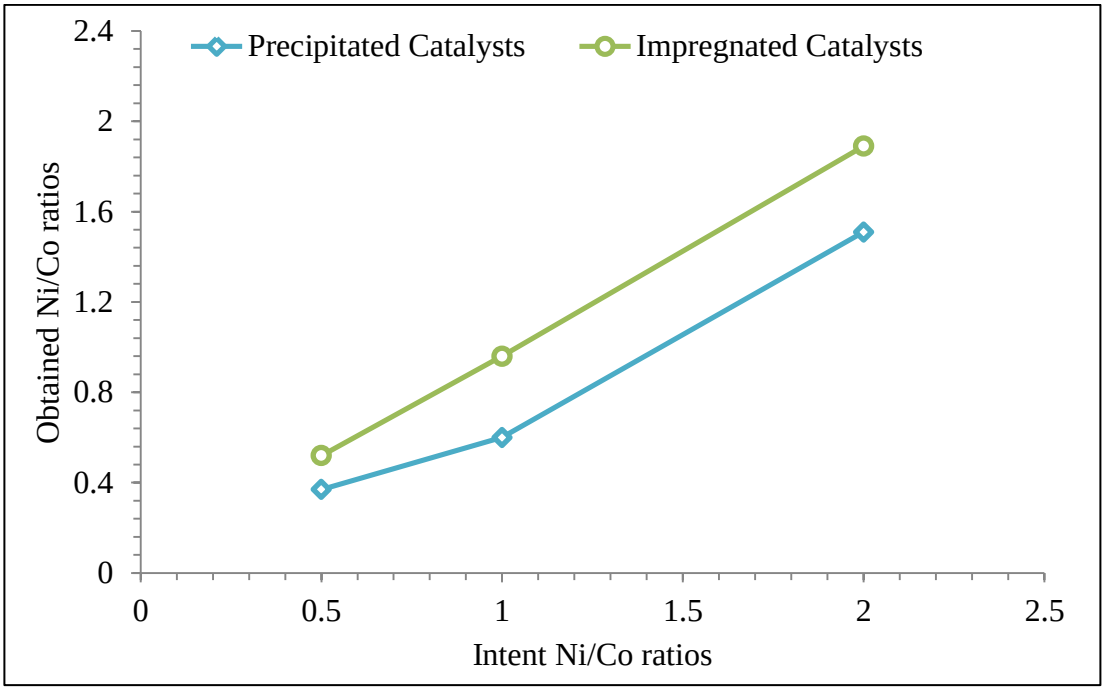

Fig. 4.3 Effect of preparation method on the intent Ni/Co ratios of the bimetallic catalysts after preparation

The effect of catalyst preparation methods on the intent Mg/Al ratio of the catalyst support is shown in Figure 4.4. It can be seen that the Mg/Al ratios are closed to each other for all the catalyst as for all the support prepared by precipitation procedure. The difference between Mg/Al ratio and related intent value might be because of the difference between solubility product of Mg and Al hydroxides as shown in Table 4.6.

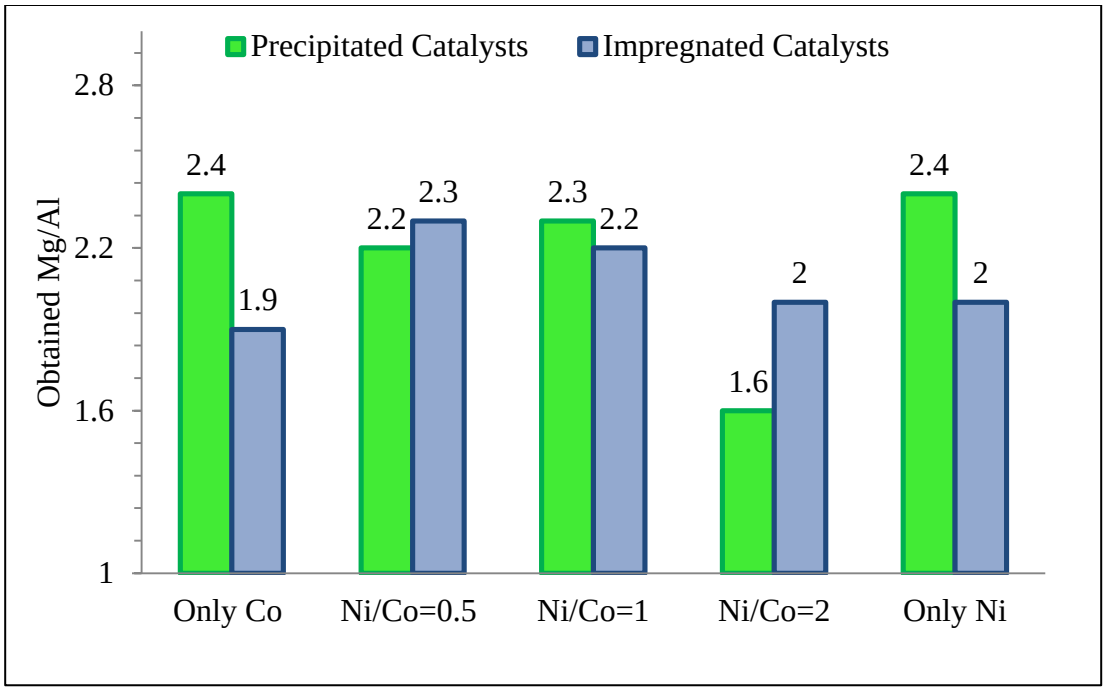

Fig. 4.4 Effect of preparation method on the obtained Mg/Al ratios of the catalysts after preparation

4.2.3 XAS ANALYSIS

All the prepared catalysts (Table 3.1 and Table 3.2) was reduced in a cell reactor in the presence of H_2 (3.5%) and He mixture at 750 °C or 850 °C for 4 h. The catalysts were cooled down to the room temperature in presence of He. With He protection in the cell reactor, the XAS was scanned. Then EXANS data were analyzed with WinXas3.2 software to get the numerical results.

During catalyst reduction, some amounts of metal were reduced in metal forms. Zhang *et al.* (2007) observed that in order to have an active Ni-Co/AlMgO_x bimetallic catalyst, metal particle size of the reduced catalyst should be smaller than 100 Å. In the precipitation method the metal particles grow inside the pores of the support that allows limited growth of particles. On the other hand, in impregnation method the metal

particles grow on the surface of the support which does not limit the metal particle size. Therefore the final metal particle size after reduction is bigger in impregnated catalyst as compared to the precipitated catalyst. In impregnation method the metals acquire the position on the prepared surface; therefore during the reduction process the metals easily migrate and grow to bigger particles. While in precipitation it is harder for metals to migrate and grow as they are located inside the support structure.

The Ni K-edge and Co K-edge of the precipitated CopCat-Ni2Co4 catalyst (with Ni/Co ratio of 0.6) was analyzed at 750 °C and 850 °C. Reconsider it that the amount of reduced Co at 850 °C was greater than 750 °C. However, the particle size at 850 °C was larger than 100 Å, which is not desired for CDRM reaction according Zhang (2008).

Table 4.7 Co K-edge XANS and EXAFS results for Ni/Co ratio 0.6 at both 750 °C and 850 °C

Precipitated catalysts	Treatment	Co-O*	Co	Co size Å
CopCat-Ni2Co4	750 ˚C , H_2	0.80	0.20	
	850 ˚C , H_2	0.33	0.67	>100

***** CoO is used to represent Co^{2+}. It is not the exact structures in catalysts.

Table 4.8 shows XANES result of the catalysts at 750 °C reduction temperature. Table 4.8 indicates that no matter how the catalysts were prepared, the Ni reduced more than Co in all bimetallic catalysts. Also, cobalt mostly is an unreduced (Co-O-Co) form, especially in the precipitated catalysts. In precipitated catalysts, the metallic Co did not show any reducibility while with increasing Ni content; Co was able to be reduced. In the other words, increasing Ni content helps Co reduction.

Table 4.8 XANES results of the prepared catalysts, 750 °C reduction temperature, H_2 (3.5%) and He mixture

Precipitated catalyst	Ni	NiO*	Co	CoO*	Impregnated catalyst	Ni	NiO*	Co	CoO*
Co6	-	-	0	1	Co5	-	-	0.43	0.57
Ni1Co4	0.52	0.48	0.20	0.80	Ni2Co3	0.82	0.18	0.37	0.63
Ni2Co4	0.52	0.48	0.20	0.80	Ni3Co3	0.83	0.17	0.37	0.63
Ni3Co2	0.55	0.48	0.25	0.75	Ni3Co2	0.79	0.21	0.51	0.49
Ni4	0.87	0.13	-	-	Ni5	0.84	0.16	-	-

***** NiO and CoO are used to represent Ni^{2+} and Co^{2+}. They are not the exact structures in catalysts.

Table 4.8 shows that impregnated catalysts are reduced more in form of metals, especially in case of Co which was almost two times as compared to the precipitated catalysts. Furthermore, the Co monometallic catalyst prepared by precipitation method did not show any reduction ability of metal, whereas, the Co from impregnation method showed 43% reduction.

The EXAFS analysis was carried out to obtain the information about the particle size. Table 4.9 shows EXAFS result of the catalysts at 750 °C reduction temperature. Table 4.9 represents that the precipitated catalysts grow smaller particle sizes than the impregnated catalysts as explained earlier. Also, the Co monometallic impregnated catalyst has the reduced particle size greater than 100 Å which is not favoured for CDRM reaction.

Table 4.9 EXAFS results of the prepared catalysts, 750 °C reduction temperature, H_2 (3.5%) and He mixture

Precipitated catalyst	Ni-Ni Bond, Å	Particle Size, Å	Co-Co Bond, Å	Particle Size, Å	Impregnated catalyst	Ni-Ni Bond, Å	Particle Size, Å	Co-Co Bond, Å	Particle Size, Å
Co6	-	-	-	-	Co5	-	-	2.50	>100
Ni1Co4	2.50	40	2.51	-	Ni2Co3	2.48	80	2.50	80
Ni2Co4	2.49	40	2.51	-	Ni3Co3	2.48	75	2.49	80
Ni3Co2	2.50	50	2.51	-	Ni3Co2	2.48	90	2.49	80
Ni4	2.48	70	-	-	Ni5	2.48	90	-	-

***** NiO and CoO are used to represent Ni^{2+} and Co^{2+}. They are not the exact structures in catalysts.

Table 4.9 indicates that the reduced metal particle size was lower than 100 Å for the bimetallic catalysts that were prepared at 750 °C. However, the particle size was more than 100 Å for precipitated CopCat-Ni2Co4 catalyst at 850 °C (Table 4.7). EXAFS results showed that the reduced Co size in the ImpCat-Co5 catalyst was more than 100 Å. This means that the Co monometallic impregnated catalyst may not have desired activity in comparison with other catalysts.

Table 4.10 and 4.11 show a summary of XAS and ICP analysis done on the prepared catalysts.

Table 4.10 Reduced metal content (wt %) of precipitated catalysts from XANES and ICP results

Participated catalysts	Nickel content (wt %)	Cobalt content (wt %)	Fraction of reduced Nickel	Fraction of reduced Cobalt	Reduced Ni content (wt %)	Reduced Co content (wt %)
Co6	0	5.9	0	0	0.00	0.00
Ni1Co4	1.52	4.18	0.52	0.2	0.79	0.84
Ni2Co4	2.67	4.53	0.52	0.2	1.39	0.91
Ni3Co2	2.83	1.87	0.55	0.25	1.56	0.47
Ni4	4.9	0	0.87	0	4.26	0.00

Table 4.11 Reduced metal content (wt %) of impregnated catalysts from XANES and ICP results

Impregnated catalysts	Nickel content (wt %)	Cobalt content (wt %)	Fraction of reduced Nickel	Fraction of reduced Cobalt	Reduced Ni content (wt %)	Reduced Co content (wt %)
Co5	0	6.6	0	0.43	0.00	2.84
Ni2Co3	1.93	3.67	0.82	0.37	1.58	1.36
Ni3Co3	2.94	3.06	0.83	0.37	2.44	1.13
Ni3Co2	4	2.1	0.79	0.51	3.16	1.07
Ni5	5.9	0	0.84	0	4.96	0.00

4.3 CATALYST ACTIVITY TEST

To observe the effects of preparation method and Ni/Co ratio, the prepared catalysts were tested for CDRM reaction. The experimental conditions were as explained in section 3.3.1. The results were compiled according to the procedure and equations as described in section 3.4. To compare the effects of catalysts on CDRM reaction, the data for the first 11 h of each reaction is shown in this section.

4.3.1 EFFECT OF Ni/Co RATIO ON CDRM REACTION (PRECIPITATED CATALYSTS)

Figures 4.5 and 4.6 show the conversion of CH_4 and CO_2, respectively. The CO_2 conversion has the same trend as shown for CH_4 conversion. Also, as expected, conversion of former is slightly higher than the latter because of the occurrence of RWGSR which is supplied from reactants and H_2 produced in CDRM reaction. Figures 4.5 and 4.6 depict that the cobalt catalyst did not show an acceptable activity which was close to 9% of conversion after 11 h. Also, the CopCat-Ni2Co4 (Ni/Co ratio of 0.6) showed higher conversion than the other bimetallic and Ni monometallic catalysts, while the difference was insignificant. In case of CO_2 conversion, the conversions for the catalysts containing Ni were close to each other for the first 11 h. This could be due to the proposed mechanism at which CO_2 is activated by support.

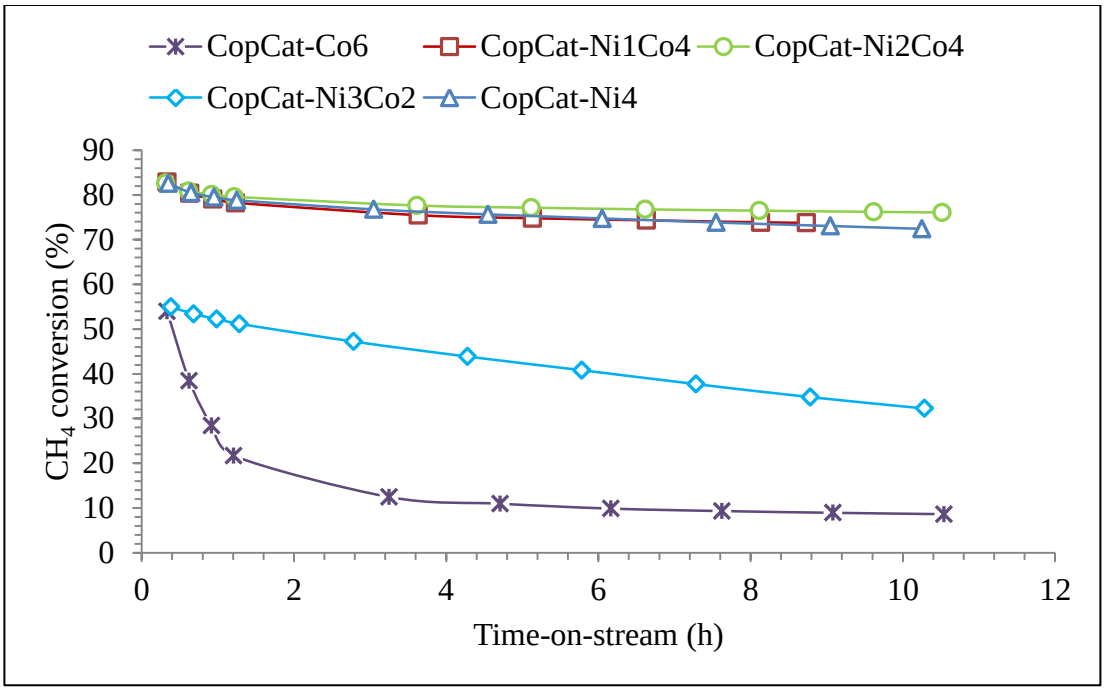

Fig. 4.5 Activity and stability of Ni-Co precipitated catalysts in term of CH_4 conversion; reaction conditions: 710 °C, 1atm, 558000 mL/g_c.h (GHSV), and $CH_4/CO_2/N_2$=1/1/1, catalyst load of 0.02 g

Table 4.12 presents the conversions of CH_4 and CO_2 in the beginning and at the end of 11 h period. The effect of RWGSR on consumption rate of carbon dioxide is more tangible than methane as the CO_2 conversion is higher than CH_4. The larger difference between CH_4 and CO_2 conversions show a larger impact of RWGSR that may result in more CO production reducing the H_2/CO ratio. Therefore, the closer the H_2/CO ratio to unity the lower the contribution of side reaction (RWGSR).

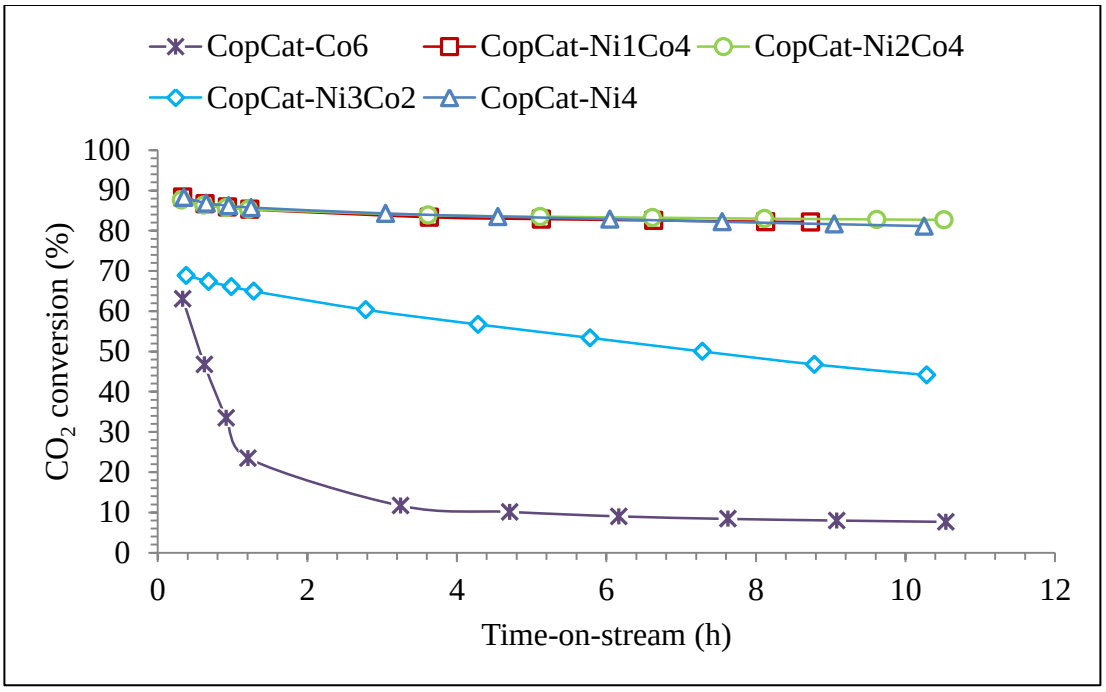

Fig. 4.6 Activity and stability of Ni-Co precipitated catalysts in term of CO_2 conversion; reaction conditions: 710 °C, 1atm, 558000 mL/g_c.h (GHSV), and $CH_4/CO_2/N_2$=1/1/1, catalyst load of 0.02 g

Table 4.12 Activity and stability of Ni-Co precipitated catalysts in terms of CH_4 and CO_2 conversions at the beginning and after 11 h

Catalyst	CH_4 conversion (%)		CO_2 conversion (%)	
	Beginning	End	Beginning	End
CopCat-Co6	54	8.6	63	7.6
CopCat-Ni2Co5	82.8	73.7	88.4	82.1
CopCat-Ni3Co5	82.7	76.1	87.6	82.7
CopCat-Ni3Co2	54.9	32.2	68.9	44.1
CopCat-Ni5	82.6	72.4	88.3	81.1

Apart from catalytic activity, selectivity is defined as one of the most important criterion of selecting a suitable catalyst. In our case selectivity may change H_2/CO ratio

significantly. Figure 4.7 shows the product H_2/CO ratios versus time for the tested catalysts. Due to instrument limitation[1], the H_2/CO was not calculated for CopCat-Co6 as illustrated in Figure 4.7.

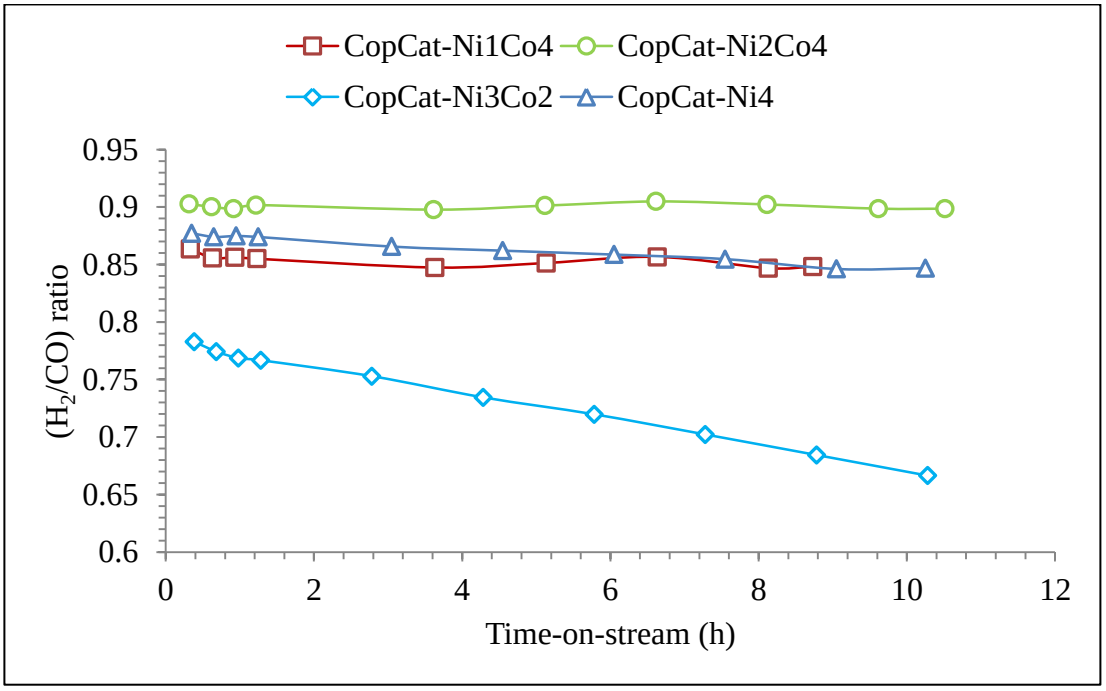

Fig. 4.7 H_2/CO ratios of precipitated catalysts; reaction conditions: 710 °C, 1atm, 558000 mL/g_c.h (GHSV), and $CH_4/CO_2/N_2$=1/1/1, catalyst load of 0.02 g

Figure 4.7 shows that bimetallic catalysts have higher H2/CO ratio than the monometallic catalyst indicating higher selectivity of precipitated bimetallic catalysts compared to precipitated monometallic catalyst. Also, the CopCat-Ni2Co4 (Ni/Co ratio of 0.6) has the highest H_2/CO ratio during the testing period suggesting a lower side reaction (RWGSR) and higher selectivity among other catalysts.

Based on the results obtained from catalyst activity tests, the CopCat-Ni2Co4 (Ni/Co ratio of 0.6) gained more selectivity as compared to the other precipitated

[1] TCD was not able to detect hydrogen peak when the conversion of reactants was lower than 20%

catalysts. It can be confirmed by comparing the reactant conversion and H_2/CO ratio as shown in Figure 4.5, 4.6, and 4.7.

To summarize, the CopCat-Ni2Co4 (Ni/Co ratio of 0.6) bimetallic catalyst prepared by precipitation method has almost the same activity in comparison with the other catalysts, but it had the highest selectivity among the other precipitated catalysts during CDRM reaction. Also, it is observed that a higher percentage of reduced metals does not lead to higher activity and selectivity. This can be confirmed by comparing the activity and selectivity of Ni monometallic catalyst (87% reduced Ni) and CopCat-Ni2Co4 bimetallic catalyst (52% reduced Ni).

4.3.2 Effect of Ni/Co ratio on CDRM reaction (impregnated catalysts)

Generally, it is expected that the catalysts with higher nickel content show better activity. Also, like the precipitated catalysts, a higher CO_2 conversion is expected due to the RWGSR. Additionally, the catalysts with higher reduced metal content may show better activity for CDRM reaction.

Figure 4.8 illustrates the CH_4 conversion, and Figure 4.9 shows the CO_2 conversion versus time on stream while using impregnated catalysts. Also, Table 4.13 shows the reactants conversion at the beginning and at the end of 11 h of reaction. It can be seen that ImpCat-Co5 catalyst is not active for CDRM reaction. The reason could be interpreted by XAS results since the only catalyst having the reduced Co particle with size more than 100 Å is ImpCat-Co6 catalyst. On the other hand Bouarab et al. (2004) reported that supported Co catalysts gave better results in comparison with Ni in terms

of carbon formation implying that presence of Co in the Ni-Co bimetallic catalyst ameliorates the carbon formation resistance of bimetallic catalysts.

In addition, it can be observed that increasing the Ni content of the bimetallic catalysts increased the reactant conversion. Regarding, XAS results more reduction took place by increasing Ni content; therefore, more activity is gained. Also, ImpCat-Ni5 has almost the same activity in term of methane conversion in comparison with the bimetallic catalysts. On the other hand, increasing the amount of Ni from Ni/Co ratio of 1.9 (ImpCat-Ni3Co2) to only Ni (ImpCat-Ni5) does not make significant change in the amount of methane conversion. It can be concluded that excess amount of Ni content more than Ni/Co=1.9 may not improve the catalyst activity.

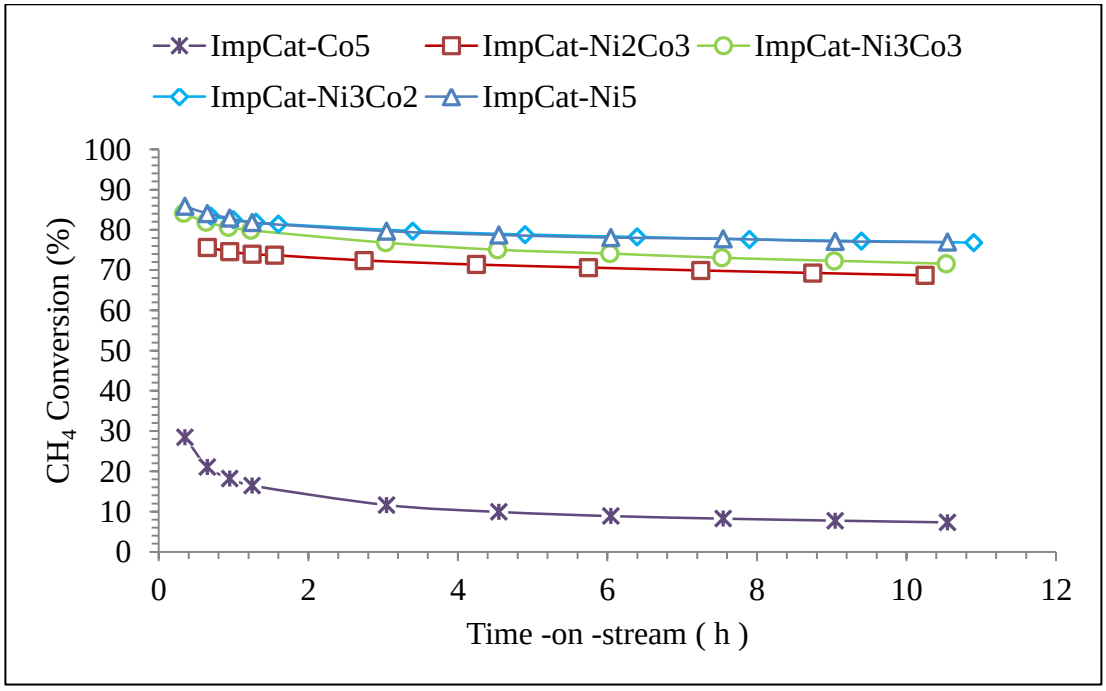

Fig. 4.8 Activity and stability of Ni-Co impregnated catalysts in term of CH_4 conversion; reaction conditions: 710 °C, 1atm, 558000 mL/g_c.h (GHSV), and $CH_4/CO_2/N_2$=1/1/1, catalyst load of 0.02 g

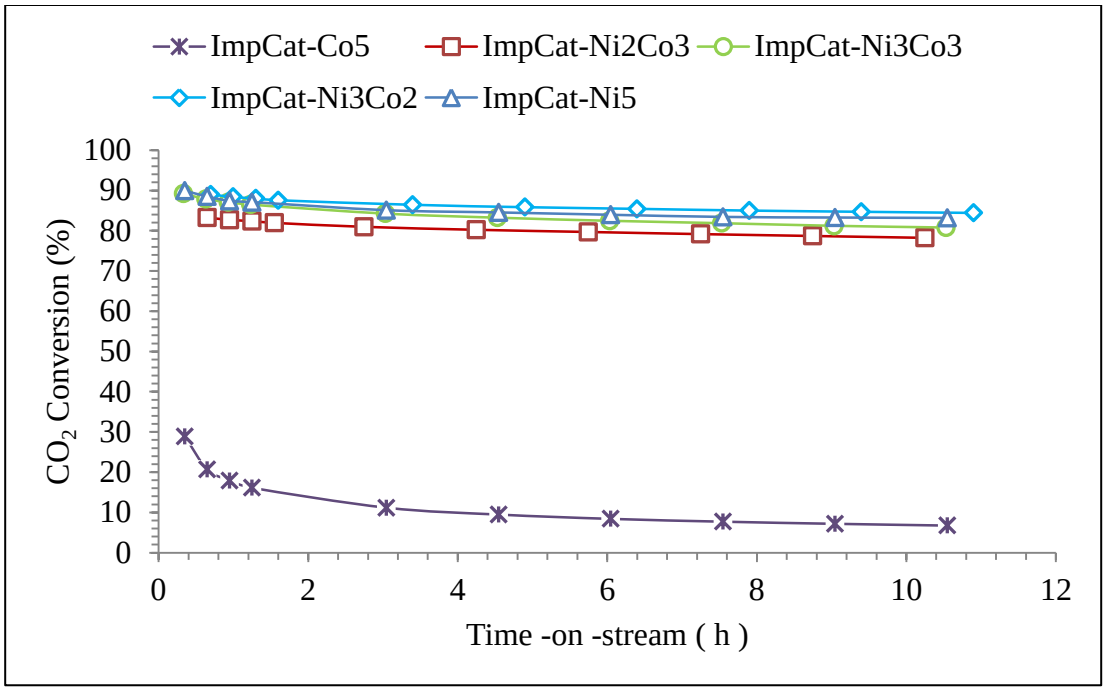

Fig. 4.9 Activity and stability of Ni-Co impregnated catalysts in term of CO_2 conversion; reaction conditions: 710 °C, 1atm, 558000 mL/g_c.h (GHSV), and $CH_4/CO_2/N_2$=1/1/1, catalyst load of 0.02 g

Table 4.13 Activity and stability of Ni-Co impregnated catalysts in terms of CH_4 and CO_2 conversions at the beginning and after 11 h

Catalyst	CH_4 conversion (%)		CO_2conversion (%)	
	Beginning	End	Beginning	End
ImpCat-Co5	28.5	7.3	28.9	6.7
ImpCat-Ni2Co3	75.6	68.7	83.3	78.2
ImpCat-Ni3Co3	84.1	71.6	89.3	80.8
ImpCat-Ni3Co2	83.4	76.8	89	84.4
ImpCat-Ni5	85.8	77	89.9	83.2

Table 4.13 provides basic information about the impacts of the side reaction (RWGSR) which can be observed due to differences between CH_4 and CO_2 conversions.

To observe the effect of side reaction (RWGSR) on the CDRM reaction over different impregnated catalysts, the H_2/CO ratios are depicted versus time as presented in Figure 4.10. Generally, the closeness value of H_2/CO to unity indicates that RWGSR has negligible contribution. Higher H_2/CO ratio associated with Ni monometallic catalyst indicating the catalyst is more selective for CDRM than RWGSR among the other impregnated bimetallic catalysts as illustrated in Figure 4.10. As it can be seen, increase in Ni content raises H_2/CO ratio and consequently the selectivity of the catalysts towards CDRM reaction.

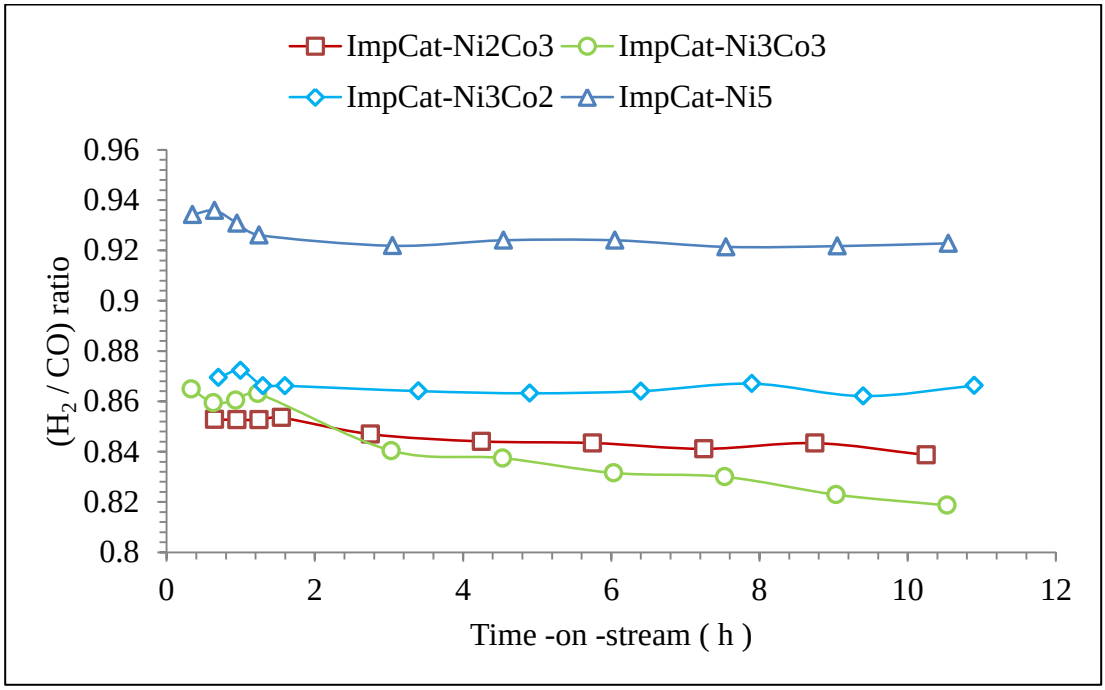

Fig. 4.10 H_2/CO ratios of Impregnated catalysts; reaction conditions: 710 °C, 1atm, 558000 mL/g_c.h (GHSV), and $CH_4/CO_2/N_2$=1/1/1, catalyst load of 0.02 g

A general trend can be concluded in this section to see how Ni content can affect the performance of the impregnated catalysts. The Catalysts with Ni/Co ratio equal or greater than 1 obtained conversions of about 84% for CH_4 and 89% for CO_2 after 30 min of reaction time. More specifically, the only Ni monometallic catalyst had the highest conversion and selectivity towards CDRM reaction resulting in the highest H_2/CO ratio as for the product stream.

4.3.3 Effects of preparation methods for the Ni-Co/$AlMgO_x$ catalysts for CDRM reaction

This section describes the effects of preparation methods on the catalysts activity for CDRM reaction. First of all the effects of preparation methods on the performance of monometallic catalysts are described. Then, the bimetallic catalyst with almost the same Ni/Co ratio[1] is investigated. Finally, the catalysts that showed better performance for CDRM reaction among each group will be selected.

4.3.3.1 Effect of preparation method for monometallic catalysts

Figure 4.11 and 4.12 show reactant conversions and H_2/CO ratios using monometallic catalysts on CDRM reaction. As discussed in sections 4.3.1 and 4.3.2, the conversion of the Co monometallic catalysts was relatively low[2] within the first 11 h of the reaction. On one hand, Ni monometallic catalysts gained quite high activity[3] for CDRM reaction. On the other hand, ImpCat-Ni5 sample has higher activity than the

[1] CopCat-Ni2Co4 (Ni/Co = 0.5), and ImpCat-Ni2Co3 (Ni/Co = 0.6)
[2] Less than 10% conversion for both reactants
[3] More than 80% of conversion for both reactants

precipitated catalyst because of either highly reduced Ni metal on the surface or large values of Ni loading.

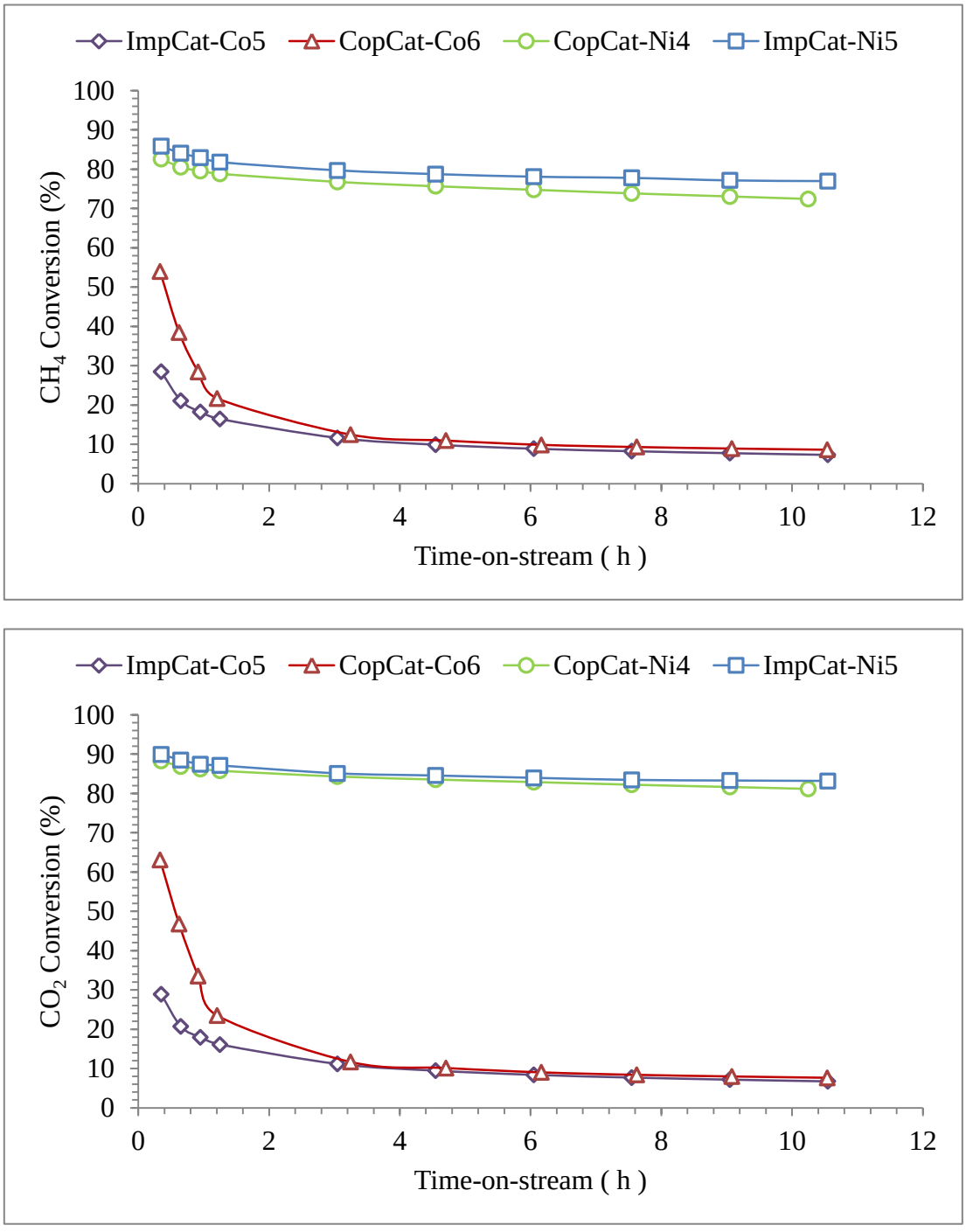

Fig. 4.11 Activity and stability of monometallic catalysts in term of reactant conversion; reaction conditions: 710 °C, 1 atm, 558000 mL/g_c.h (GHSV), and $CH_4/CO_2/N_2$=1/1/1, catalyst load of 0.02 g

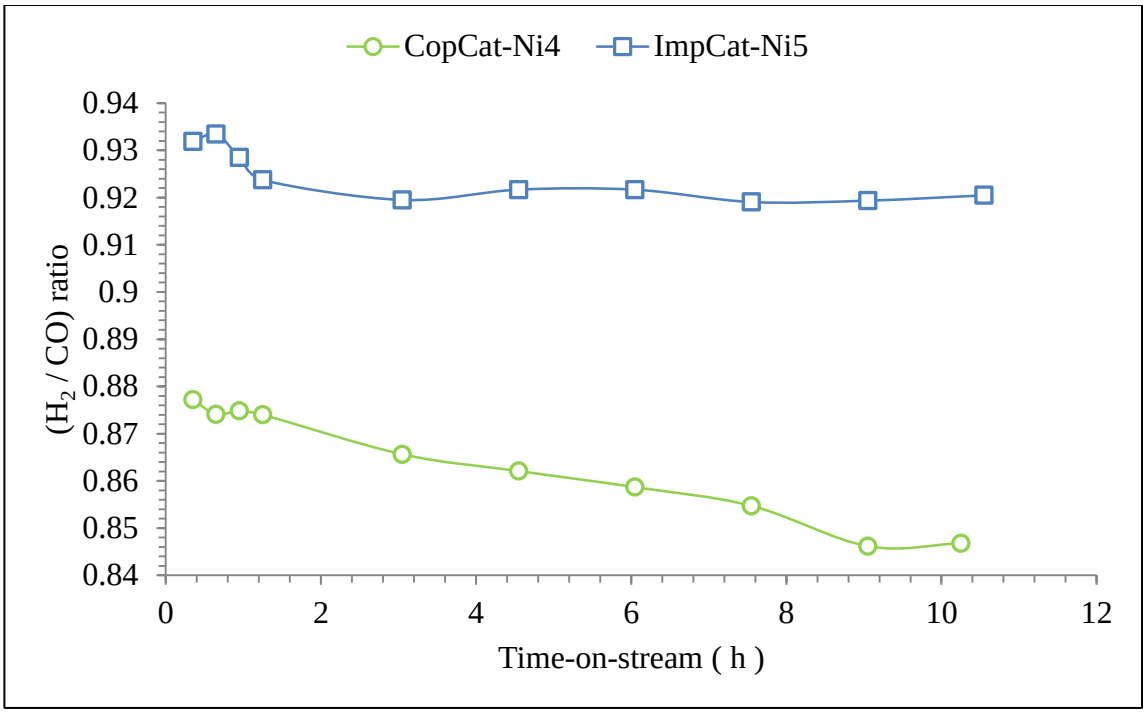

Fig. 4.12 H_2/CO ratios of the monometallic catalysts; reaction conditions: 710 °C, 1atm, 558000 mL/g_c.h (GHSV), and $CH_4/CO_2/N_2$=1/1/1, catalyst load of 0.02 g

4.3.3.2 Effect of preparation method for Ni-Co bimetallic catalysts

Although the available Ni content of precipitated catalyst was significantly lower than impregnated one, precipitated catalyst had more activity than impregnated one as shown in Figure 4.13.

Figure 4.14 shows that the precipitated catalyst has higher H2/CO ratio during the 15 h of reaction time. The results are in agreement with Zhang's (Zhang et al., 2007) study.

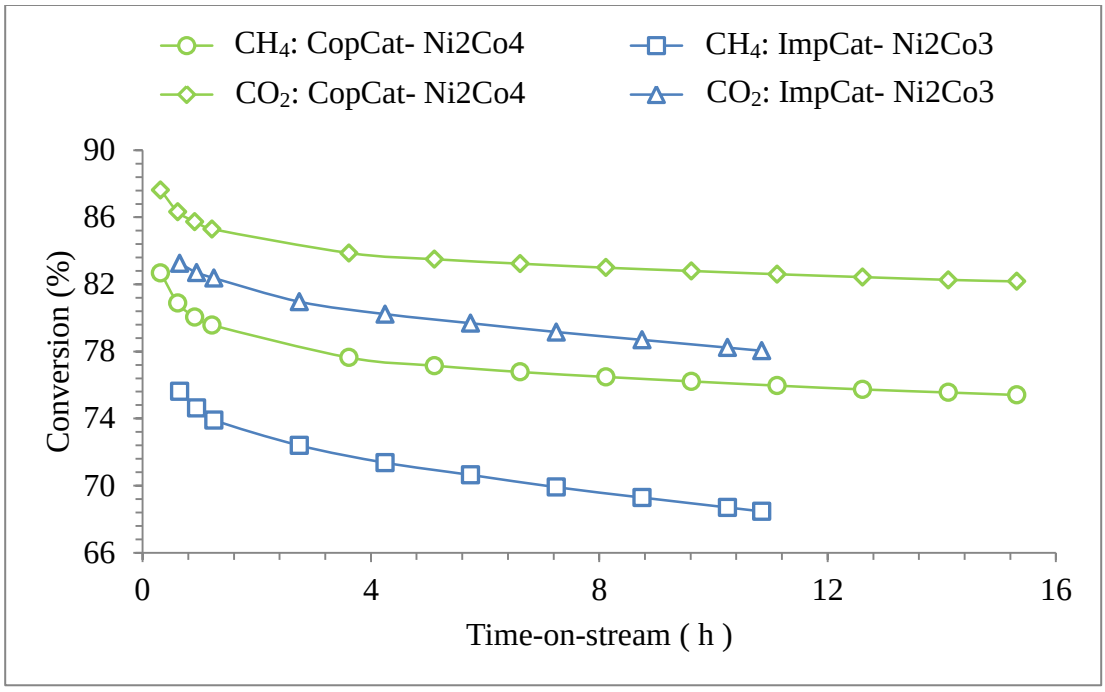

Fig. 4.13 Activity and stability of bimetallic catalysts in term of reactant conversions; reaction conditions: 710 °C, 1atm, 558000 mL/g_c.h (GHSV), and $CH_4/CO_2/N_2$=1/1/1, catalyst load of 0.02 g

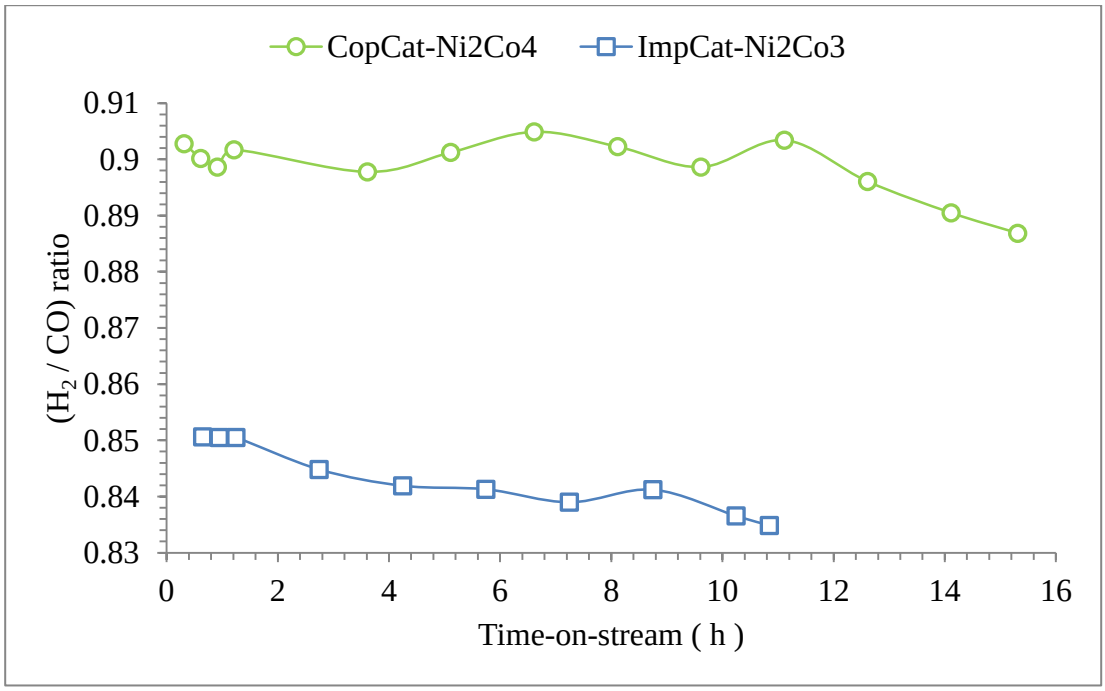

Fig. 4.14 H_2/CO ratios of Ni/Co bimetallic catalysts; reaction conditions: 710 °C, 1atm, 558000 mL/g_c.h (GHSV), and $CH_4/CO_2/N_2$=1/1/1, catalyst load of 0.02 g

4.3.3.3 OVERALL COMPARISON

According to sections 4.3.1 and 4.3.2, the CopCat-Ni2Co4 bimetallic (Ni/Co ratio of 0.6) and the CopCat-Ni4 monometallic catalysts were chosen among the precipitated samples. Similarly, the ImpCat-Ni3Co2 bimetallic (Ni/Co ratio of 1.9) and the ImpCat-Ni5 monometallic catalysts were selected from the impregnated samples. Figure 4.15 shows reactant conversions of the CDRM reaction over the selected catalysts.

As Figure 4.15 shows, the initial conversions for the impregnated samples are slightly higher than the precipitated samples. However, after the first 8 h of the reaction CH_4 conversion of the Impregnated catalysts dropped slightly while the conversion of CopCat-Ni2Co4 catalyst remained almost constant.

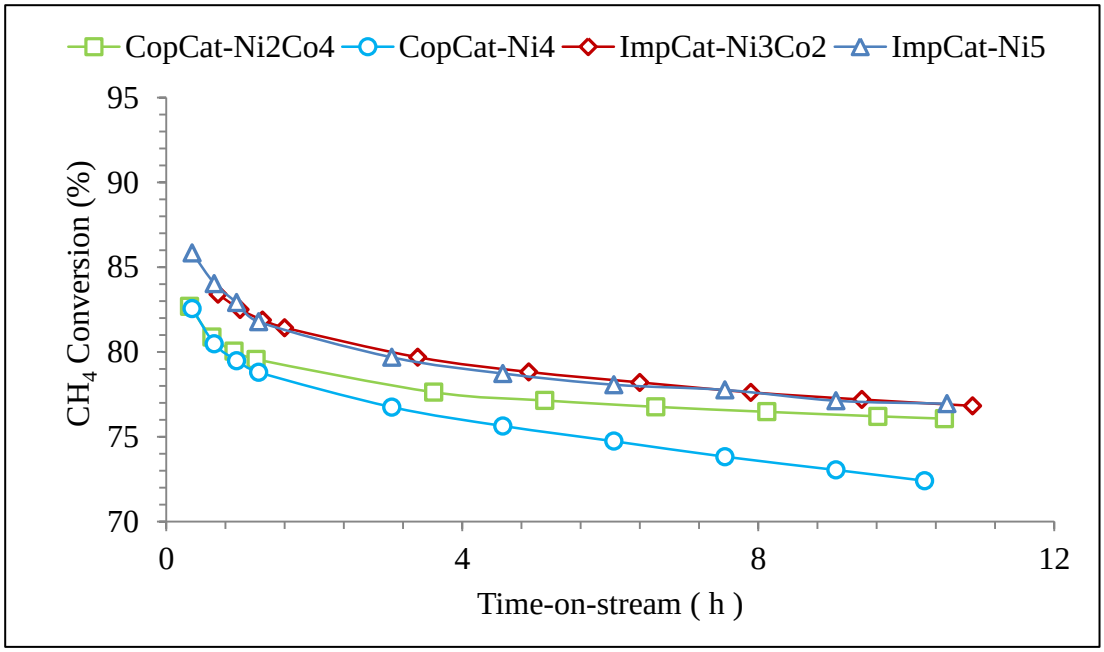

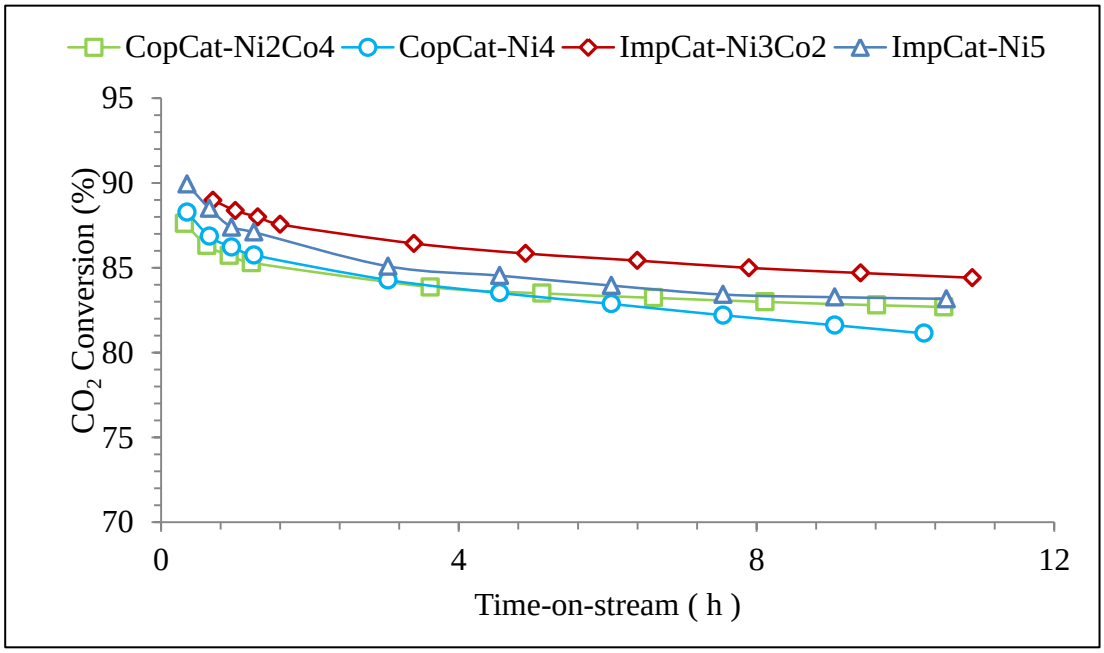

Fig. 4.15 Activity and stability of Ni-Co catalysts in term of reactant conversions; reaction conditions: 710 °C, 1 atm, 558000 mL/g_c.h (GHSV), and $CH_4/CO_2/N_2$=1/1/1, catalyst load of 0.02 g

A further comparison is made among different H_2/CO ratios as shown in Figure 4.16. It can be observed that the H_2/CO ratio has the highest value for the impregnated monometallic Ni catalyst (ImpCat-Ni5). It should be noted that except the precipitated monometallic Ni catalyst the values of H_2/CO for all the others stay fairly stable.

One of the most influential factors determining the performance of a catalyst is the related amount of reduced metals content which is shown in Tables 4.10 and 4.11. Based on the total amount of reduced metals content associated with each catalyst the consumption rate of reactants are shown in Figures 4.17 and 4.18.

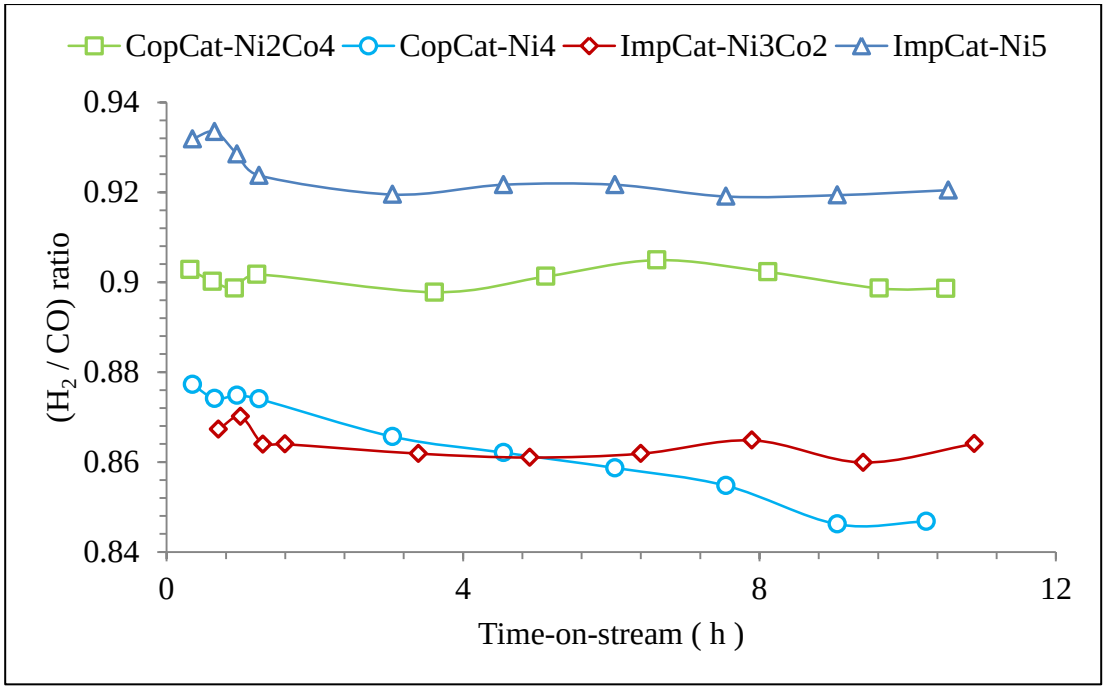

Fig. 4.16 H_2/CO ratios of Ni-Co catalysts; reaction conditions: 710 °C, 1atm, 558000 mL/g_c.h (GHSV), and $CH_4/CO_2/N_2$=1/1/1, catalyst loading of 0.02 g

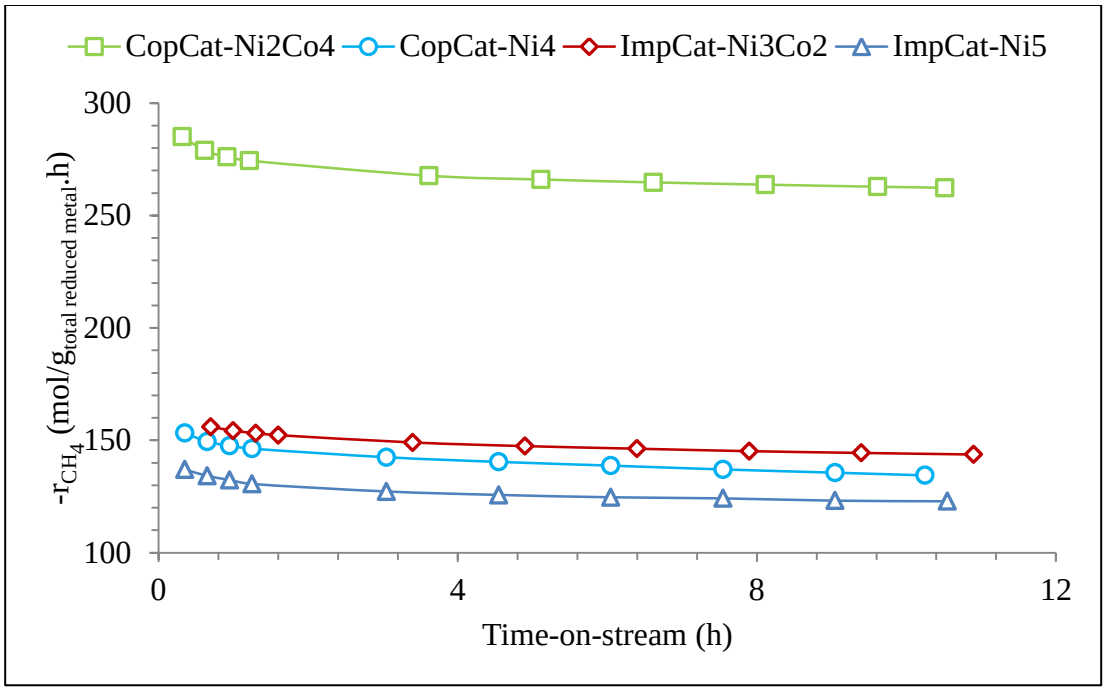

Fig. 4.17 CH_4 rates of CDRM reaction based on the total reduced metal weight of the catalysts

Regarding amount of reduced metal content Figure 4.18 clearly shows that the performance of the CopCat-Ni2Co4 catalyst (Ni/Co ratio of 0.6) is approximately two times than that of the only Ni impregnated catalyst. Zhang *et al.* (2007) and Bouarab *et al.* (2004) observed that the presence of Co in Ni-Co catalyst is necessary to improve the carbon formation resistance of the catalyst. In other words the presence of Co improves the selectivity of catalyst while the only Co monometallic catalyst is not active for CDRM reaction, as shown in Figure 4.11. Furthermore, the presence of Co in the precipitated Ni-Co bimetallic catalysts reduces the number of Ni active sites making RWGSR less favorable compared to the ImpCat-Ni5 catalyst. Thus, presence of Co is a must to get desired performance for CDRM reaction.

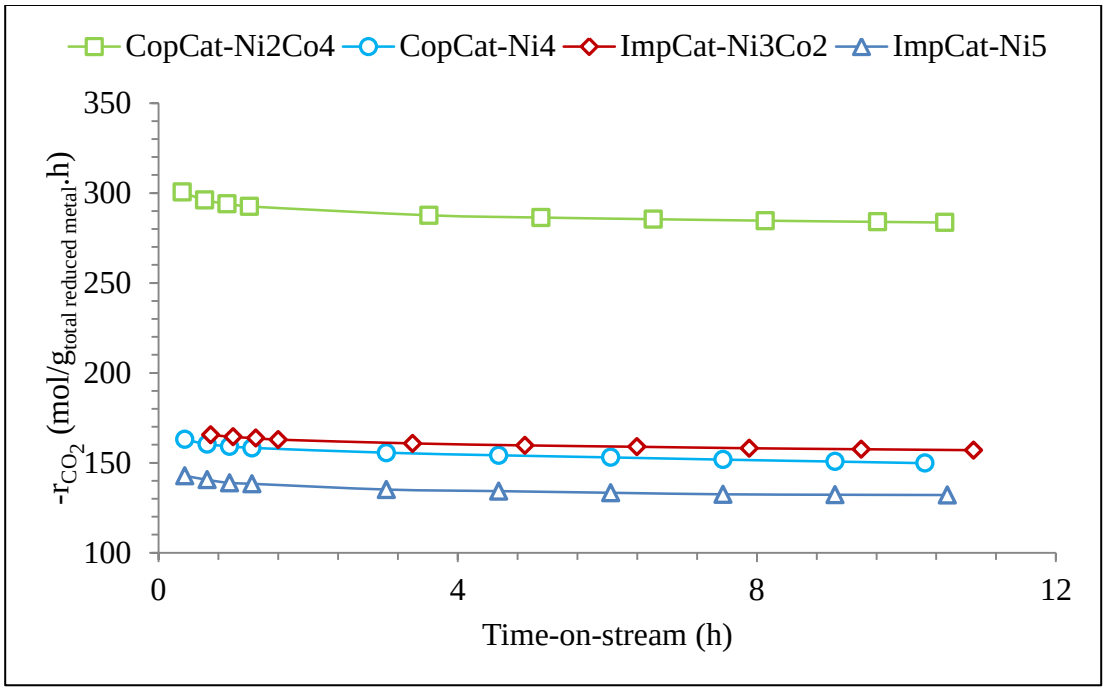

Fig. 4.18 CO_2 rates of CDRM reaction based on the total reduced metal weight of the catalysts

Based on the above discussion, Ni-Co/AlMgO_x catalyst with Ni/Co ratio of 0.6 (CopCat-Ni2Co4) is selected as the optimum catalyst for CDRM reaction.

4.4 Life-time activity and stability test of Ni-Co bimetallic catalyst (CopCat-Ni2Co4 with Ni/Co ratio of 0.6)

To meet the requirement of Carbon Science Inc., the stability and activity of the Ni-Co/AlMgO_x catalyst with Ni/Co ratio of 0.6 (CopCat-Ni2Co4) as the optimum catalyst for CDRM reaction was tested for almost 1600 h with the procedure described in section 3.3.2.

Based on the previous studies done in our research group desired stability and conversion were expected especially at 760 °C by using the Ni/Co ratio of 0.6 precipitated catalyst (CopCat-Ni2Co4) for CDRM reaction. The reactant conversion and production rate are shown in Figures 4.19 and 4.20. Also, Table 4.14 summarizes the reactant conversion and formation rate of products for the life-time test.

The test was performed within 65 days at two different temperatures i.e. 710 °C and 760 °C. The catalyst showed better performance in terms of activity and stability at 760 °C[1] as compared to 710 °C as shown in Figure 4.19. The CH_4 conversion at 710 °C dropped from 90% to 72% within 42 days. More interestingly, there was a significant increase in reactant conversions as soon as the temperature increased to 760 °C after the 42nd day of reaction. The reactant conversion remained stable after 23 days on. It is noteworthy that there was not only an immediate recovery in conversion but also an improvement in stability. Figure 4.22 reveals formation rate of products.

[1] Almost 93% CH_4 conversion and 95% CO_2 conversion

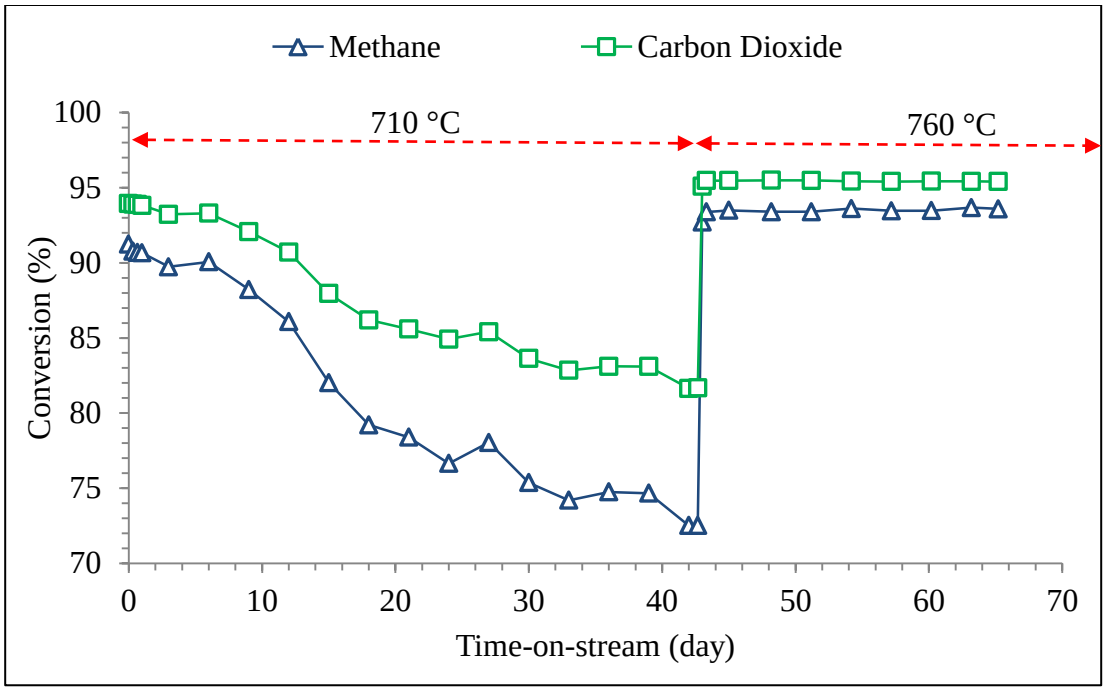

Fig. 4.19 Activity and stability of CopCat-Ni2Co4 with Ni/Co ratio of 0.6 catalyst in term of reactant conversions of CDRM reaction; reaction conditions: 710 °C for the first 42 days and 760 °C for the rest, 1 atm, 110,000 mL/g_c.h (GHSV), and $CH_4/CO_2/N_2$=1/1/1, catalyst load of 0.05 g.

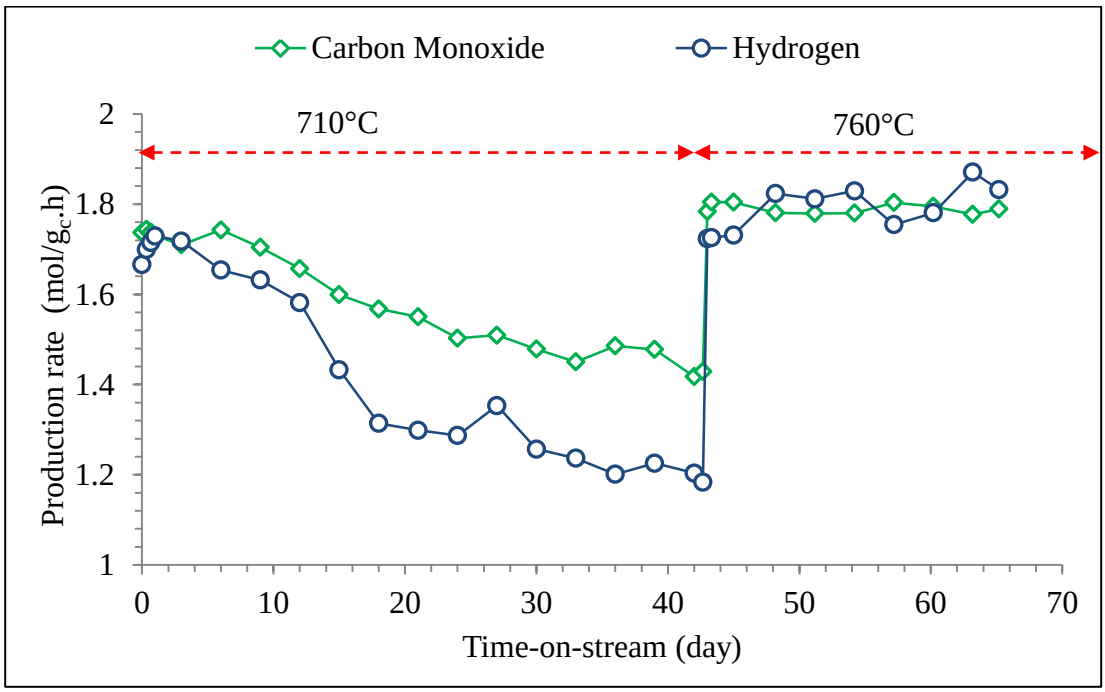

Fig. 4.20 Production rates of the life-time CDRM test, reaction conditions: 710 °C for the first 42 days and 760 °C for the rest, 1 atm, 110,000 mL/g_c.h (GHSV), and $CH_4/CO_2/N_2$=1/1/1, catalyst load of 0.05 g

Table 4.14 Formation rate of products and reactant conversions of the life-time test using CopCat-Ni2Co4 with Ni/Co ratio of 0.6, at 710 °C and 760 °C

Time (day)	Temperature (°C)	CH_4 conversion (%)	CO_2 conversion (%)	Rate of H_2 (mol/g_c.h)	Rate of CO (mol/g_c.h)
1st	710	90	94	1.70	1.74
20th	710	78	85.5	1.32	1.54
42th	710	72.5	81.5	1.20	1.42
43th	760	93	95	1.72	1.78
65th	760	93.5	95.5	1.78	1.79

Regarding Figure 4.21 there is a decreasing trend for H_2/CO ratio while it fluctuates versus time at 710 °C. On the other hand, at 760 °C although the H_2/CO ratio is fluctuating, it remained steady around 1.. This behaviour was described by Wei *et al.* (2000) as a periodic cycle of carbon deposition and elimination on the catalyst. Richardson (1998) called this phenomenon as an effective periodic carbon deposition and elimination stabilizing catalytic performance.

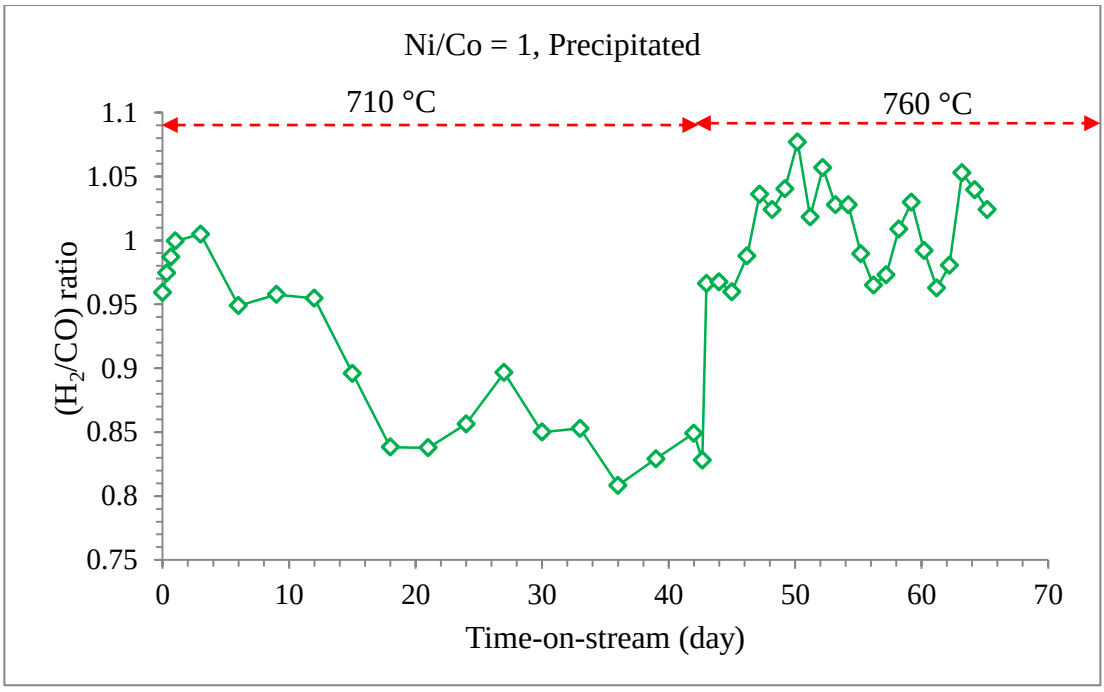

Fig. 4.21 H_2/CO ratio during the life-time test period at 710 °C and 760 °C

To conclude, the precipitated Ni-Co/$AlMgO_x$ catalyst with Ni/Co ratio of 0.6 has a high stability for CDRM reaction. This behavior improved when the reaction temperature was increased from 710 °C to 760 °C during the life-time test for 65 days.

4.5 Catalyst poisoning with 30 ppm of H_2S

As mentioned, both natural gas and landfill gas as the main sources of CH_4 may contain sulfur containing compounds[1] as the poison. In order to investigate the effects of sulphur compounds on the activity of catalyst, all the prepared catalysts were poisoned with 30 ppm of H_2S. The procedure for poisoning the catalysts was introduced in section 3.3.3. Among the catalysts prepared by both precipitation and impregnation methods, the monometallic Co catalysts were not active compared to other catalysts; therefore the

[1] Mainly H_2S

poisoning test was not conducted for them. This part of research is mainly focused on the activity and regeneration capability of the catalysts poisoned by H_2S.

In addition, after the poisoning, activities of the catalyst prepared by precipitation and impregnation techniques were compared based on the reduced metal contents.

Running the tests three sections are distinguished called “before poisoning” (P-1), “during poisoning” (P-2), and “after poisoning” (P-3). The reaction conditions for the P-1 and P-3 sections were the same as explained in section 3.3.1. For the P-2, the flow rates of the gases were adjusted in order to keep the equimolar mixture of CH_4, CO_2, and N_2. Because of instrument limitations, catalyst loadings, and poison availability a certain value of poisonous gas is chosen. The catalysts were poisoned by 30 ppm of H_2S and the temperature of the reaction was kept constant at 710 °C (the beginning of P-2). To make sure that all the catalysts are poisoned, the H_2S poisoning was stopped as soon as GC could not recognize the H_2 peak (the end of P-2) indicating the catalyst is totally poisoned with H_2S. Then the flow rates of CH_4, CO_2, and N_2 gases were adjusted to the condition prior to the poisoning (beginning of P-3). In this section, t=0 is the time at which H_2S was injected to the reactor (beginning of P-2).

Figure 4.22 shows results of the CO_2 conversion for the precipitated catalysts during and after H_2S poisoning (P-2 and P-3). As soon as poisoning starts a rapid drop in conversion of all catalysts is observed. In spite of very low conversions[1], all the precipitated bimetallic catalysts are still active. However, in case of Ni monometallic

[1] CO_2 conversion in the range of 10-15%

catalyst, the conversion starts to increase versus time while poisoning. The results indicate that catalyst with higher Ni content than Co has more ability of regeneration after being poisoned implying that the presence of Ni is essential for regeneration after poisoning. As presented in Table 4.8, Ni monometallic catalyst has a higher percentage of metal reduction among the others resulting in faster regeneration than the bimetallic catalysts.

Table 4.15 indicates the reactants conversion before, after, and at the end of the poisoning test. The CH_4 conversion trends of the catalysts were the same as CO_2 as shown in Figure 4.23.

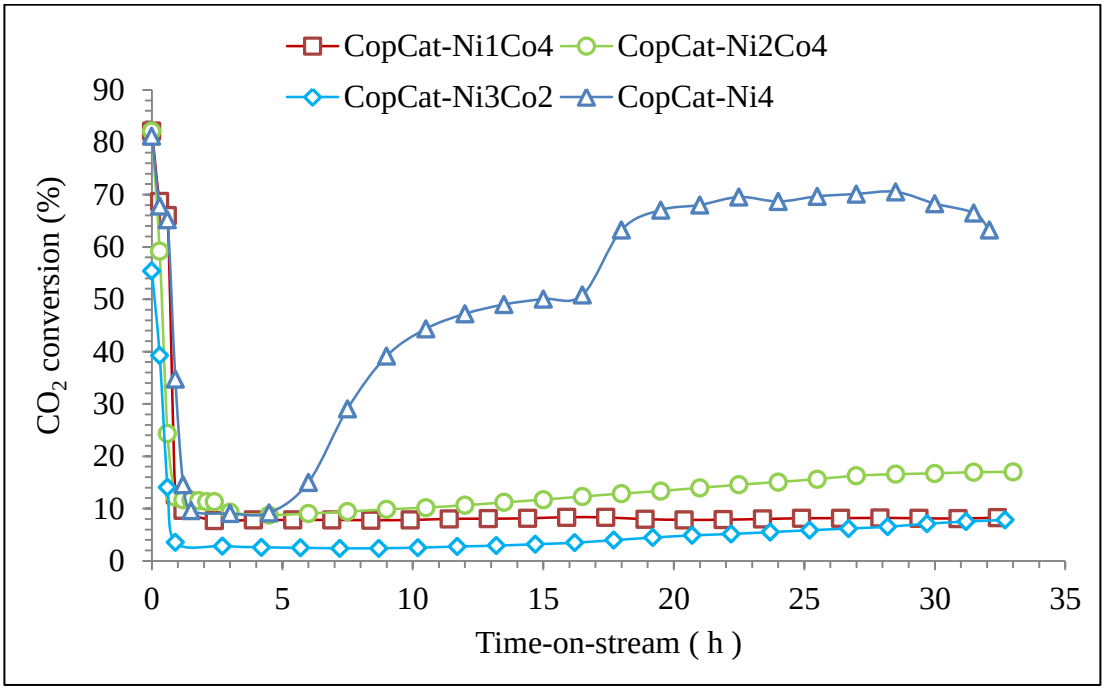

Fig. 4.22 Activity of Ni-Co precipitated catalysts in term of CO_2 conversions during H_2S poisoning test; CDRM reaction conditions: 710 °C, 1 atm, 558,000 mL/g_c.h (GHSV), and $CH_4/CO_2/N_2$=1/1/1, catalyst load of 0.02 g, 30 ppm H_2S

Table 4.15 Reactant conversions for the poisoning test, precipitated catalysts

Catalyst	CH_4 conversion (%)			CO_2 conversion (%)		
	before H_2S	after H_2S	end	before H_2S	after H_2S	end
CopCat-Co6	54	-	8.6	63	-	7.6
CopCat-Ni1Co4	82.8	8.8	8.8	88.4	7.7	8.6
CopCat-Ni2Co4	82.7	10.1	12.4	87.6	9.3	16.7
CopCat-Ni3Co2	54.9	2.9	4.6	68.9	3.5	8.5
CopCat-Ni4	82.6	8.8	63.6	88.3	9.6	63.2

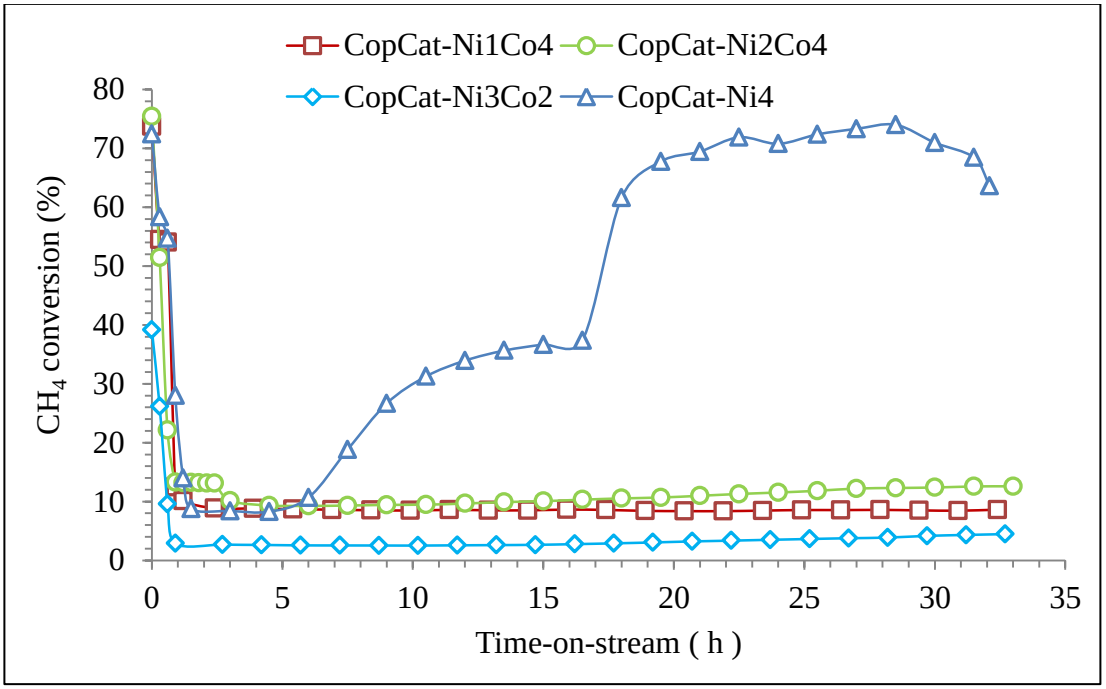

Fig. 4.23 Activity of Ni-Co precipitated catalysts in term of CH_4 conversions during H_2S poisoning test; CDRM reaction conditions: 710 °C, 1 atm, 558,000 mL/g_c.h (GHSV), and $CH_4/CO_2/N_2$=1/1/1, catalyst load of 0.02 g, 30 ppm H_2S

Figure 4.24 and 4.25 illustrate the results of catalyst poisoning test using 30 ppm of H_2S for the catalysts prepared by impregnation method. It can be observed that catalysts with higher Ni content can be quickly regenerated after being exposed to hydrogen sulfide. Also, the results indicate that the bimetallic catalyst prepared by impregnation method regenerate themselves faster than the precipitated ones implying that the impregnated catalysts with higher metal content on the surface have higher degree of reduction as shown in Tables 4.5 and 4.8. Table 4.16 presents the results of the poisoning test for impregnated catalyst. Despite the quick regeneration step, the longest deactivation time recorded for Ni monometallic catalyst showing more resistibility of Nickel toward H_2S poison.

Table 4.16 Reactant conversions for the poisoning test, impregnated catalysts

Catalyst	CH_4 conversion (%)			CO_2 conversion (%)		
	before H_2S	after H_2S	end	before H_2S	after H_2S	end
ImpCat-Co5	28.5	-	7.2	29	-	6.5
ImpCat-Ni2Co3	75.6	7.9	8.3	83.2	7.7	10
ImpCat-Ni3Co3	84.1	8.6	33.8	89.2	8.9	47.4
ImpCat-Ni3Co2	83.4	8.4	52.4	89	8.4	64.6
ImpCat-Ni5	84	7.7	64.6	88.5	8.4	65.7

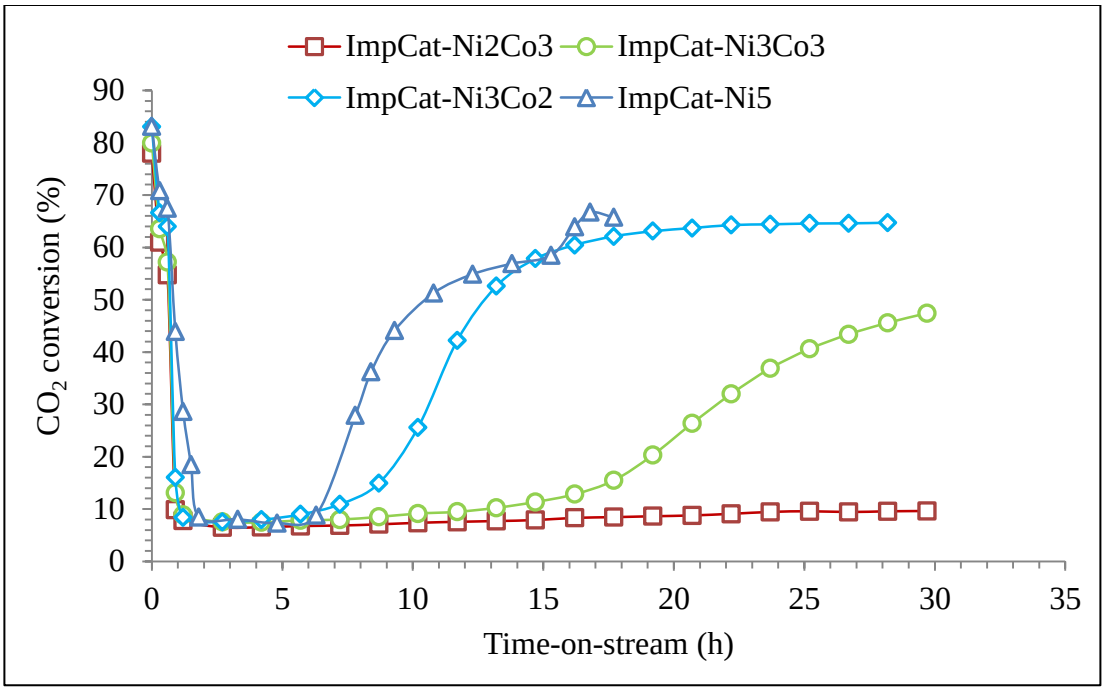

Fig. 4.24 Activity of Ni-Co impregnated catalysts in term of CO_2 conversions during H_2S poisoning test; CDRM reaction conditions: 710 °C, 1 atm, 558,000 mL/g_c.h (GHSV), and $CH_4/CO_2/N_2$=1/1/1, catalyst load of 0.02 g, 30 ppm H_2S

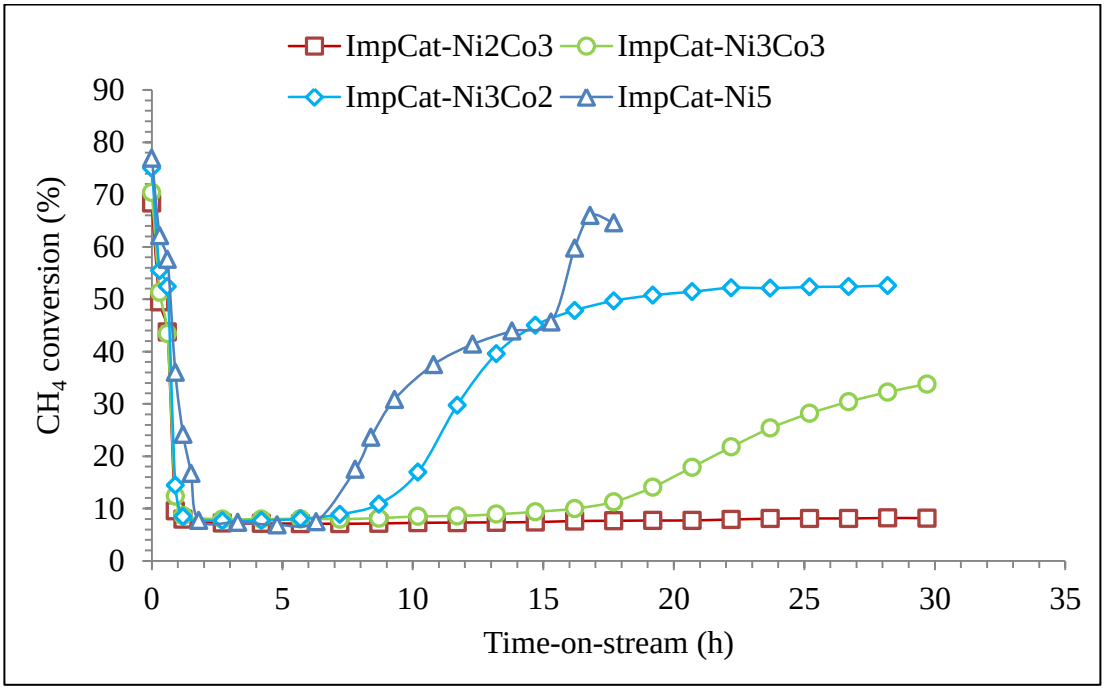

Fig. 4.25 Activity of Ni-Co impregnated catalysts in term of CH_4 conversions during H_2S poisoning test; CDRM reaction conditions: 710 °C, 1 atm, 558,000 mL/g_c.h (GHSV), and $CH_4/CO_2/N_2$=1/1/1, catalyst load of 0.02 g, 30 ppm H_2S

To summarize, higher Ni content, increases the regeneration capability of the catalysts, no matter which method selected for preparation. On the other hand, the regeneration ability for the bimetallic impregnated catalysts was higher than precipitated catalysts. Also, the same regeneration behavior associated with both impregnated and precipitated Ni monometallic catalysts is observed as a result of having significantly close values of reduced Ni content as shown in Table 4.10 and 4.11. One may link the regeneration difficulties to pore blockage of the precipitated catalyst. The majority of sulfur compounds may block the active sites forming a stable structure on the catalyst surface (Metal-S). Consequently, the blocked sites will not be able to adsorb the CH_X species anymore[1]. This justification can be proposed as a possible pathway for deactivation mechanism within poisoning period. It can be concluded that the regeneration time becomes shorter as the Ni/Co ratio increases although the regeneration is not complete.

[1] Based on the proposed mechanism for CDRM reaction in section 2.4.4.

CHAPTER 5: CONCLUSION AND RECOMMENDATION

5.1 CONCLUSION

- All the prepared catalysts with various Ni/Co ratios by impregnation and precipitation methods, had BET surface area greater than 100 m^2/g_c.
- It was observed that due to the lack of metal-metal interactions in impregnated catalysts the obtained Ni/Co and Mg/Al ratios were closer to the intent ones as compared to the precipitated catalysts.
- In the impregnated catalysts the amounts of reduced metals were almost two times of the precipitated catalysts. Furthermore, only the Co monometallic catalyst prepared by precipitation method did not show any Co reduction.
- No matter how the catalysts were prepared, the percentage of reduced Ni was very close in Ni monometallic catalysts.
- The amount of reduced metals at 850 °C was more than those at 750 °C, but the reduced metal particle size was lower than 100 Å for the bimetallic catalysts that were prepared at 750 °C. Whereas, the particle size was more than 100 Å for bimetallic catalysts that were prepared at 850 °C.
- The CO_2 conversion had the same trend as CH_4 conversion in all the prepared catalysts for CDRM reaction at 710 °C.

- The Co monometallic catalysts prepared by impregnation and precipitation did not show a good activity for CDRM reaction as compared to the other prepared bimetallic and metallic catalysts.
- The CopCat-Ni2Co4 catalyst (Ni/Co ratio of 0.6) leads the CDRM reaction to produce H_2/CO ratio (0.95-1.05) is achieved by dry reforming theoretically indicating that the catalyst is not suffering from a significant side reaction (RWGSR) effect resulting in a desirable selectivity.
- The only Ni monometallic catalyst prepared by impregnation had the highest conversion and also the lowest side reaction for CDRM reaction at 710 °C.
- The precipitated bimetallic catalyst with Ni/Co ratio of 0.6 (CopCat-Ni2Co4) was more stable as compared to the impregnated Ni monometallic (CopCat-Ni4) catalyst.
- The precipitated Ni-Co/AlMgOx catalyst with Ni/Co ratio of 0.6 has a high stability for CDRM reaction. This behavior improved when the reaction temperature was increased from 710 °C to 760 °C during the life-time test for 65 days.
- The catalysts containing more Ni showed better H_2S resistance and regeneration after poisoning whether they were prepared by precipitation or impregnation method.
- The bimetallic impregnated catalysts regenerated themselves better as compared to the precipitated ones, which could be due to their higher metal content on the surface and reduction than the precipitated catalysts.

- The same regeneration behavior associated with both impregnated and precipitated Ni monometallic catalysts is observed as a result of having significantly close values of reduced Ni content.

5.2 RECOMMENDATION

As general recommendations:

1- The H_2S poisoning test should be repeated with various concentrations of H_2S in order to obtain an optimum concentration of H_2S that may have a reduced effect on the catalyst performance.
2- Studying the stability of the catalyst for a periodic H_2S poisoning could be investigated.
3- To understand how H_2S poisons the catalyst, detailed characterization analyses are needed.

Some specific recommendations for the precipitated Ni-Co catalyst of ratio 1 to be used as a working catalyst in industry:

1- Finding the maximum H_2S concentration that may not affect the catalyst performance for long term use.
2- In reality natural gas mainly contains methane and relatively low concentrations of other gases compounds including sulfur containing compounds (H_2S, mercaptans, thiophen, ...). The effects of such impurities should be investigated on the catalyst performance.

3- To pelletize the catalyst, a suitable binder needs to be selected so that industrial shapes could leave desired impacts on the catalyst performance. In this way, catalyst shows a better performance in terms of mechanical properties such as high abrasion and attribution resistances. The pelletized catalyst on the bottom of a fixed bed in operation could be able to tolerate either the force from the above catalyst or the applied force by pressure drop as a result of oncoming gas flow.

REFERENCES

1. Arbag, H., Yasyerli, S., Yasyerli, N., Dogu, G., "Activity and stability enhancement of Ni-MCM-41 catalysts by Rh incorporation for hydrogen from dry reforming of methane", international journal of hydrogen energy 35 (2010) 2296–2304.
2. Aparicio, P., F., Ramos, I., R., Ruiz, A., G., "On the applicability of membrane technology to the catalysed dry reforming of methane", J. Applied Catalysis A: General, Volume 237, Issues 1-2, November 2002, Pages 239-252.
3. Barreto, L., Makihira, A., Riahi, K., "The hydrogen economy in the 21st century: a sustainable development scenario", International Journal of Hydrogen Energy, Volume 28, Issue 3, March 2003, Pages 267-284.
4. Barroso-Quiroga, M. M., Castro-Luna, A. E., "Catalytic activity and effect of modifiers on Ni-based catalysts for the dry reforming of methane", international journal of hydrogen energy 35 (2010) 6052–6056.
5. Bellido, J. D. A., Assaf, E. M., "Effect of the Y_2O_3-ZrO_2 support composition on nickel catalyst evaluated in dry reforming of methane", Applied Catalysis A: General 352 (2009) 179‑187.
6. Bellido, J. D. A., De Souza, J. E., Jean-Claude M'Peko, Assaf, E. M., " Effect of adding CaO to ZrO2 support on nickel catalyst activity in dry reforming of methane", Applied Catalysis A: General 358 (2009) 215–223.

7. Bitter, J., Seshan, K., and Lercher, A., "The state of zirconia supported platinum catalysts for CO_2/CH_4 reforming," J. Catal. 171, 279-286 (1997).
8. Bitter, J., Seshan, K., and Lercher, A., "Mono and bi-functional pathways of CO_2/CH_4 reforming over Pt and Rh based catalysts," J. Catal. 176, 93-101 (1998).
9. Bouarab, R., Akdim, O., Auroux, A., Cherifi, O., Mirodatos,C., "Effect of MgO additive on catalytic properties of Co/SiO2 in the dry reforming of methane", Appl. Catal. A, 2004, 264, pages 161–168.
10. Bradford, M., C., Vannice, M., A., "Catalytic reforming of methane with carbon dioxide over nickel catalysts I. Catalyst characterization and activity", Applied Catalysis A: General, Volume 142, Issue 1, 1 August 1996, Pages 73-96.
11. Bradford, and M.C.J., Vannice, M.A., "CO_2 reforming of CH_4," Catal. Rev. Sci. Eng. 41, 1 (1999).
12. Bradford, M., C., Vannice, M., A., "CO_2 Reforming of CH_4 over Supported Pt Catalysts", Journal of Catalysis, Volume 173, Issue 1, 1 January 1998, Pages 157-171.
13. Brunauer, S., Emmett, P. H., and Teller, E., J. Am. Chem. Soc., 60, 309, (1938).
14. Cornaglia, L., M., Múnera, J., Irusta, S., Lombardo, E.A., "Raman studies of Rh and Pt on La_2O_3 catalysts used in a membrane reactor for hydrogen production", Applied Catalysis A: General, Volume 263, Issue 1, 28 May 2004, Pages 91-101.
15. Dowden, D.A., Schnell, C.R., and Walker, G.T., "The design of complex catalysts," Fourth International Congress on Catalysis, Rice University, Houston, pages 1120-1131 (1968).

16. Environment Canada, "http://www.ec.gc.ca/gesghg/default.asp?lang=En&n=72E6D4E2-1", Jun 2011.
17. ErdoÈhelyi, A., CsereÂnyi, J., Papp, E., Solymosi, F., "Catalytic reaction of methane with carbon dioxide over supported palladium", J. Applied Catalysis A: General, Volume 108, Issue 2, 3 February 1994, Pages 205-219.
18. ErdoÈhelyi, A., Fodor, K., Solymosi, F., "Reaction of CH_4 with CO_2 and H_2O over supported Ir catalyst", Studies in Surface Science and Catalysis, Volume 107, 1997, Pages 525-530.
19. Fidalgo, B., Zubizarreta, L., Bermúdez, J.M., Arenillas, A., Menéndez, J.A., "Synthesis of carbon-supported nickel catalysts for the dry reforming of CH_4", Fuel Processing Technology 91 (2010) 765–769.
20. Frusteri, F., Arena, F., Calogero, G., Torre, T., Parmaliana, A, "Potassium-enhanced stability of Ni/MgO catalysts in the dry-reforming of methane", Catalysis Communications 2 (2001) 49-56.
21. García-Diéguez, M., Finocchio, E., Larrubia, M. A., Alemany, L.J., Busca, G., "Characterization of alumina-supported Pt, Ni and PtNi alloy catalysts for the dry reforming of methane", Journal of Catalysis 274 (2010) 11–20.
22. Goff, S. P., Wang, S. I., *Chem. Eng. Prog.* 1987, Aug, 46.
23. Guo, J. J., Lou, H., Zhao, H., Chai, D. F., Zheng, X. M., "Dry reforming of methane over nickel catalysts supported on magnesium aluminate spinels", Appl. Catal. A 2004, 273, pages 75–82.
24. Hickman, D.A., and Schmidt, L.D., "Production of syngas by direct catalytic oxidation of methane," Science 259, 343-345 (1993).

25. IPCC http://www.ipcc.ch/pdf/assessment-report/ar4/syr/ar4_syr_spm.pdf, AR4 SYR SPM page 5, July 2009.
26. Jensen, M.B., Ra`berg, L.B., Olafsen Sja`stad, A., Olsbye, U., "Mechanistic study of the dry reforming of propane to synthesis gas over a Ni/Mg(Al)O catalyst", Catalysis Today 145 (2009) 114–120.
27. Juan-Juan, J., Roma´n-Martı´nez, M.C., Illa´n-Go´mez, M.J., "Effect of potassium content in the activity of K-promoted Ni/Al_2O_3 catalysts for the dry reforming of methane", Applied Catalysis A: General 301(2006) 9–15.
28. Kang, K. M., Kim, H. W., Shim, I.W., Kwak, H. Y., " Catalytic test of supported Ni catalysts with core/shell structure for dry reforming of methane", Fuel Processing Technology 92 (2011) 1236–1243.
29. Kroll, V.C.H., Swaan, H.M., and Mirodatos, C., "Methane reforming reaction with carbon dioxide over Ni/SiO2 catalyst: II. A nechanistic study," J. Catal. 164, 387-398 (1996).
30. Kroll, V.C.H., Swaan, H.M., and Mirodatos, C., "Methane reforming reaction with carbon dioxide over Ni/SiO2 catalyst: I. deactivation studies," J. Catal. 161, 409-422 (1996).
31. Miller, J.T., Kropf, A.J., Zha, Y., Regalbuto, J.R., Delannoy, L., Louis, C., Bus, E. and van Bokhoven, J.A. J. Catal. 240, 222 (2006).
32. Múnera, J., Irusta, S. Cornaglia, L. Lombardo, E., "CO_2 reforming of methane as a source of hydrogen using a membrane reactor", Applied Catalysis A: General 245 (2003) 383–395.
33. J. Applied Catalysis A: General 263 (2004) 91–101.

34. Ocsachoque, M., Pompeo, F., Gonzalez, G., "Rh–Ni/CeO_2–Al_2O_3 catalysts for methane dry reforming", Catalysis Today (2011).
35. Omata, K., Nukui, N., Hottai, T., Showa, Y., Yamada, M., "Strontium carbonate supported cobalt catalyst for dry reforming of methane under pressure", Catalysis Communications 5 (2004) 755–758.
36. Pena, M.A., Gomez, J.P., and Fierro, J.L.G., "New catalytic routes for syngas and hydrogen production", Appl. Catal. A 144, 7-57 (1996).
37. Pompeo, F., Nichio, N. N., Gonza´lez, M. G., Montes, M., "Characterization of Ni/SiO_2 and Ni/Li-SiO_2 catalysts for methane dry reforming", Catalysis Today 107–108 (2005) 856–862.
38. Quincoces, C. E., Basaldella, E. I., De Vargas, S. P., Gonza´lez, M. G., "Ni/γ-Al_2O_3 catalyst from kaolinite for the dry reforming of methane", Materials Letters 58 (2004) 272– 275.
39. Ramachandran, R., Menon, R., K., "An overview of industrial uses of hydrogen", International Journal of Hydrogen Energy, Volume 23, Issue 7, July 1998, Pages 593-598.
40. Richardson, B., Turk, B., and Twigg, M.V., Appl. Catal. A 148, 97 (1996).Aparicio, L.M., "Transient Isotopic Studies and Microkinetic Modeling of Methane Reforming over Nickel Catalysts," J. Catal. 165, 262-274 (1997).
41. Richardson, J.T., "Principles of catalyst development," Plenum Press, New York, 28-31 (1989).

42. San-Jose´ -Alonso, D., Juan-Juan, J., Illa´n-Go´ mez, M.J., Roma´ n-Martý´nez, M.C., " Ni, Co and bimetallic Ni–Co catalysts for the dry reforming of methane", Applied Catalysis A: General 371 (2009) 54–59.
43. Satterfield C. N., "Heterogeneous Catalysis in Practice", McGraw-Hill (1991).
44. Schuurman, Y., Marquez-Alvarez. C., Kroll, V.C.H., and Mirodatos, C., "Unraveling mechanistic features for the methane reforming by carbon dioxide over different metals and supports by TAP experiments," Catal. Today 46, 185-192 (1998).
45. Solymosi, F., Kustan, G., and Erdohelyi, A., "Catalytic reaction of CH_4 with CO_2 over aluminasupported Pt metals," Catal. Lett. 11, 149-156 (1991).
46. Solymosi, F., "The bonding, structure and reactions of CO_2 adsorbed on clean and promoted metal surfaces," J. Mol. Catl., 65, 337-358 (1991).
47. Takanabe, K., Nagaoka, K., Nariai, K., and Aika, K.I, "Titania-supported cobalt and nickel bimetallic catalysts for carbon dioxide reforming of methane," J. Catal. 232, 268-275 (2005).
48. Teuner, S.C.; Neumann, P.; Linde, F.V., "The CALCOR standard and CALCOR economy processes", Oil Gas European Magazine 3, 44 (2001).
49. Tsai, H-L, Wang, C-S, "Thermodynamic equilibrium prediction for natural gas dry reforming in thermal plasma reformer", journal of Zhōngguó gōngchéng xuékān, ISSN 0253-3839, 2008, vol. 31, n°5, pp. 891-896.
50. Tsipouriari, V.A., and Verykios, X.E., "Carbon and oxygen reaction pathways of CO_2 reforming of methane over Ni/La_2O_3 and Ni/Al2O3 catalysts studied by isotopic tracing techniques," J. Catal. 187, 85-94 (1999).

51. Tsipouriari, V.A., and Verykios, X.E., "Kinetic study of the catalytic reforming of methane with carbon dioxide to synthesis gas over Ni/La2O3 catalyst," Catal. Today 64, 83-90 (2001).
52. Udengaard, N.R.; Hansen, J.-H. B.; Hanson, D. C.; Stal, J. A., "Sulfur passivated reforming process lowers syngas H_2/CO ratio", Oil & Gas Journal, 90, 62 (1992).
53. Uniongas Company report, "http://www.uniongas.com/aboutus/aboutng/composition.asp#",Jun, 2011.
54. Wang, N., Chua, W., Zhangb, T., Zhaoc, X. S., "Manganese promoting effects on the Co-Ce-Zr-Ox nano catalysts for methane dry reforming with carbon dioxide to hydrogen and carbon monoxide", Chemical Engineering Journal 170 (2011) 457–463.
55. Wei, J.-M., Xu, B.-Q., Li, J.-L., Cheng, Z.-X., and Zhu, Q.-M., "Ultra stable Ni/ZrO2 catalyst for carbon dioxide reforming of methane," Appl. Catal. A 196 L167-169 (2000).
56. Wijngaarden R.J., Kronberg, A., and Westerterp, K.R., "Industrial catalysis – optimizing catalysts and processes," WILEY-VCH Verlag GmbH, D-69496 Weinheim, 25-59, (1998).
57. Xi, Ch., Wang, H, "Effects of Preparation Conditions and Ni/Co Ratio on Ni-Co Bimetallic Catalyst Performance for CO_2 Reforming of CH_4", 21st NAM conference, San Francisco, CA, 2009.
58. YAW, T., C., AMIN, N., A., "Analysis of carbon dioxide reforming of methane via thermodynamic equilibrium approach", Universiti Teknologi Malaysia, Jurnal Teknologi, 43(F) Dis. 2005: 31–50.

59. Zhang, A., Zhu, A., Chen, B., Zhang, Sh., Au, Ch., Shi, Ch., "In-situ synthesis of nickel modified molybdenum carbide catalyst for dry reforming of methane", Catalysis Communications, 12 (2011), pages 803–807.
60. Zhang, J., "Research and development of nickel based catalyst for carbon dioxide formation of methane", PhD thesis, department of chemical engineering, university of Saskatchewan, summer (2008).
61. Zhang, J., Wang, H., Dalai, A., K., "Development of stable bimetallic catalysts for carbon dioxide reforming of methane", Journal of Catalysis, Volume 249, Issue 2, 25 July 2007, Pages 300-310.
62. Zhang, Z., Tsipouriari, V., A., Efstathiou, A., M., Verykios, X., E., "Reforming of Methane with Carbon Dioxide to Synthesis Gas over Supported Rhodium Catalysts: Effects of Support and Metal Crystallite Size on Reaction Activity and Deactivation Characteristics", Journal of Catalysis, Volume 158, Issue 1, January 1996, Pages 51-63.

APPENDIX A: CALIBRATION OF MASS FLOW (MFC) CONTROLLER

To calibrate the MFC, N_2 was used. Then for gases other than N_2, the flow rate of N_2 was converted to the corresponding gas flow rate using heat capacity of gases at constant pressure as shown in Table A.1. Equation A-1 was used to convert the flow rates.

$$F_j = F_{N_2} \times \frac{C_{N_2}}{C_j} \qquad \text{(A-1)}$$

where, j stands for CH_4, CO_2, or H_2.

Table A.1 Heat capacity values of H_2, N_2, CO_2, and CH_4 at 21 °C.

Gas	Heat capacity (Cp)
N_2	0.2885
H_2	0.2847
CO_2	0.3749
CH_4	0.3547

In the following calibration curves for mass flow controller, each point stands as the average of 10 measured flow rates with the same set-point.

A: N_2 mass flow controller (set-point vs measurement at STP)

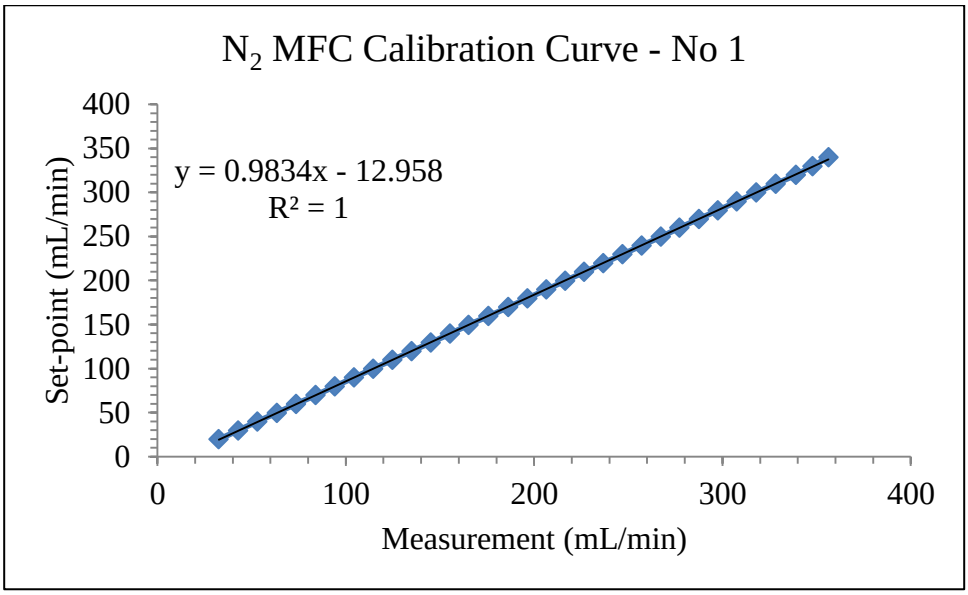

Fig. A.1 Calibration curve for N_2 mass flow controller

B: CH_4 mass flow controller (set-point vs measurement at STP)

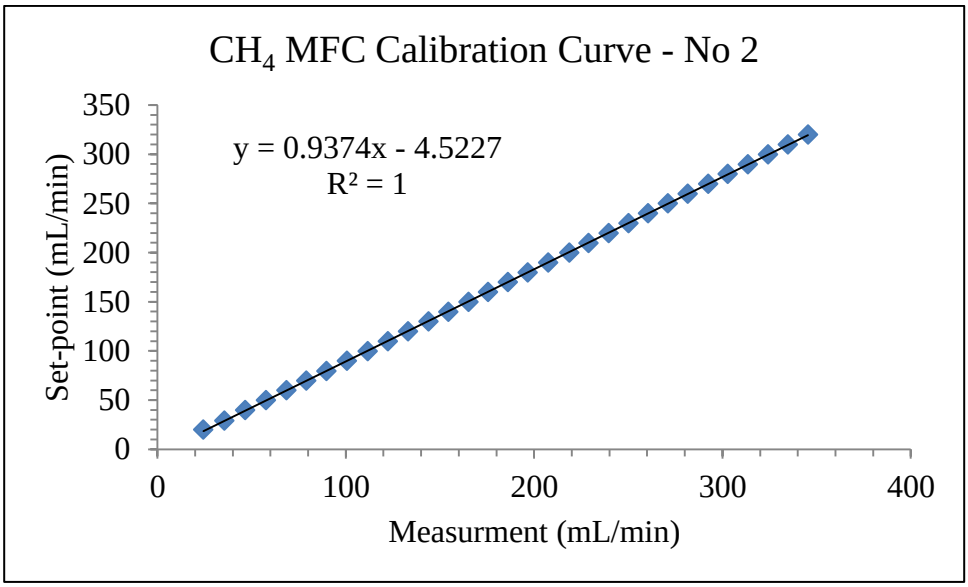

Fig. A.2 Calibration curve for CH_4 mass flow controller

C: CO_2 mass flow controller (set-point vs measurement at STP)

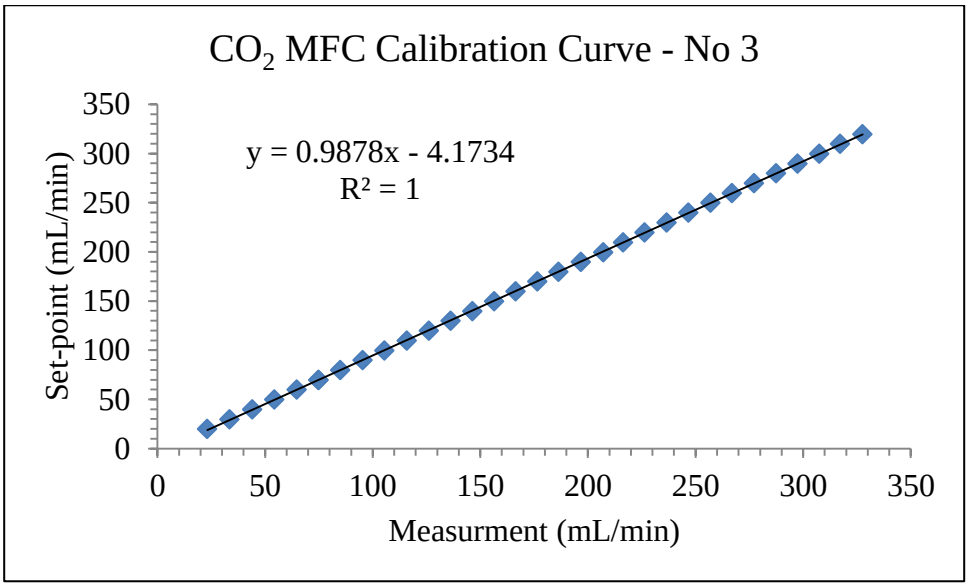

Fig. A.3 Calibration curve for CO_2 mass flow controller

D: H_2 mass flow controller (set-point vs measurement at STP)

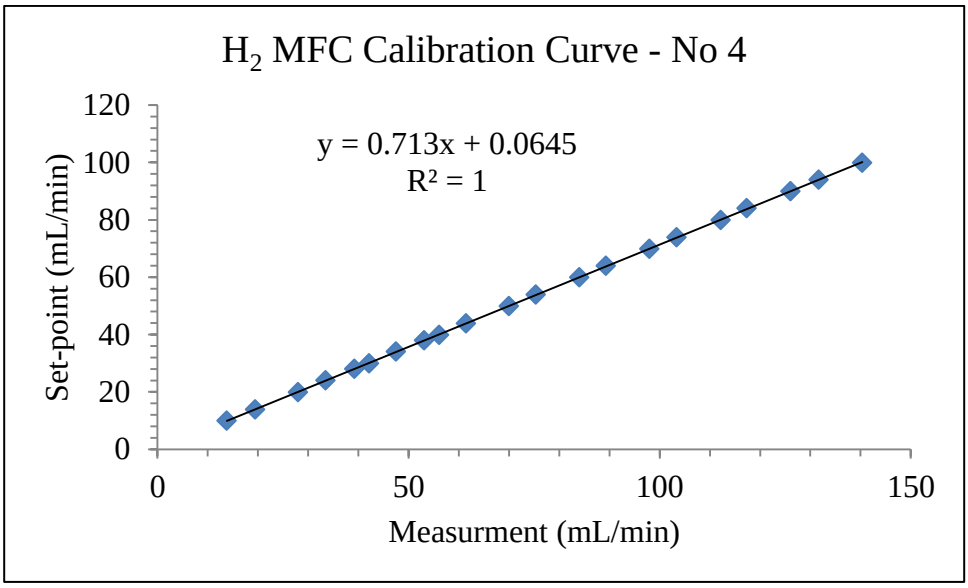

Fig. A.4 Calibration curve for H_2 mass flow controller

APPENDIX B: CALIBRATION OF GAS CHROMATOGRAPHY

To calibrate the Gas Chromatography (GC), at least three times injection for each concentration was done. Then the average area was calculated to use in the calibration curve. Also the Standard Deviation of the obtained data is calculated based on the following equation:

$$STD = \sqrt{\frac{1}{N}\sum_{i=1}^{N}(x_i - \bar{x})^2} \quad \text{(B-1)}$$

where,

STD : standard deviation of the obtained areas for each concentration,

N: number of injections at each concentration,

x_i: GC measured area for each injection with same concentration,

$\bar{x}$: average of the GC measured areas for each injection with same concentration.

A: GC calibration curve for H_2 (area vs concentration (%v/v))

Table B.1 GC calibration data for H_2

Ret. Time	Level	Concentration (%v/v)	Area	STD
1.37	1	6.60	16.35	0.19
1.37	2	10.00	20.75	0.03
1.37	3	18.00	37.98	0.06
1.36	4	26.00	55.23	0.09
1.36	5	32.00	69.21	0.34
1.36	6	40.00	87.40	0.14

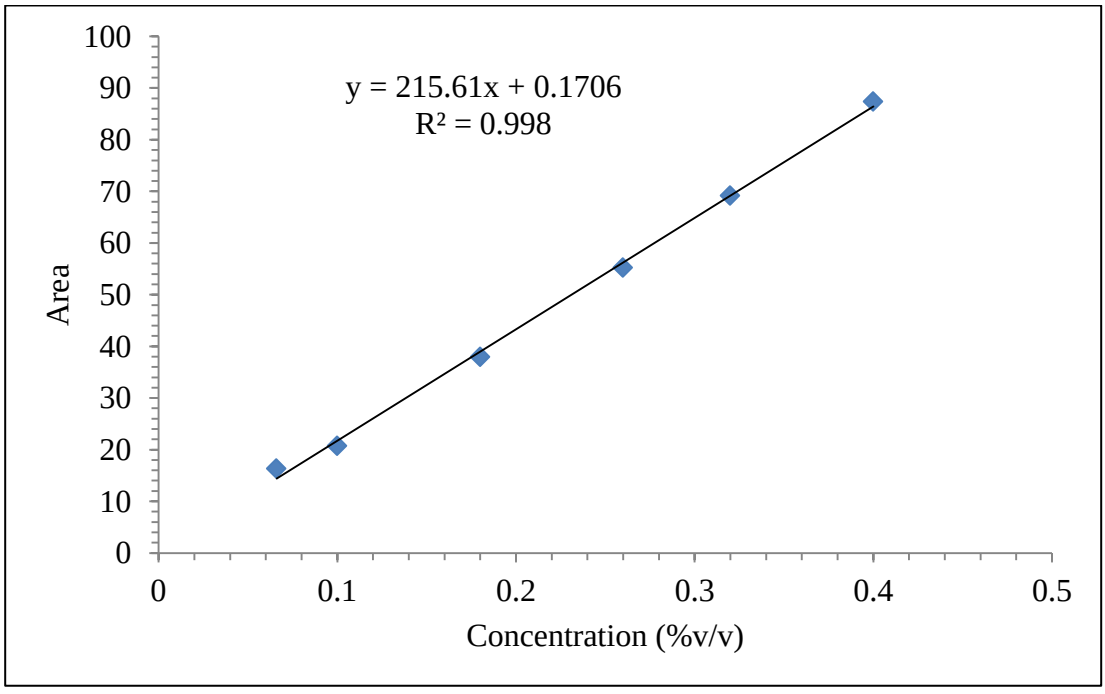

Fig. B.1 GC calibration curve for H_2

B: GC calibration curve for N_2 (area vs concentration (%v/v))

Table B.2 GC calibration data for N_2

Ret. Time	Level	Concentration (%v/v)	Area	STD
3.546	1	10.2	4172.48	34.82
3.532	2	19.94	6076.19	14.48
3.516	3	29.73	8258.92	2.75
3.50	4	39.97	10628.14	15.40

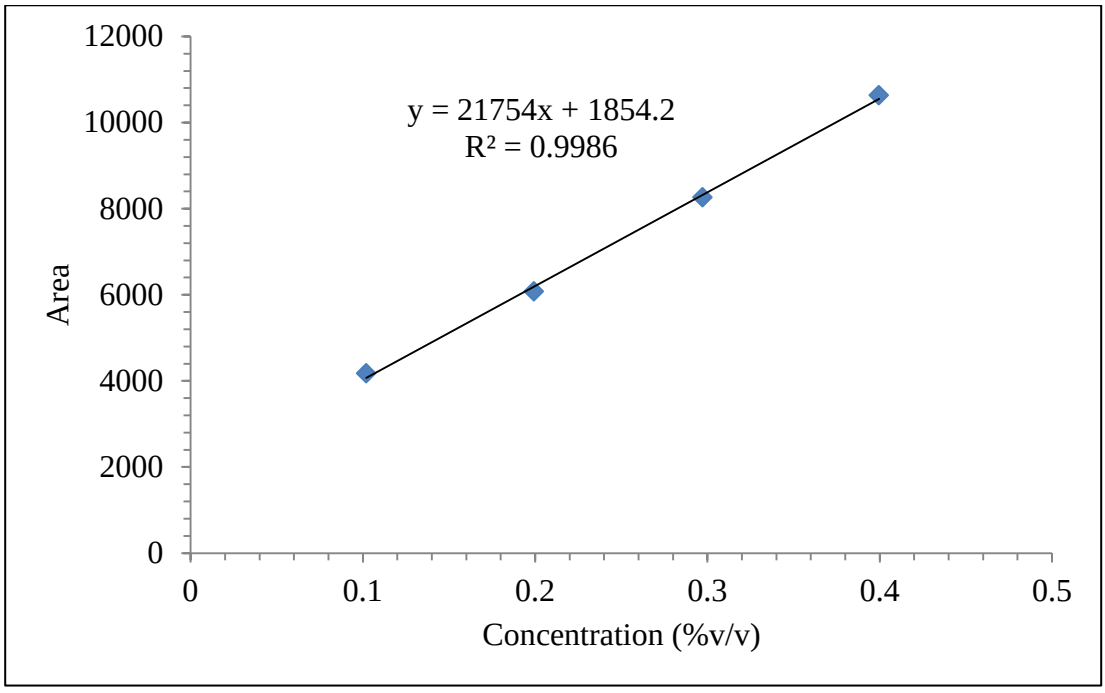

Fig. B.2 GC calibration curve for N_2

C: GC calibration curve for CO (area vs concentration (%v/v))

Table B.3 GC calibration data for CO

Ret. Time	Level	Concentration (%v/v)	Area	STD
4.45	1	6.60	1427.55	6.51
4.45	2	10.00	2196.99	3.49
4.43	3	18.00	3956.71	1.03
4.41	4	26.00	5693.98	1.28
4.40	5	32.00	7045.00	15.60
4.39	6	40.00	8718.22	16.44

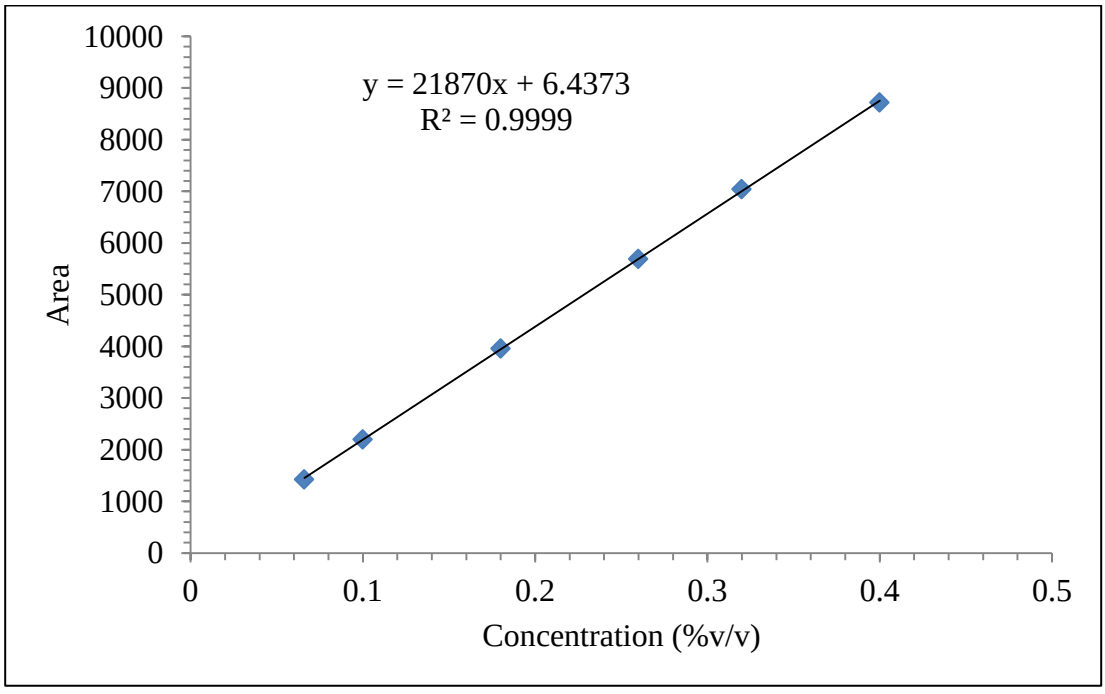

Fig. B.3 GC calibration curve for CO

D: GC calibration curve for CH_4 (area vs concentration (%v/v))

Table B.4 GC calibration data for CH_4

Ret. Time	Level	concentration (%v/v)	Area	STD
7.62	1	2.50	470.56	0.64
7.62	2	10.00	1583.54	0.44
7.59	3	19.90	3036.29	1.52
7.56	4	34.42	5528.09	4.97

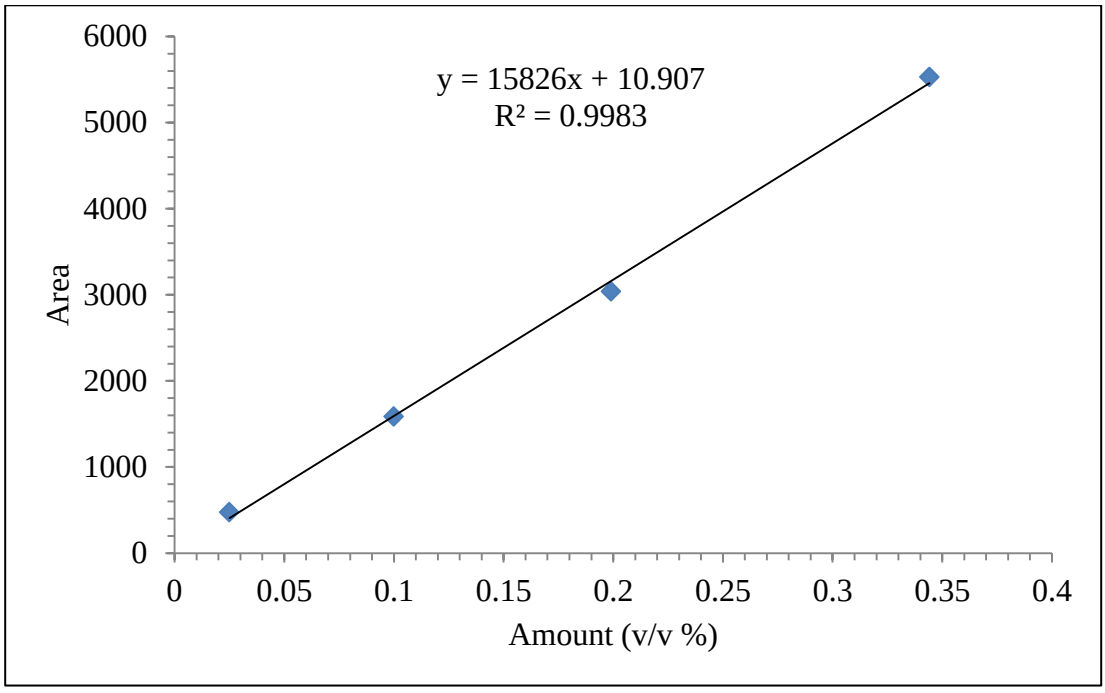

Fig. B.4 GC calibration curve for CH_4

E: GC calibration curve for CO_2 (area vs concentration (%v/v))

Table B.5 GC calibration data for CO_2

Ret. Time	Level	concentration (%v/v)	Area	STD
11.17	1	3.00	693.29	0.25
11.14	2	10.00	2071.19	0.45
11.11	3	19.80	4224.00	3.59
11.08	4	26.00	5897.01	6.28
11.05	5	35.25	8349.34	5.66

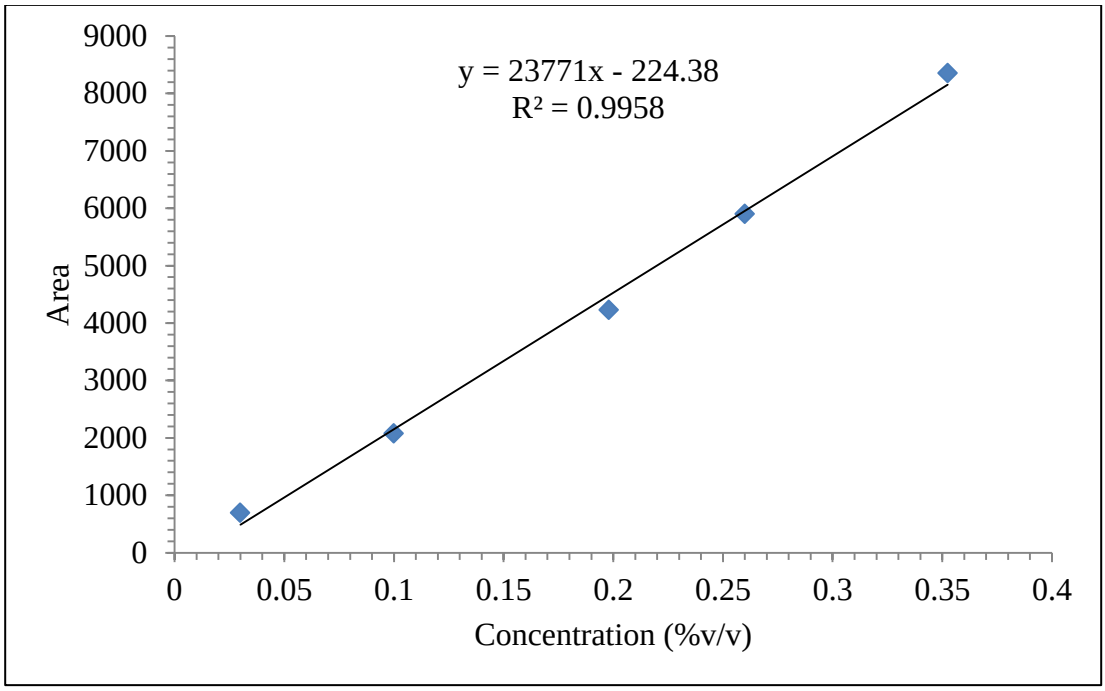

Fig. B.5 GC calibration curve for CO_2

APPENDIX C: TEMPERATURE CALIBRATION IN THE MIDDLE OF THE REACTOR

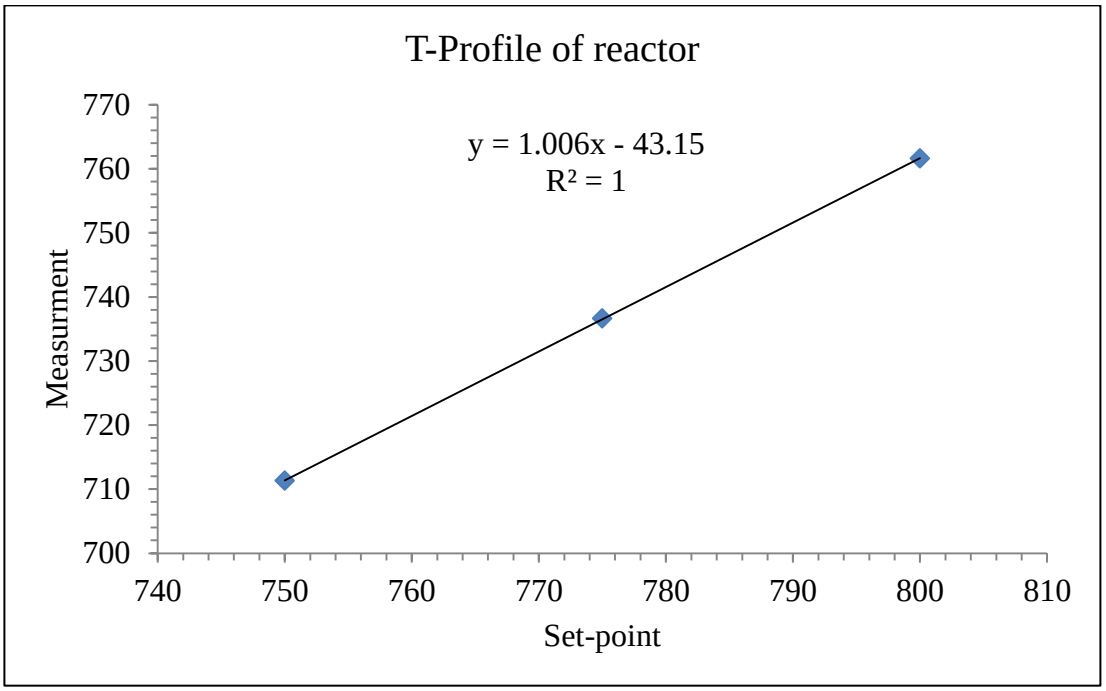

Fig. C.1 Heater temperature calibration in the middle of the reactor during CDRM reaction

APPENDIX D: CARBON BALANCE

mole of C in = mole of CH_4 in + mole of CO_2 in (D-1)

mole of C Out = mole of CH_4 out + mole of CO_2 out + 2*mole of CO out (D-2)

Regarding equations D-1 and D-2, carbon flow (mol/h) in both inlet and outlet stream of the reactor using CopCat-Ni3Co2 catalyst on CDRM reaction is presented in Figure D.1.

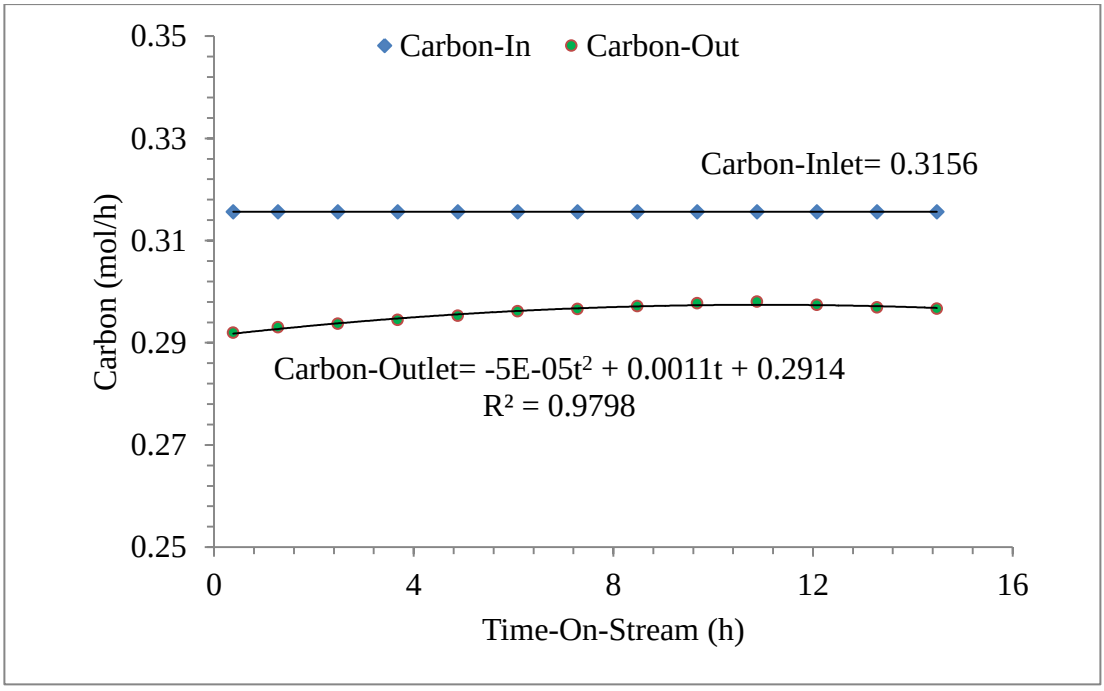

Fig.D. 1 Carbon flow in inlet and outlet streams of the reactor using CopCat-Ni3Co2 catalyst for CDRM reaction

The overall amount of carbon within TOS (14h is calculated) is integrated from the area below each line which shown in Figure D.1 as shown in Table D.1.

Table D. 1 Carbon balance for CopCat-Ni3Co2 within 14h

Overall (h)	Carbon-Inlet (mol)	Carbon-Outlet (mol)	C balance	
			mol	%
14	4.45	4.17	0.28	6.2

APPENDIX E: CATALYST CHARACTERIZATION ANALYSIS

E-1 BET surface area

BET surface area is known as an important property for many kinds of materials and especially solid catalysts. B.E.T. (or BET) stands for Brunauer, Emmett, and Teller, the scientists who proposed the theory for measuring the surface area (Brunauer et al., 1938). The concept of the theory is based on the Langmuir theory. Different methods are used to calculate and measure the BET surface area, but most of them are based on isothermal adsorption of nitrogen. The BET is measured by the use of nitrogen adsorption/desorption isotherms at liquid nitrogen temperature and relative pressures. The BET equation is:

$$\frac{1}{Q\left[\left(\frac{P_0}{P}\right)-1\right]} = \frac{c-1}{Q_m c}\left(\frac{P}{P_0}\right) + \frac{1}{Q_m c} \qquad \text{(E-1)}$$

where,

Q: the adsorbed gas quantity,

P_0: saturation pressure of the adsorbed gas,

P: equilibrium pressure of the adsorbed gas,

Q_m: quantity of the monolayer adsorbed gas,

c: BET constant.

The BET plot is gained by plotting $\frac{1}{Q\left[\left(\frac{P_0}{P}\right)-1\right]}$ on the y-axis versus $\left(\frac{P}{P_0}\right)$ on the x-axis. *c* and Q_m can be calculated by using the slope and y-intercept of the BET plot. Then, $S_{BET,Total}$ and S_{BET} will be calculated by the following equations:

$$S_{BET,Total} = \frac{Q_m N s}{V} \quad \text{(E-2)}$$

$$S_{BET} = \frac{S_{BET,Total}}{a} \quad \text{(E-3)}$$

where,

N: Avogadro's number = 6.022×10^{23},

s: molecular cross-sectional area,

V: molar volume of adsorbed gas,

A: molar mass of adsorbed species.

There are two parts, degassing and analysis. Degassing is to remove the dissolved gases from liquids, especially water. After degassing the sample is analysed for BET surface area. BET analysis also gives information about pores size and pore volume of the samples.

E-2: XAS analysis

In XAS method the core electron is excited by tuning the photon energy. Then after the excitation, a spectrum is generated through the XAS data. The spectrum

contains three main regions which are shown in Figure E.1. The regions orderly are Pre-edge, XANES, and EXAFS (Miller et al., 2006).

The name of "edge" is subjected to the excited core electron. The principle quantum numbers n=1, 2, 3 respectively relate to the K-, L-, and M- edge. To be more illustrative the excitation of 1s electron happens at K-edge, while 2s and 2p occur at L-edge.

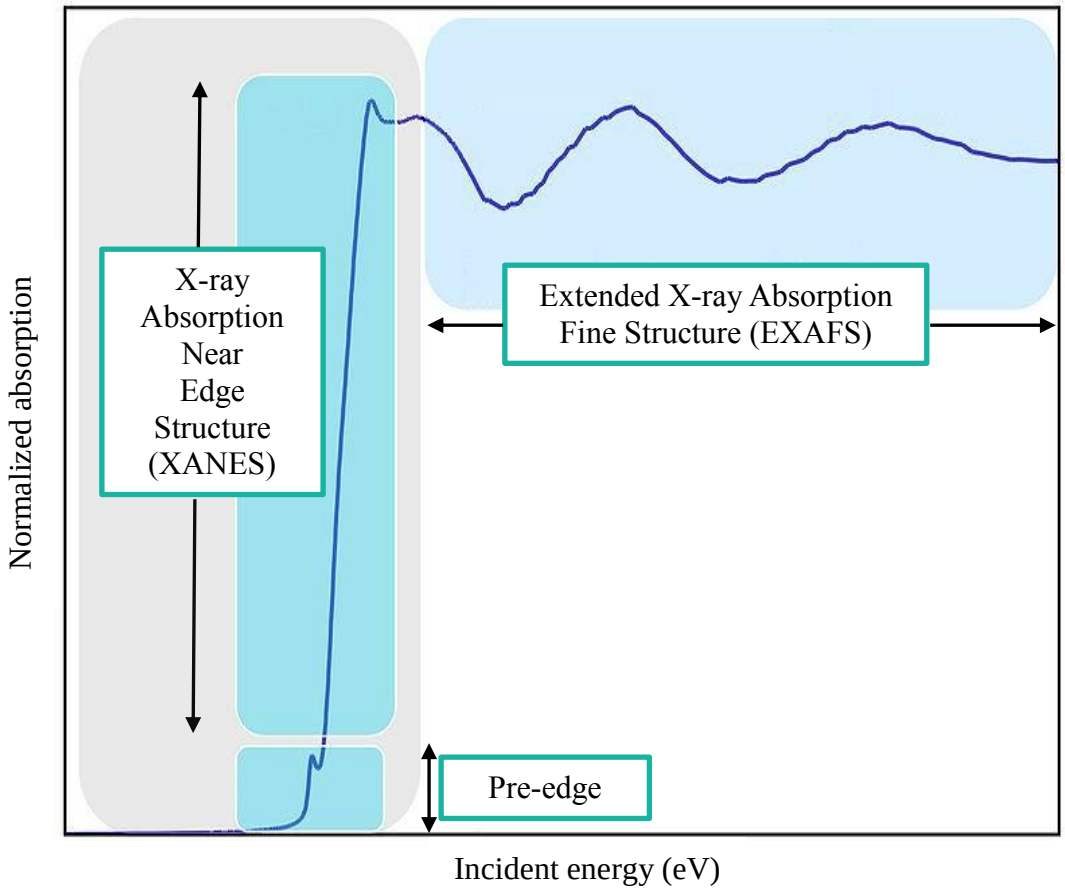

Fig. E.1 Three main regions in an XAS spectrum

Three main regions in an XAS spectrum schematically as shown in Figure E.1 are as follows:

1) Pre-edge: The name is given to the region in the energies lower than rising edge.

2) XANES: The main region above the Pre-edge is called XANES (X-ray Absorption Near-Edge Structure) or NEXAFS (Near-edge X-ray Absorption Fine Structure).

3) EXAFS: The region at energies above pre-edge is called EXAFS (Extended X-ray Absorption Fine Structure). EXAFS corresponds to scattering of the released photoelectron of neighbouring atoms.

APPENDIX F: OVEN TEMPERATURE PROFILE OF GC

Table F.1 GC oven temperature values

Oven ramp	Ramp rate (°C/min)	Next T (°C)	Hold time (min)	Run time (min)
Initial	-	40	3.00	3.00
Ramp 1	10.00	60	1.00	6.00
Ramp 2	35.00	125	5.20	13.06
Post run		40	0.00	13.06

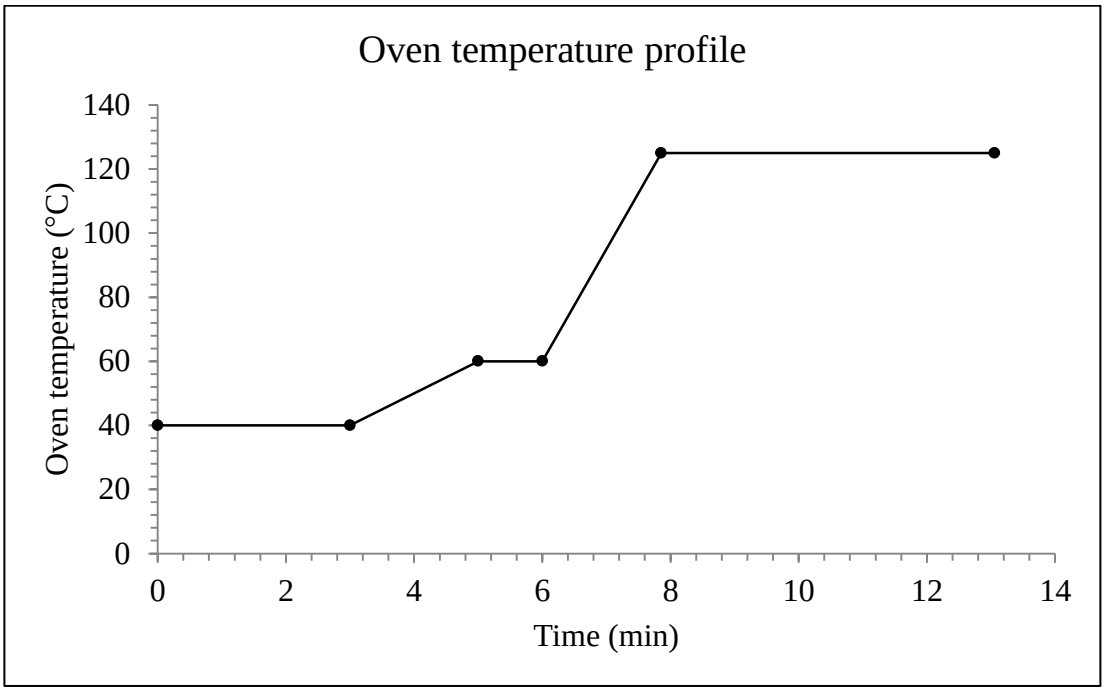

Fig. F.1 Oven temperature profile of GC

4